PhD degree in Molecular Medicine

European School of Molecular Medicine (SEMM),

University of Milan and University of Naples "Federico II"

Faculty of Medicine

THESIS

CROSS-TALK BETWEEN RAL AND RAC PATHWAYS IN THE CONTROL OF CELL MIGRATION

Amel SADOU

Matricola n. R08429

Supervisor: **Pr Giorgio SCITA**

IFOM-IEO Campus, Milan

Anno accademico 2011-2012

RESUME (français)

Le mode de coordination parmi les différentes molécules qui régulent la migration reste très peu connu. Ce travail traite de deux voies de transduction régulant la migration : la voie Rac1/WRC (Wave Regulatory Complex) qui contrôle la formation du réseau d'actine au front des cellules migrantes, et la voie RalB/exocyst, dont les mécanismes moléculaires de son implication dans la motilité cellulaire étaient inconnus au début de cette thèse. Rac1 et RalB sont des petites protéines G des familles Rho et Ras, respectivement. Les complexes WRC et exocyst sont leurs effecteurs directs.

Au cours de la recherche de connexions entre l'exocyst et des régulateurs de la migration, nous avons trouvé que deux sous-unités de l'exocyst, Exo70 et Sec6, interagissent directement in vitro avec Abi et Cyfip, respectivement, deux sous unités du WRC. De plus, nous avons trouvé que les sous-unités de l'exocyst peuvent interagir in vitro avec le WRC entier. Nous avons également montré que ces deux complexes s'associent in vivo. Sur le plan fonctionnel, l'exocyst est requis pour le positionnement du complexe WRC au front des cellules migrantes.

D'autre part, nous avons également trouvé que deux autres sous-unités de l'exocyst Sec8 and Exo84, interagissent avec SH3BP1 (une RhoGAP) en double hybride et en co-immunoprécipitation. SH3BP1 se localise au front des cellules migrantes, et cette localisation dépend de l'exocyst. De façon intéressante, in vivo, la voie RalB/exocyst/SH3BP1 cible spécifiquement Rac1, et non Cdc42. Grâce à plusieurs approches, nous concluons que SH3BP1 est requis pour inactiver Rac1 au front.

Dans notre modèle nous proposons que RalB/exocyst régulerait la migration cellulaire en véhiculant au front de migration deux éléments majeurs de la signalisation de Rac1 : son complexe effecteur WRC, qui stimule la nucléation de filaments d'actine et son régulateur négatif SH3BP1, une GAP qui promeut l'inactivation et le cycle GDP/GTP de Rac1. En conclusion, ce travail fournit de nouvelles connexions moléculaires et fonctionnelles entre l'exocytose polarisée et la dynamique de l'actine au cours de la motilité cellulaire.

RIASSUNTO (italiano)

I meccanismi di coordinazione tra le varie molecule che regolano la migrazione restano poco conosciuti. Questo lavoro tratta di due vie di segnale che regolano la migrazione: la via Rac1/WCR (Wave Regulatory Complex) che controlla la formazione della rete di actina al fronte delle cellule migranti; e la via RalB/exocyst, i cui meccanismi molecolari alla base della sua implicazione nella migrazione cellulare erano ignoti all'inizio di questa tesi. Rac1 e RalB fanno rispettivamente parte delle famiglie Rho e Ras delle piccole proteine G. I complessi WRC ed exocyst sono i loro effettori diretti. Ricercando possibile connessioni tra l'exocyst e le molecole regolatrici della migrazione, abbiamo trovato che due subunità dell'exocyst, Exo70 e Sec6, interagiscono direttamente in vitro con Abi e Cyfip, che sono due subunità del complesso WRC. Inoltre abbiamo trovato che le subunità dell'exocyst possono interagire in vitro con il complesso WRC intero, contenente tutti i suoi componenti. Abbiamo mostrato che questi due complessi sono associati anche in vivo. Dal punto di vista funzionale, l'exocyst è necessaria per posizionare il complesso WRC al fronte delle cellule migranti. D'altra parte abbiamo trovato che due altre subunità dell'exocyst, Sec8 e Exo84, interagiscono con SH3BP1 (una proteina RhoGAP) grazie alla tecnica del doppio-ibrido e per co-immunoprecipitazione. SH3BP1 si trova al fronte delle cellule migranti; questa sua localizzazione dipende dalla presenza dell'exocyst. E' interessante il fatto che, in vivo, la via RalB/exocyst/SH3BP1 ha come bersaglio Rac1, e non Cdc42. Combinando diversi approcci abbiamo potuto concludere che SH3BP1 è necessaria all'inattivazione di Rac1 al fronte.

Nel nostro modello proponiamo che RalB/exocyst regola la migrazione cellulare trasportando al fronte di migrazione due elementi chiave delle vie di segnale di Rac1: il suo complesso effettore WRC, che stimola la nucleazione di filamenti di actina , e il suo regolatore negativo SH3BP1, una GAP che promuove l'inattivazione e il ciclo GDP/GTP di Rac1. In conclusione, questo lavoro ha messo in evidenza nuove connessioni molecolari e funzionali tra l'esocitosi polarizzata e le dinamiche d'actina durante la migrazione cellulare.

SUMMARY (English)

Very little is known about the coordination and the integration among the different regulators of the motility process. This work deals with two migration-regulatory pathways: the Rac1/WRC (Wave Regulatory Complex) pathway that drives the formation of the actin polymerization network at the front of motile cells; and RalB/exocyst pathway for which the molecular mechanisms underlying its implication in cell motility were still largely unknown at the beginning of this thesis. Rac1 and RalB are small GTPases of the Rho and Ras family, respectively. WRC and exocyst complexes are their direct effectors.

In searching for connections between the exocyst and migration regulators, we found that two subunits of the exocyst, Exo70 and Sec6, interact directly in vitro with two subunits of the WRC, Abi and Cyfip, respectively. Moreover, we found that exocyst subunits can interact in vitro with the whole fully-assembled WRC complex. We also showed that these two complexes associate in vivo. Functionally, the exocyst was required for WRC complex positioning at the front of migrating cells.

On the other hand, we also found that two other subunits of the exocyst, Sec8 and Exo84, interact with SH3BP1 (a RhoGAP protein) by two-hybrid assay and by co-immunoprecipitation. SH3BP1 localizes at the leading edge and this localization is dependent on the exocyst. Interestingly, in vivo, the RalB/exocyst/SH3BP1 pathway specifically targets Rac1, and not Cdc42. By a combination of approaches we concluded that SH3BP1 is required to inactivate Rac1 at the front.

In our model we propose that RalB/exocyst regulates cell migration by driving to the leading edge two key signaling elements of the Rac1 pathway: its effector WRC, that stimulates actin filament nucleation, and its negative regulator SH3BP1, a GAP promoting Rac1 inactivation and GDP/GTP cycling. In conclusion, this work provides novel molecular and functional links between polarized exocytosis and actin dynamics during cell motility.

ABBREVIATIONS

CaM	Calmodulin
DE-cadherin	Drosophila Epithelial Cadherin
bFGF	Basic fibroblast growth factor
FLIM	Fluorescence-lifetime imaging microscopy
GAP	GTPase activating protein
GDP	Guanosine diphosphtae
GEF	Guanosyl exchange factor
HEK-HT	Human embryonic kidney cell line
HGF	Hepatocyte growth factor
IGF-1	Insulin-like growth factor 1
NPF	Nucleation Promoting Factor
PH	Plecstrine Homology
PP2A	Phosphatase 2A
PLC	Phospholipase C
PLD	Phospholipase D
PP2A	Protein phosphatase type 2A
RAL	RAS like
RAL-BP1	Ral binding protein
RALGDS	Ral Guanine nucleotide dissociation stimulator
RNAi	RNA interference
SNARE	SNAP Receptor proteins
VCA domain	Verprolin homology, Cofilin homology, and Acidic region
WASP	Wiskott-Aldrich Syndrome Protein
WAVE	WASP family Verprolin-homologous
ZONAB	ZO-1-associated nucleic acid-binding protein
WRC	Wave regulatory complex

TABLE OF CONTENT

8

INTRODUCTION

CHAPTER 1:
PLAYERS

1. RAL

1.1. RAL GTPases

1.1.1. Discovery

Exploration of Ras functions in yeast provided the first evidence pointing to the importance of Ras as a hub in signal transduction (Van Aelst et al., 1994). This concept has been extended to mammalian cells, where Ras proteins were found to mediate the transduction of various signaling pathways emanating from plasma membrane receptors by directly associating with at least three major signal transducers: Raf, PI3Kinase and RalGEFs (Downward, 2003). Mutations in the effector domain of Ras enabled to dissect the contribution of each of these effectors and transduction patwhays to oncogenic Ras functions.

Ral proteins (Ras like) are small G proteins belonging to Ras superfamily. In addition they act downstream of Ras since RalGEFs, direct effectors of Ras, are also direct activators of Ral. They share the biochemical properties typical of all GTPases: cycling between a non active GDPlinked form, to an active GTP-linked form. Ral-encoding genes were isolated from a cDNA library of immortalized simian B-lymphocytes, by using a degenerated probe specific to Ras family domains (Chardin and Tavitian, 1986).

1.1.2. Structure

RalGTPases exist in all multicellular organisms (one gene in fly, two in humans, and four in zebrafish). In mammalian cells, two different genes encode RalA and RalB proteins; they are located on 7p15-p13 and 2cen-q13 respectively (Chardin and Taviatian, 1989). RalA and RalB are monomeric proteins of 206 aminoacids, with a predicted molecular weight of 23.5 KDa. RalA

and RalB show 85% of homology. In fact, these two proteins are 100% identical over the two "switch" regions (Figure I1).

Despite this structural homology, RalA and RalB clearly have different functions as it will be discussed later in this manuscript.

The main domain of Ral is the GTPase domain (residues 12-178). It contains four GTP binding motifs, which are conserved in all small GTPases. Within the GTPase domain, two regions called "switch" (residues 40-48 and 70-78) change conformation upon GTP binding and mediate effector binding. Effectors bind to a single switch or stretch across both. At the N-terminal, an extension of 11 amino acids is supposed to mediate interactions with phospholipase D (PLD) or phospholipase C-δ1 (PLC-δ1); at the C-terminal tail there is a short calmodulin-binding domain (Sidhu, Clough, & Bhullar, 2005).

The major differences between RalA and RalB is in the C-terminal region between residue 181 in RalB (residue 180 in RalA) and the four C-terminal residues that comprise the site of prenylation necessary for membrane association (Kinsella et al., 1991; Hancock et al., 1989; Hancock et al., 1990). This region is called the hypervariable region. It contains two phosphorylation sites in RalA (Ser183 and Ser 194) and one phosphorylation site in RalB (Ser198). The differences in the "hypervariable region" of RalA and RalB may be responsible for the different subcellular distribution of RalA and RalB. RalA localizes at the plasmamembrane and endosome, whereas RalB is present exclusively at the plasma membrane (Shipitsin and Feig, 2004).

The solutions of the various Ral crystal structure were instrumental to help defining the mechanisms of its regulation. Crystal structures of active (bound to the GTP-analogous GppNHp) and inactive (bound to GDP) RalA conformations were published

(Nicely et al., 2004), as well as the structure of the complex between active RalA and a Ral-binding domain from its Sec5 effector (Fukai et al., 2003).

The comparison between active and inactive forms suggests nucleotide-dependent switch mechanism in RalA to bind Sec5. There are two putative sites for RalA-Sec5 interaction: the first one is adjacent to switch I and the second one is modulated by switch II and obstructed in Ral inactive form (Fukai et al., 2003)

The crystal structure of the complex formed by active RalB and the Ral-binding domain of another effector, RalBP1 (Fenwick et al., 2009) revealed somedifferences with respect to the RalA-Sec5 complex, in that both switch regions directly contact the RalBP1 effector.
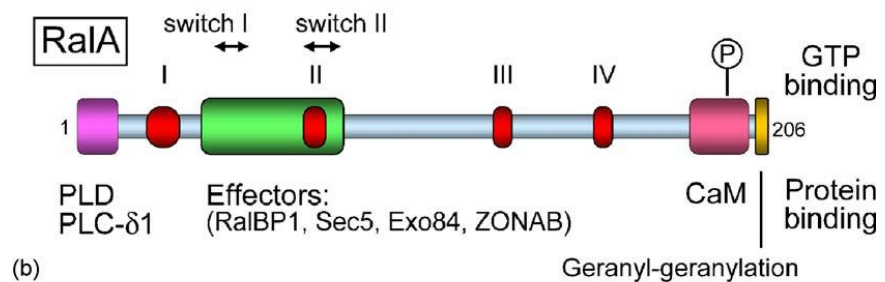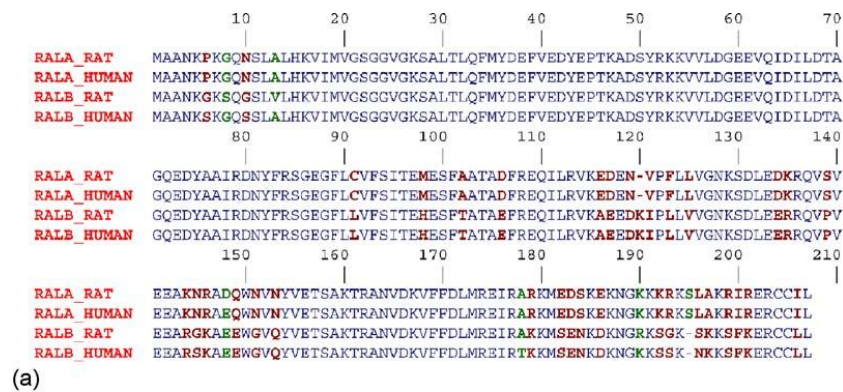
Figure I1: a) Alignment of amino acid sequence of RalA and RalB, from rats and humans. Identical amino acids (blue), 75% identity between the four sequences (green) and 50% or less (brown).

14

b) RalA domain primary structure. RalA contains 206 amino acids, with four motifs for GTP binding and hydrolysis (labelled I–IV). The switch regions of RalA are indicated (switch I-II). The N-terminal 11 amino acids bind PLD1 and PLC-δ1. The effector binding domain is represented in green. The C-terminus domain contains Calmodulin (CaM) binding domain, the phosphorylation site for Aurora-A kinase at Ser-194 (RalA only) and the site for post-translational lipid modification (van Dam and Robinson, 2006).

1.2. REGULATION

Like other small GTPases, Ral proteins act as molecular switches and timers that cycle between inactive guanosine diphosphate (GDP)-bound and active guanosine triphosphate (GTP)-bound states. In GTP-bound state, they have higher affinity for downstream effectors through which they are controlling different biological processes.

Activation of GTPases is catalyzed by GEFs (Guanosyl Exchange Factor). The interaction of GTPase with GEF destabilizes the GTPase-GDP complex and leads to the dissociation of GDP. This is followed by association of GTP because of the fact that the intracellular concentration of GTP is 10-times higher than the concentration of GDP. Inactivation of GTPases requires hydrolysis of the bound GTP to GDP. The intrinsic catalytic activities of Ral proteins are weak and GTP hydrolysis is enhanced by the intervention of GAPs (GTPase Activating Proteins) (Figure I2).
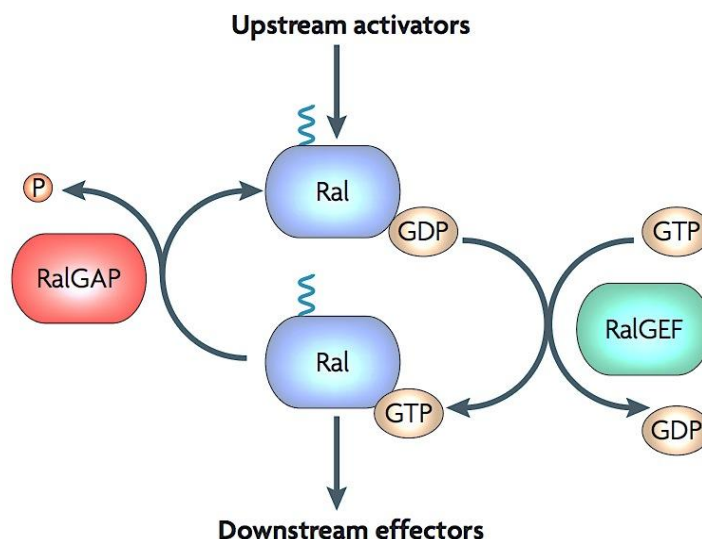
Figure I2: The cycle of Ral GTPases. Inactive Ral is loaded with GDP. RalGEF induce the release of GDP followed by GTP loading, which activates Ral. Hydrolysis of GTP is mediated by RalGAPs, which inactivates Ral (Bodemann and White, 2008).

1.2.1. Regulation by RalGEFs

Six RalGEFs have been identified in human: RalGDS, Rgl1, Rgl2, Rgl3, RalGPS1 and RalGPS2. They can be classified in two groups: RalGDS, Rgl1, Rgl2, Rgl3 have a C-terminal Ras Association domain (RA), and can be directly activated by Ras; RalGPS1 and RalGPS2 do not have a RA domain, therefore they activate Ral GTPases independently of Ras (van Dam and Robinson, 2006; Bodemann and White, 2008) (Figure I2A).

Upon binding a RalGEF, the binary Ral-GDP complex becomes a trimeric GEF-Ral-GDP complex, in which the GEF catalyses the release of the GDP, producing the nucleotide-free GEF-Ral complex; this series of reactions is reversed by rebinding of a nucleotide, predominantly GTP, leading to the active Ral-GTP complex (Vetter and Wittinghofer, 2001).

16
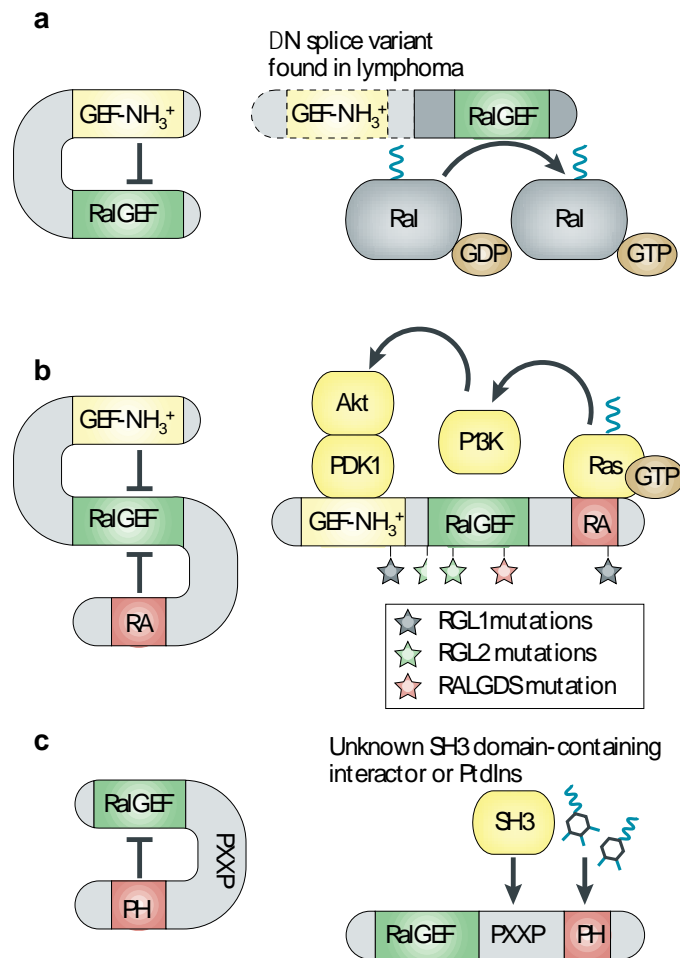
Figure I2A: he RalGEF family and their regulatory cues. An important aspect involves relief of autoinhibitory interactions of amino-terminal and/or C-terminal regulatory motifs (indicated in the figure in yellow and red, respectively) with the catalytic domain (indicated in green). **(a)** In the case of human retinal G-protein coupled receptor (RGR), N-terminal truncation mutants found in lymphoma exhibit cell transformation activity in cell culture and transgenic expression in thymocytes. **(b)** Consistently with this regulatory motif, 3-phosphoinositide-dependent protein kinase 1 (PDPK1) associates with the N terminus of RALGDS to relieve autoinhibition of catalytic activity in response to epidermal growth factor receptor activation[75,76]. RALGDS is also a direct effector of Ras–GTP through the C-terminal Ras association (RA) domain. **(c)** Finally, the RALGPS2 PXXP–PH domains have dominant inhibitory activity (c), decreasing Ral–GTP accumulation by 50% when expressed in HEK 293 cells *(Bodemann and White, 2008).*

Ras-dependent activation

Ras can activate Ral via various mechanisms.

Several works have demonstrated that Ras proteins activate Ras-dependent RalGEFs, at least in part, by relocalizing them to their target, the Ral GTPases: RalGDS, Rgl1, Rgl2 and Rgl3 bind to activated Ras through their RA domain and consequently they are translocated to the plasma membrane where they can stimulate the GDP to GTP exchange on Ral (Huang et al., 1998; Hofer et al., 1998).

The activation of RalGEFs by Ras might also occur through other Ras effectors, thePI3-Kinases: the PI3-K-dependent kinase 1 (PDK1) interacts with the N-terminal domain of RalGDS, relieves its auto-inhibitory effect and enhances GEF activity on its target Ral; this PDK1 function is not dependent upon its kinase activity (Tian et al., 2002).

The regulatory mechanisms of Ras-dependent RalGEFs are still poorly investigated. For example, a recent study suggests that phosphorylation of Rgl2 by CyclinD1-Cdk4 complex may stimulate its GEF activity (Fernandez et al., 2011).

Ras-independent activation

RalGPS1 and RalGPS2 share the core catalytic domain of other RalGEFs, but don't have a RA domain. At the C-terminal, they have a PH (Plecstrine Homology) domain suggested to be necessary for membrane targeting. They have a proline-rich motif, which allows interaction with SH3-containing adapter proteins Grb2 and Nck. The interaction with these adaptors likely contributes to RalGPS regulation (Rebhun et al., 2000).

RalGDS can also interact with β-arrestins. In leukocytes, under basal conditions, RalGDS is associated with β-arrestins in the cytosol. fMLP (formyl-Met-Leu-Phe) receptor stimulation recruits β-arrestin–RalGDS protein complexes to the plasma

membrane. β-arrestin binding to the fMLP receptor is followed by the release of RalGDS and results in Ras-independent activation of Ral. This mechanism has been implicated in cytoskeletal reorganization required for cell migration in response to chemoattractant stimulus (Bhattacharya et al., 2002).

Another way to activate Ral by a Ras-independent pathway is through modulation of Ca^{2+}. Activation of PLC increases intracellular Ca^{2+} level and was proposed to promote Ral activation, possibly via the binding of calmodulin (CaM) to Ral, (Hofer et al., 1998). Both RalA and RalB interact specifically in vitro and in vivo with calmodulin. Both RalA and RalB have a calcium dependent CaM-binding site in their C-terminal region, and a calcium independent binding site in their N-terminal region. Moreover, in vitro Ral-GTP pull-down experiments demonstrated that thrombin-induced activation of Ral in human platelets requires calmodulin, suggesting that calmodulin regulates Ral activation in human platelets (Clough et al., 2002).

1.2.2. Regulation by RalGAPs

The existence of a protein with a Ral-specific GAP activity was biochemically demonstrated using the cytosolic fraction of brain and testis (Emkey et al., 1991). It took long time to identify the coding genes because it turned out that the RalGAPs are multiprotein complexes, which require heterodimerization for their GAP activity. The first proteins with RalGAP activity were identified in 2009 and named RalGAP1 and RalGAP2. They are large heterodimeric complexes, each composed of a catalytic α1 (240 kDa) or α2 (220 kDa) subunit and a common β subunit (170 kDa) (Shirakawa et al., 2009). Akt2, also known as PKB beta, phosphorylates RalGAP2 upon insulin stimulation. This phosphorylation inhibits RalGAP2 activity and therefore activates Ral GTPases (Chen et al., 2011). Since Akt2 acts down-stream of

the Ras-effector PI3-kinases, this axis may define an additional mechanism by which Ras can activate Ral proteins.

1.2.3. Regulation by phosphorylation

Phosphorylation of RalA on Ser183 and on Ser194 by AuroraA, promotes its activation, its translocation from plasma membrane and the activation of the effector protein RalBP1 (Lim et al., 2010). PP2A Abeta, a well known tumor suppressor, dephosphorylates RalA at these sites Ser183 and Ser194, inactivating RalA and abolishing its transforming function. It was proposed that PP2A Abeta suppresses transformation of immortalized human cells by regulating the function of RalA (Sablina et al., 2007).

Phosphorylation of RalB on Ser198 by PKC was shown in vitro and in vivo. In human bladder carcinoma cells, PMA (phorbol ester [phorbol 12-myristate 13-acetate]) treatment induced S198 phosphorylation of RalB. This phosphorylation is necessary for RalB translocation from the plasma membrane to perinuclear regions, as well as for actin cytoskeletal organization, anchorage-independent growth, cell migration and lung metastasis (Wang et al., 2010).

These observations showing that RalA and RalB are phosphorylated by different kinases may contribute to their different biological functions.

1.3. EFFECTORS

1.3.1. Exocyst

The exocyst complex consists of eight subunits named Sec3, Sec5, Sec6, Sec8, Sec10, Sec15, Exo70 and Exo84, and was first identified in the secretory pathway of budding Yeast (Novick et al., 1980; TerBush et al., 1996; Finger and Novick, 1998). Exocyst

complex, which is conserved from yeast to humans, is required for polarized secretion by controlling the docking of intracellular vesicles to specific sites of the plasma membrane (He and Guo, 2009). The mammalian subunits are called EXOCs (exocyst complex components) 1-8 (figure I3A); however the yeast nomenclature is still currently used (figure I3).

Yest	Mammalian
SEC3	EXOC1
SEC5	EXOC2
SEC6	EXOC3
SEC8	EXOC4
SEC10	EXOC5
SEC15	EXOC6
EXO70	EXOC7
EXO84	EXOC8

Figure I3A: Yest and mammalian nomenclature of exocyst subunits.

Two exocyst subunits, Sec5 and Exo84, interact with the active form of Ral GTPases. Thus, they are direct effectors of RalA and RalB. The functions of the Ral-Exocyst are not fully understood, but RalA silencing experiments suggested that RalA is required for the assembly of the full octameric complex (Moskalenko et al., 2002; Moskalenko et al., 2003).

The functional aspects of exocyst will be presented later in the manuscript (Chapiter 2.3).
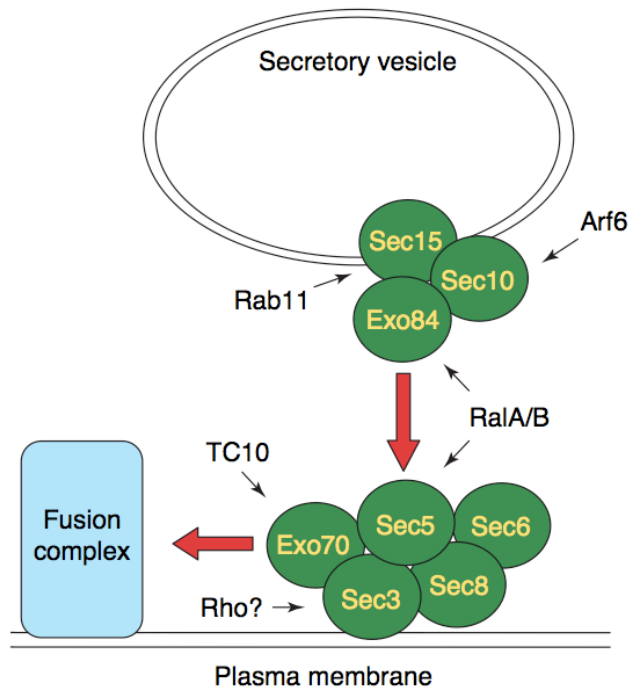
Figure I3: RalGTPases promote exocyst assembly. *This model proposes that RalGTPases interact with Sec5 and Exo84 to assemble the exocyst complex by combining two subcomplexes: the Exo84 subcomplex on secretory vesicles and the Sec5 subcomplex on plasma membrane target sites. Other GTPases can also associate with exocyst subunits, as indicated by the arrows, and might participate in dynamic regulation of this secretory machinery (Camonis and White, 2005).*

1.3.2. RalBP1

RalBP1 (Ral Binding Protein 1), also known as RLIP76, was the first identified effector of Ral GTPases. It interacts with the active form of RalA and RalB (Cantor et al., 1995; Jullien-Flores et al., 1995). RalBP1 contains a Ral binding domain and a Rho GAP domain, which has a GAP activity on Rac and Cdc42 (Jullien-Flores et al., 1995). RalBP1 interacts also with AP2 (adaptor protein 2, adaptor protein for clathrin binding to membrane), during transferrin and EGF receptor endocytosis; and with POB1 (RalBP1-binding protein, regulates receptor-mediated endocytosis)

during internalization of insulin. These interactions suggest that RalBP1 is an important actor of endocytosis machinery (Nakashima et al., 1999; Jullien-Flores et al., 2000).

RalBP1 interacts also with Cdk1 and this interaction is necessary for phosphorylation of Epsin (clathrin-mediated endocytosis protein) by Cdk1 during mitosis in a Ral dependent manner. Phosphorylated Epsin is no longer competent for endocytosis suggesting that Ral might regulate inhibition of endocytosis during mitosis through this mechanism (Rossé et al., 2003).

1.3.3. PLD1

Phospholipase D (PLD) hydrolyzes the phosphatidylcholine, one of the four major glycerolipids, to phosphatidic acid and free choline. Phosphatidic acid is the intracellular lipid mediator of many of the biological functions attributed to PLD. In mammals, PLD activity regulates the actin cytoskeleton, vesicle trafficking for secretion and endocytosis, and receptor signaling (Jenkins and Frohman, 2005).

The activation of PLD1 by phorbol esters, growth factor receptor tyrosine kinases and oncogenic tyrosine kinase v-Src is dependent on RalA. PLD1 directly binds to the N-terminal region of Ral GTPase in a nucleotide-independent manner (Jiang et al., 1995; Schmidt et al., 1998; Voss et al., 1999). RalA and Arf6 (a GTPase implicated in endocytosis and endocytic vesicle recycling) cooperate to activate PLD1, a potential functional mechanism to link vesicles trafficking and signal transduction (Luo et al., 1998).

1.3.4. ZONAB

ZONAB (ZO-1-associated nucleic acid-binding protein) is a transcription factor of the Y-box family and plays a role in regulating epithelial cell proliferation and cell density. At low cell

density, a pool of ZONAB is nuclear and represses transcription, while at high cell densities, relocation of ZONAB from the nucleus relieves transcriptional repression. ZONAB binds to RalA in a GTP-dependent manner, and this interaction increases with the increase of cell densitiy and cell-cell contacts resulting in derepression of ZONAB-regulated transcription (Frankel et al., 2005).

1.3.5. PLC-δ1

PLC (Phospholipase C) is a family of enzymes responsible for hydrolysis of the membrane lipid phosphatidylinositol bisphosphate. RalA and RalB bind to PLC-δ1 in a GTP-independent manner, and promote its activity *in vitro* and *in vivo* (Sidhu et al., 2005). A more recent study showed that the angiotensin II type 1 receptor (AT1R), a G protein-coupled receptors important for the blood pressure regulation, activates PLC-δ1 through RalA. Activation of AT1R recruits β-arrestin-RalGDS complex to activate RalA and activation of RalA is necessary for PLC-δ1 activation. This mechanism may be important for physiological cardiovascular function (Godin et al., 2010).

1.4.   BIOLOGICAL FUNCTIONS

1.4.1. Cell migration

A role for Ral in cell migration was first described in *Drosophila melanogaster:* the expression of the dominant-negative Ral gene delayed the onset of migration of "border cells" (specific follicle cells that migrate in the egg chamber during the fly oogenesis), without affecting their migratory speed (Lee et al., 1996). In mammalian cells, it was shown that dominant-negative mutants of Ras and Ral inhibited chemotaxis of mouse myoblast

24

cell line C2C12 in response to bFGF (Basic fibroblast growth factor), HGF (Hepatocyte growth factor) and IGF-1 (Insulin-like growth factor 1). Expression of an activated mutant of either Ras or Ral resulted in increased motility of myoblasts (Suzuki et al., 2000).

The individual roles of RalA and RalB in cell migration were clarified thanks to the development of the RNAi technology. In human bladder and prostate cancer cell lines, depletion of RalB resulted in reduction in cell migration. Interestingly, simultaneous depletion of both RalA and RalB had no effect on migration, which suggests that RalA and RalB might act as antagonists (Oxford et al., 2005).

Our team similarly showed that RalB, but not RalA, is required for the cell migration of non-transformed NRK (normal rat kidney) cells. Furthermore, the exocyst complex, but not the RhoGAP RalBP1, was found to be required downstream of RalB, indicating the existence of a RalB/exocyst pathway controlling cell migration. It was shown that RalB promotes assembly of exocyst complex and mobilization of exocyst to the leading edge of moving cells (Rossé et al., 2006).

The work of other groups indicated that another Ral effector, RalBP1, is implicated in the regulation of cell migration. RalBP1 is also an effector of R-Ras and is required for adhesion-induced Rac activation through Arf6, and for the resulting cell spreading and migration of NIH3T3 cells (Goldfinger et al., 2006).

In human prostate cancer, RalA is important for invasion in vivo and metastasis formation (Yin et al., 2007) and RalA expression is associated with human tumor progression (Varambally et al., 2005). RalBP1 was identified playing a similar role as RalA in prostate cancer cells. In fact, depletion of RalA and RalBP1 in PC3 human prostate cancer cells inhibited cell migration and bone metastasis (Wu et al., 2010).

It is still not clear whether RalBP1, which has a GAP domain working on Rac and Cdc42 in vitro (Jullien-Flores et al., 1995), really acts as a GAP for Rac and Cdc42 during cell motility in vivo.

1.4.2. Apoptosis

RalB/Sec5/TBK1 pathway

RalB is implicated in survival of tumour-derived cell lines (but not of non-transformed cell lines). In fact, tumor cells are selectively dependent on RalB expression and not on RalA expression, suggesting that RalB GTPase may induce survival pathways that are crucial for counteracting oncogene-driven apoptotic propensities (Chien and White, 2003). A RalB/exocyst/TBK1 pathway has been identified as a mediator of the anti-apoptotic activity of RalB in cancer cells. TBK1 (atypical IkappaB kinase family member) is a non-conventional activator of the NFkB pathway. RalB promotes Sec5/TBK1 assembly, which activates TBK1. This activation inhibits the initiation of apoptotic programs (Chien et al., 2006).

RalB/Sec5/JNK pathway

Various reports are supporting anti-apoptotic roles of Ral proteins through the regulation of the JNK pathway. Activation of the JNK pathway might have a pro-apoptotic or an anti-apoptotic role depending on cell type and stimulus (Lin and Dibling, 2002).

In *Drosophila* sensory organs, it was shown that Ral behaves as a negative regulator of JNK pathway, and that the exocyst complex is required for the execution of Ral apoptotic function. Notably, the Ral-JNK signaling is conserved in mammalian cells. In fact, to determine which signaling pathways are implicated in Ral-dependent apoptotic phenotype, genetic analysis was performed in our team. *Drosophyla* strains with reduced Ral

activity were crossed with straines defective in various apoptotic pathways, and the resulting apoptotic phenotypes was used as functional read out. More specifically, both loss-of-function mutations (as well as the expression of the dominant negative form) or the ectopic expression of different members of the apoptotic pathways were used to either interefere or to activate these pathways.

This Genetic interactions analysis demonstrated that: (i) Ral regulates apoptotic programs acting as an upstream negative regulator of JNK activity and a positive activator of p38 MAP kinase; (ii) the main effector of Ral, the exocyst complex, is required for the execution of Ral function in apoptosis; (iii) a cascade connecting Ral through the exocyst to HGK/MSN (Ste20 kinase in mammals and in Drosophila respectevely) was identified as the molecular basis of Ral action on JNK; (iv) Ral-dependent restriction of JNK activation and the exocyst/HGK relationship are conserved in mammalian cells (Balakireva et al., 2006).

In A14 cells (mouse fibroblasts expressing human insulin receptors), expression of an activated version of Rgl2 (with a CAAX motif at C-terminal) induced phosphorylation of c-Jun. This phosphorylation is abolished by the expression of a dominant-negative mutant of Ral GTPases (de Ruiter et al., 2000). In a mouse model of skin carcinogenesis, RalGDS was necessary for Ras induced transformation by providing a survival signal to tumor cells. In this model, JNK activation by RalGDS was shown to be responsible for the increased survival (González-García et al., 2005).

1.4.3. Cytokinesis

Cytokinesis is the last step of cell division that leads to the physical separation of the daughter cells. Abscission of the intracellular bridge is the last step of this process.

In our laboratory, we showed that RalA and RalB have distinct roles in two different steps of cytokinesis. RalA is localized at the cleavage furrow and is necessary for the stabilization and elongation of the intracellular bridge. RalB is localized in the intracellular bridge and is necessary for abscission. Depletion of RalA or RalB leads to different failures of cytokinesis. Depletion of RalA induces accumulation of bi-nucleate cells and depletion RalB induces accumulation of bridged cells (Cascone et al., 2008). The functions of RalA and RalB in cytokinesis are mediated by their exocyst effector (see Chapter 2.3).

1.4.4. Autophagy

Autophagy is a highly conserved homeostatic pathway by which cells degrade damaged proteins and organelles. Portions of cytoplasm are sequestered within double-membrane cytosolic vesicles (autophagosome) and degraded upon fusion with lysosomes. Autophagy might be induced in response to nutrient starvations and is essential for cell survival in these conditions.

It has been shown that RalA functions as an indispensable signal mediator for the nutrient-sensing system, by positively regulating the mTorc1 complex, which is an inhibitor of autophagy (Maehama et al., 2008).

More recently, it has been shown that RalB, but not RalA, and Exo84 are necessary for autophagosome formation and that constitutively active RalB (RalB-G23V) is sufficient to activate autophagy in human epithelial cells (Bodemann et al., 2011). These results suggest that RalB-Exo84 effector complex is a key regulator of the cellular response to nutrient deprivation.

1.5. RAL IMPLICATION IN CANCER

The interest in studying the role of Ral proteins in oncogenesis started from the discovery that their specific exchange factors are effectors of Ras oncoproteins.

This chapter describes different observations that put Ral pathway as a major actor in the transmission of oncogenic signals and in the control of metastases formation in human cancer.

1.5.1. Ral in oncogenic transformation

Ral itself is not an oncogene, but an actor of oncogenic transformation. The historical foci-assay approach with murine NHI3T3 cells brought to light the capability of Rals to contribute to Ras oncogenic transformation.

After Raf, RalGDS was identified as a second Ras binding protein that can induce oncogenic transformation. More specifically, RalGDS was shown to cooperate synergistically with mutationally activated Raf to induce foci of growth and morphologically transformed NIH 3T3 cells. Moreover, inhibition of RalGEFs activity by expression of dominant negative mutant of Ral blocks Ras dependent transformation of the fibroblastic cell line NIH3T3 (White et al., 1996). Constitutively activated Ral alone cannot induce oncogenic transformation, but it enhances the transforming activities of both Ras and Raf. Moreover, the expression of dominant negative RalA suppressed the transforming activities of these two oncogenes (Urano et al., 1996).

Few years ago, thanks to the development of human cancerogenesis models (Hahn et al., 1999), important dissimilarities between human and mouse transformation processes were shown, suggesting that the underlying mechanisms are not identical (Hamad et al., 2002; Rangarajan et al., 2004). Many studies in murine models had supported a model in which Raf serine/threonin kinase (c-Raf1, A-Raf et B-Raf) are

the major actors of the transmission of oncogenic properties of Ras proteins. On the contrary, in human cells, RalGEF, and not the Raf or PI3-kinase pathway, is sufficient to mediate Ras transformation (Hamad et al., 2002).

In several human cell lines (fibroblasts, astrocytes and embryonic kidney cells (HEK)), oncogenic capacities of Ras seem to be recapitulated by Ral activation through: expression of ectopic mutant Ras (Ras mutant that activates specifically Ral pathway) or by the constitutive activation of Rlf (Rlf-CAAX), the exchange factor of Ral (Hamad et al., 2002).

Cell type specific differences about pathways required in transformation were discovered (Rangarajan et al., 2004). Immortalized human fibroblasts need activation of Raf and RalGEFs, immortalized human embryonic kidney cells (HEK-HT) need activation of PI3K and RalGEFs, and epithelial mammary cells need activation of the three pathways. In this work, the important result regarding Ral is that RalGEF/Ral pathway is always required (figure I4).
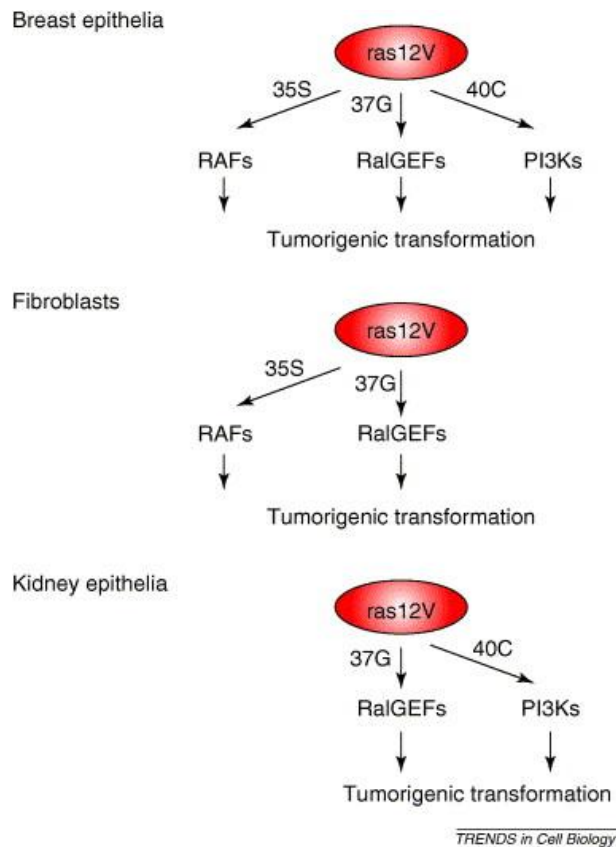
Figure I4: Pivotal contribution of Ral activation to oncogenic Ras-induced tumorigenicity. A variety of primary human cell types isolated from normal tissue can acquire tumorigenic phenotypes upon forced expression of telomerase together with SV40 large and small T-antigen and oncogenic Ras (ras12V). Substitution of ras12V with effector mutations that discriminate between three families of Ras targets – Raf (ras12V,35S), RalGDS (ras12V,37G) and phosphoinositide 3-kinase (PI3K) (ras12V,40C) – reveals selective requirements for activation of these pathways to drive tumorigenic transformation of breast epithelia, fibroblasts and kidney epithelia. While these three cell types display dissimilar sensitivity to Ras-induced activation of Raf family and PI3K family proteins (as indicated by the arrows), activation of Ral GTPases is apparently a common prerequisite to development of tumors in nude mice (Camonis et al. 2005).

Downstream Ral, a role for exocyst subunits Sec5 and Exo84 has been reported in RalGEF-mediated transformation of HEK-HT cells, in oncogenic Ras-mediated tumorigenesis of human cells and in the proliferation of Ras-transformed human cells, suggesting that Rals promote oncogenic Ras-mediated tumorigenesis through, at least in part, its exocyst effector (Issaq et al., 2010).

Activation of RalA seems to be a critical step in tumorigenesis of human cells. RalA is activated in a large panel of cell lines derived from human pancreatic tumors. About 90% of pancreatic cancer has Ras mutation. Chronic depletion of RalA in these cell lines inhibits the ability of cells to form tumors after subcutaneous injection in nude mice (Lim et al., 2006).

Additional evidence about implication of Ral in oncogenesis comes from the discovery made by Sablina (Sablina et al., 2007) that RalA is a target of phosphatase 2A (PP2A). Biallelic mutations of the subunit Ab of PP2A are frequently found in many human tumors. RalA is phosphorylated on serine 183 and 194, potentially by Aurora A kinase. These phosphorylation sites are PP2A substrates, and are associated to a 5 times increase of active RalA pool. Disphosphorylation of RalA by PP2A is a major mechanism of cell proliferation restriction by PP2A. These results suggest that PP2A subunit Ab acts as tumor suppressor by regulating RalA function.

1.5.2. Ral controls the proliferation/survival balance of human cancer cells

Discrete interlocking contribution of Ral GTPases to proliferation and survival of cancer cells was described in cell lines derived from human tumors using loss of function analysis (Chien and White, 2003). In this work, RalB was found to be essential for

the survival of variety of tumor cells, but not of normal epithelial cell lines. On the other side RalA was not essential for the survival or proliferation of adherent culture cells, but it was required for proliferation of anchorage-independent cancer cells.

A functional interaction between RalA and RalB is supported by the observation that depletion of RalA inhibits the sensitivity of tumor cells to RalB depletion (Camonis and White, 2005). In other words, cancer cells need RalB expression and cannot survive without it, pointing to the notion that RalB renders cancer cell addicted. RalA depletion abrogated cancer cell addition to RalB, suggesting RalA and RalB activities must be in equilibrium in cancer cells.

The fact that RalA or RalB depletion causes diverse phenotype in normal and cancer cells indicates that the two Rals may collaborate in the maintenance of oncogenic transformation by controlling survival and proliferation signals. Proliferative pressure dependent on RalA should be counterbalanced by inhibition of apoptosis dependent on RalB (Figure I5). The mechanistic basis of this divergence of RalA and RalB functions remains still to be clarified. One likely possibility rests in a different cell compartmentalization of the two Ral proteins. Alternatively, RalA and RalB may have different affinities for their effectors, due to the small difference in aminoacids around the effector domain.

TRENDS in Cell Biology
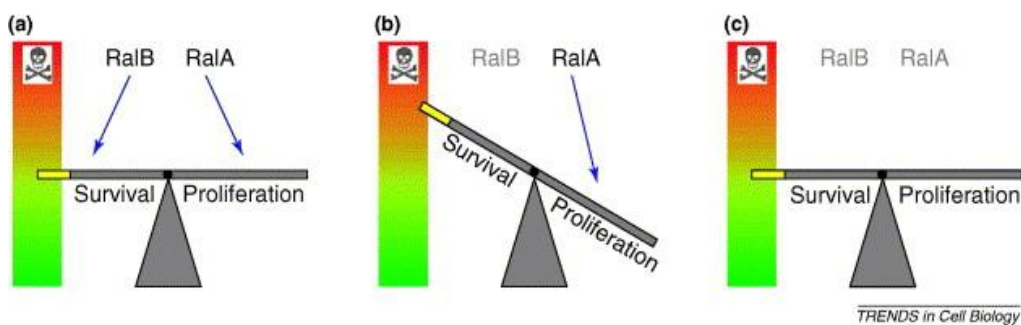
Figure I5: The RalA–RalB balancing act in tumor cells.
Under conditions of oncogene-induced stress, the increased
apoptotic propensity driven by RalA is offset by RalB-dependent
survival signals (a). Inhibition of RalB function under these
conditions therefore leads to apoptosis (b). Reducing
proliferative pressure by inhibition of RalA restores balance to
the system, relieving dependency on RalB survival signals (c).
This relationship, suggests that RalB-dependent survival
pathways represent conceptually ideal targets for anticancer
drugs with high tumor-cell-specific potency (Camonis and White,
2005).

1.5.3. Ral in metastasis formation

Cancer cells spread by infiltrating adjacent tissues (invasion) and subsequently traveling to distant organs through the blood or lymph vessels (metastasis). Metastatic progression is a multistep process. Tumor cells, particularly those of epithelial origin, frequently loose in their initial stages cadherin-based cell–cell adhesion, become able to degrade the basement membrane and acquire a motile phenotype. Remodeling of the actin cytoskeleton plays a crucial role in all these steps.

Several works supported the notion that RalGEF-Ral signaling is implicated in tumor invasion.

For example, 3T3 cells transformed by mutant Ras[V12G37,] a Ras effector mutant that activates RalGEF but not Raf or PI3 kinase, form aggressive metastasis, indicating that the signaling pathway mediated by RalGEFs facilitates, in combination with ERK pathways, the acquisition of an invasive phenotype (Ward et al., 2001). Consistently, RalB dominant negative inhibits metastatic activity of Ras[V12G37].

In in *vivo* experimental metastasis assay, using chinese hamster cells (Tchevkina et al., 2005), Ha-Ras was shown to stimulate mestatasis formation via Ras-RalGDS-RalA pathway.

RalA alone is able to increase the mestatatic activity of fibroblasts spontaneously transformed or transformed by Rous sarcoma virus. Moreover, during *in vivo* selection, cells acquire a high metastatic potential after activation of endogenous RalA.

Chronic RalA depletion inhibits the formation of bone mestastasis by human prostate cancer (DU145 cells). Consistently, activation of Ral pathway is necessary and sufficient for bone mestastasis formation by DU145 cells. The requirement of Ral A for bone metastasis is probably cell specific: in fact, RalA depletion or RalB depletion in mammary cancer cells (MDA-MB-231), or in colorectal cancer cells (HT29), does not inhibit bone metastasis formation (Yin et al., 2007)

1.5.4. Mutations and abnormal expression of Ral pathway components are found in human cancers

The previous paragraphs summarized the accumulating evidence that the Ral pathway is implicated in oncogenesis using in vitro cell lines or mouse in vivo models. This notion was corroborated and strengthened by the discovery of mutations of the components of the Ral pathway in human tumors. For example, mutations of Rgl1 and exocyst subunit Sec6 were reported in breast cancer. Similarly, RalGDS and exocyst subunit Sec8 where found in colon cancer (Sjoblom et al., 2006). Notably, missense RalA mutation was found to occur in one of a panel of bladder carcinoma cell line (UM-UC-6 cell line).

Deregulation of Ral pathway components was reported at expression level. RalA was discovered to be overexpressed in metastatic prostate cancer (Varambally et al., 2005). RalA mRNA was found also significantly overexpressed in human bladder cancer. Moreover, RalA overexpression is further associated with invasion. RalB was shown to be reduced in hepatocellular carcinoma, seminoma, ovarian carcinoma, and meningioma (Smith

et al., 2007). It was also shown that RLIP is overexpressed in lung and ovary cancer (Awasthi et al., 2008).

The discovery that Ral regulators and effectors are deregulated in human cancer reinforce to the notion that Ral maybe a major axis of oncogenic signaling downstream of Ras.

2. EXOCYST

2.1. DISCOVERY

Exocyst is an eight subunit complex: EXOC1/Sec3, EXOC2/Sec5, EXOC3/Sec6, EXOC4/Sec8, EXOC5/Sec10, EXOC6/Sec15, EXOC7/Exo70 and EXOC8/Exo84 (human/yeast nomenclature). Mutations of these subunits were identified in yeast in a screening for secretion mutants (Novick et al., 1980). Analysis of this complex, in particular in yeast, consolidates its role in polarized secretion (TerBush and Novick, 1995): In yeast, exocyst contributes to post-Golgian vesicle targetting to the plasmamembrane via an interaction with Rab GTPase Sec4p (Guo et al., 1999). This complex is highly conserved in yeast, *Drosophila* and human (Hsu et al., 1996).

Even though the exocyst complex mediates many of the Ral cellular functions and it is considered the major RalA/B effector, the functional relevance of the Ral binding to Exocyst is still not fully understood. A tentative working model has been proposed in which Sec5 and Exo84 belong to two different sub-complexes of exocyst and Ral proteins assemble the complex by interacting with both (Camonis and White, 2005) (Figure I3).

Crystallography of exocyst subunits, Sec3 (Baek et al., 2010; Yamashita et al., 2010), Sec5 (Fukai et al., 2003), Sec6 (Sivaram et al., 2006), Sec15 (Wu et al., 2005), Exo84 (Jin et al.,2005; Dong et al., 2005) and Exo70 (Dong et al., 2005; Hamburger et al., 2006;

Moore et al., 2007). In spite of low sequence homology (less than 10%) between esocyst subunits Sec6, Sec15 and Exo84 and Exo70, crystallography shows that they share the same novel fold, made of compact helical-bundle repeats connected by flexible linkers (Croteau et al., 2009).
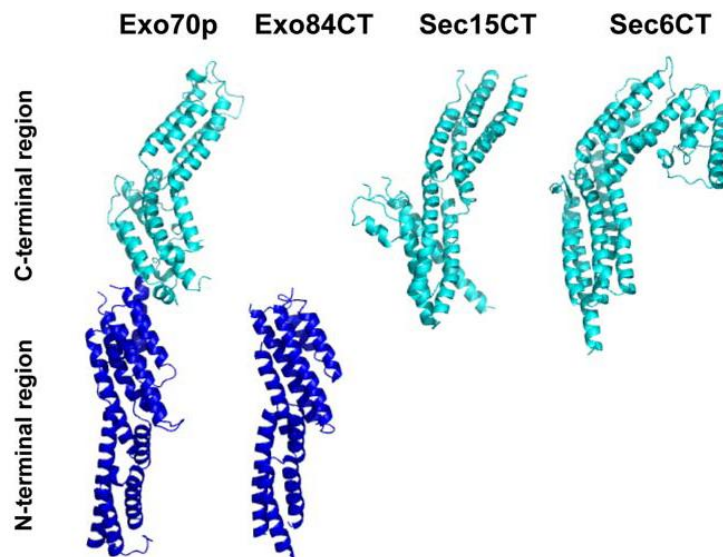
Figure I5A: The exocyst subunits share the same helical bundle structures. *The known structures of the exocyst subunits are shown: Exo70, Exo84, Sec15 and Sec6.*

2.2. BIOLOGICAL FUNCTIONS

The exocyst complex has been shown to be required for several biological processes involving membrane plasticity.

2.2.1. Vesicle trafficking

The role of exocyst in exocytosis was historically studied in yeast. During exocytosis vesicles are formed from a donor compartment, translocated to the plasmamembrane, where tethering, docking and fusion take place. This phenomenon requires SNARE (SNAP Receptor) proteins. Pairing of SNARE on vesicle (v-SNAREs) with target membrane SNAREs (t-SNAREs) is

crucial (Brown and Pfeffer, 2010). Exocyst was found to be highly concentrated at regions were vesicle fusion was very active; it was proposed that the exocyst directs vesicles or restricts their fusion (TerBush and Novick, 1995). Moreover, always in yeast, the exocyst complex was implicated in the delivery of post-Golgi vesicles to the plasma membrane (Terbush et al. 1996). In epithelial cell line MDCK, exocyst is required to specify the delivery of vesicles containing membrane proteins to sites of cell-cell contact (Grindstaff et al., 1998; Lipschutz et al., 2000).

The exocyst collaborates with SNARE in vesicle tethering. It was shown that the subunit Sec6 of the exocyst binds to t-SNARE at the plasma membrane (Sivaram et al. 2005). The exocyst keeps the vesicle bound to the plasmamembrane until the SNARE-dependent fusion machinery acts (Munson M, Novick P. 2006). It was proposed that the exocyst as a dynamic complex (Terbush et al. 1996) can have many binding partners, and integrate a large number of signals helping in determining the proper conditions to facilitate SNARE pairing (Brown and Pfeffer, 2010).

2.2.2. Polarization of epithelial cells

Exocyst is an important regulator of epithelial polarity in Drosophila Melanogaster, but the mechanisms of its action is still partially known. A model was proposed (Langevin et al., 2005), whereby the physical interaction between Armadillo/beta-catenin and Sec10 allows the exocyst to regulate Drosophila Epithelial Cadherin (DE-cadherin) trafficking. New pieces of evidence show that epithelial polarity in the *Drosophila* embryo requires the exocyst complex subunit homolog Exo84. Exo84 regulates Crumbs localization, a key determinant of epithelial apical identity (Blankenship et al., 2007).

After establishment of E-cadherin-dependent cell-cell contacts, Sec6 and Sec8 subunits are recruited to the lateral

membrane (Grindstaff et al., 1998; Yeaman et al., 2004). So, it was proposed that the exocyst promotes the formation of basolateral domain of epithelial cells by directing Golgi-derived vesicles to cell-cell contact sites.

It remains not clear whether the exocyst contribution to epithelial polarity is, at least in part, due to its role in polarized secretion, by mediating exocytosis from Golgi or by regulating endosome recycling.

2.2.3. Neuronal development

Exocyst components, because of their function in polarized secretion, have been involved in different aspects of neuronal development, which consists in a succession of events ending with synapse formation.

For examples, the exocyst was shown to be implicated in synaptogenesis: it specifies sites for targeting vesicles at domains of neurite outgrowth and potential active zones (Hazuka et al., 1999). During Drosophila development, photoreceptor cells (PRCs) with reduced Sec6 show transport failure and accumulation of secretory vesicles (Beronja et al., 2005). Sec5 and Sec6 subunits play an important role in neurite growth, synaptic transmission and oocyte polarization (Murthy et al., 2003, Murthy et al., 2005; Murthy and Schwarz, 2004).

Ral GTPases are mediators of neurite branching. The two Ral proteins, RalA and RalB, promote branching through distinct pathways, involving the exocyst complex and phospholipase D, respectively (Lalli and Hall, 2005). Neuron cells depleted of the exocyst subunits Sec6, Sec8 or Exo84, lost their polarity; consistently, the exocyst was found to interact locally with the PAR polarity complex. Moreover, at early stages of neuronal polarization, RalA local activation regulates spatially the exocyst and favours exocyst assembly in nascent axon (Lalli, 2009).

2.2.4. Cell migration

It is hard to dissociate between exocyst function in exocytosis and exocyst function in cell migration. A series of very convincing observations supporting this concept were obtained thanks to live TIRF microscopy: exocytic vesicles were preferentially distributed close to the leading edge of motile astrocytes cells, the exocytic process was found to be organized into hotspots, and the polarized delivery of vesicles and their clustering in hotspots was dependent on the intact exocyst complex. Clearly, the exocyst plays a role in vesicle delivering to the leading edge and in determining the tethering sites during polarized cell motility (Letinic et al, 2009).

In our group, it was shown that depletion of various exocyst subunits impairs the motility of NRK cells by using both wound-healing and Boyden chamber motility assays. The exocyst requires RalB to localize at the leading edge and to fully assemble (Rossé et al. 2006).

2.2.5. Cytokinesis

The role of the exocyst complex in cytokinesis was first identified in Yeast. It was shown that the exocyst complex is required for the formation of the cleavage site and cell separation (Wang et al., 2002; Dobbelaere and Barral, 2004). Ingression of the cleavage furrow requires addition of new membrane by vesicle transport and fusion, and the loss of exocyst abolishes the completion of furrow ingression (VerPlank and Li, 2005). In mammalian cells, it was shown that the exocyst is localized at the intracellular bridge and its disruption inhibits abscission (Gromley et al., 2005).

3. WAVE REGULATORY COMPLEX (WRC)

Cell motility depends on the assembly of actin filaments at their leading edge to generate force that pushes the plasma membrane and propels cells forward. This process is tightly regulated in space and time so that the assembly of a branched network of actin filaments is restricted beneath the advancing plasmamembrane. As these filaments grow, they push the membrane forward.

3.1. NUCLEATING ACTIN

Cells use two major mechanisms to nucleate new actin filaments: a mechanism is mediated by the Arp2/3 complex and another one is mediated by Formins. Arp2/3 and Formins act in different ways.

Arp2/3 complex produces branched actin filament starting on a preexisting actin network. The free end of the new filament elongates until a capping protein terminates growth. The branched network that is generated as consequence of Arp2/3 activation is capable of generating protrusive forces that propels lamellipodia protrusion, adhesion, phagocytosis, endocytosis, vesicle and organelle motility trafficking within and from Golgi apparatus and exocytosis (Goley and Welch, 2006).

Formins produce unbranched filaments for actin bundles found in filopodia and the cytokinetic contractile ring (Wallar and Alberts, 2003). Formin remains associated with the growing end of the filament, providing an anchor and protection against capping.

3.2. THE Arp2/3 COMPLEX

The Arp2/3 complex is a stable assembly of seven proteins: Arp2, Arp3, and the subunits p40/ARPC1, p34/ARPC2, p21/ARPC3, p20/ARPC4 and p16/ARPC5 (Machesky et al., 1994;

Mullins et al., 1998) (Figure I6). Arp2 and Arp3 belong to the family of actin-related proteins (Arps) and are predicted to share the same protein fold as actin, although the amino acid sequence is divergent from that of conventional actins (Kelleher et al., 1995).

Two models have been proposed to explain how the activated Arp2/3 complex interacts with a filament to initiate branching: the first one favours the possibility that the Arp2/3 complex branches by binding to the side of pre-existing filaments (Amann and Pollard, 2001; Higgs and Pollard, 1999); the second, instead, proposes that branching can occur only at the barbed ends of growing filaments (Boujemaa-Paterski et al., 2001; Pantaloni et al., 2000; Pantaloni et al., 2001). Whatever the case, a consensus has been reached that the Arp2/3 complex generates a branched array of actin filaments.

At the side of a pre-existing filament (mother filament), the Arp2/3 complex can nucleate a new filament (daughter filaments) at an angle of 70°, thus generating y-branched actin network (Machesky et al., 1994; Mullins et al., 1998) (Figure I6). This property accounts for the central role of the Arp2/3 complex in the formation of highly branched actin filament structures at the leading edge of lamellipodia in motile eukaryotic cells (Svitkina and Borisy, 1999).
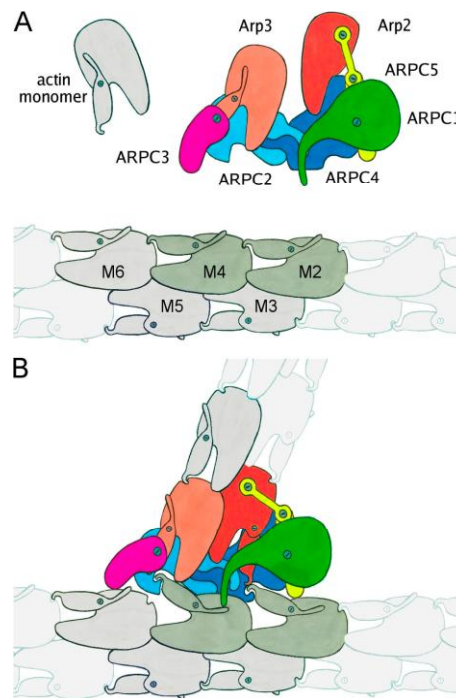
Figure I6: Schematic representations of the precursors and assembled components of the branch junction. (A) Inactive Arp2/3 complex and a standard actin filament. (B) Model of the branch junction (Rouiller et al. 2008).

Actin remodelling in the lamellipodium is also coupled to the formation of adhesive contacts that link the actin cytoskeleton to the extracellular matrix. Emerging evidences indicate that the Arp2/3 complex might be recruited to sites of nascent focal contacts through a direct interaction with the linker region of vinculin, a protein associated to the cytosolic domain of integrin receptor (DeMali et al., 2002). Similarly, direct linkages between the actin polymerization machinery and adhesion molecules have also been reported in the context of cell-cell adhesion. Recently, it has been observed that E-cadherin interacts with the Arp2/3 complex to promote local actin assembly and lamellipodial protrusion during the formation of early cell–cell adhesive contacts

(Kovacs et al., 2002). Alpha-Catenin can compete for actin filaments, and thus it can abolish the activity of Arp2/3. This suggests the following model: at adherent junctions, beta-catenin form clusters and recruits alpha-catenin that can inhibit the Arp2/3 complex, and so inhibits lamellipodia formation, in order to form stable contact point (Pokutta et al., 2008).

Very interestingly, the Arp2/3 compelx interacts with the exocyst complex, in particular with the Exo70 subunit. Exo70 was shown to regulate actin polymerization at the leading edges of migrating cells, via direct control of Arp2/3 activation (Zuo et al., 2006).

Notably, the Arp2/3 complex is autoinhibited. In order to be activated it requires the engagament with Nucleation Promoting Factor (NPF) proteins. Members of the WASP (Wiskott-Aldrich Syndrome Protein) and WAVE (WASP family Verprolin-homologous) families of proteins are the major NPFs proteins for the Arp2/3 complex. The NPF binds directly the Arp2/3 and delivers an actin monomer that forms with Arp2/3 a starting nucleus for new filament (Figure I6).

Structural basis of actin branching is now highly debated because of the dendritic nucleation model challenging.

Electron tomography revealed the three dimensional organization of lamellipodia and showed that in lamellipodia from four cell types, actin filaments are almost exclusively unbranched. Majority of apparent filament junctions proved to be overlapping filaments, rather than branched end-to-side junctions (Urban et al. 2010, Small, 2010). However, there are several important shared points about Arp2/3 and WRC. Arp2/3 is a major actin nucleation factor at the leading edge, it is highly enriched at the leading edge and is an effector of WRC, which localizes at the leading edge (Higgs, 2011). Two electron electron microscopy

techniques probably counterbalance their potential artefacts about existence of branched actin filaments in lamellipodia (Yang et al. 2011). The size on the studied region, their density and the length of the observed filaments make orbservable branches rare (Insall, 2011) (Figure I7A).
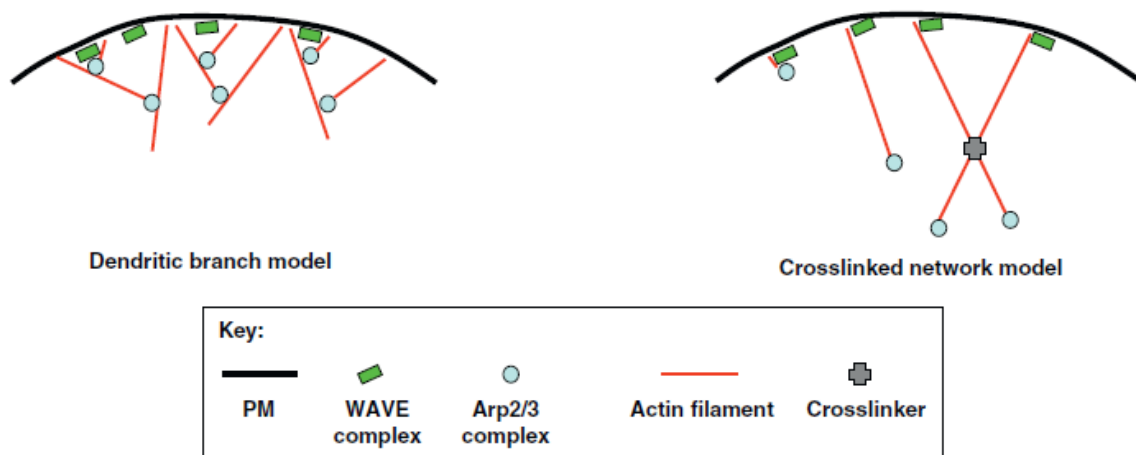
Figure I7A: Two models of leading edge actin network architecture. Left: dendritic branch model. WRC activates Arp2/3 complex. Arp2/3 complex is also activated by binding to the side of an actin filament close to the plasmamembrane. This coactivation by WRC and filament side binding results in branch formation, with Arp2/3 complex forming the link between the pointed end of the new filament and the side of the activating filament. *Right: crosslinked network model.* WRC activates Arp2/3 complex but it does not bind to the side of an existing filament, so that branches do not assemble (Higgs, 2011).

3.3. WASP AND WRC ACTIVATE Arp2/3

A large family of NPFs were identified through the presence of a characteristic C-terminal VCA domain (Verprolin homology, Cofilin homology, and Acidic region). This family is subdivided into four NPF subfamilies based on their N-terminal domains: WASP, WAVE and more recently WASH, WHAMM (Linardopoulou et al.,

2007; Campellone et al., 2008; Zuchero et al., 2009) and JMY (Rottner et al., 2010). The WASP (Wiskott-Aldrich Syndrome Protein) and WAVE (WASP family Verprolin-homologous) are the most studied, they activate Arp2/3 complex in responses to signaling events downstream of the Rho-family GTPases Cdc42 and Rac.

WASP protein was identified as the causative gene of Wiskott-Aldrich Syndrome, a rare, X-linked disease characterized by immunodeficiency, thrombocytopenia and eczema (Derry et al., 1994). Expression of WASP is restricted to hematopoietic cells, hence the restricted defects in the syndrome. The other member of WASP group in mammals, neural WASP (N-WASP), originally identified in brain tissues, is more widely expressed than WASP (Miki et al., 1996).

WAVE1 protein was isolated in a database search for WASP-like proteins (Machesky et al., 1998) and subsequently two other members of WAVE family, WAVE2 and WAVE3, have been identified (Suetsugu et al., 1999). In mammals, WAVE2 is ubiquitously expressed while WAVE1 and WAVE3 are particularly enriched in brain.

The VCA region is the minimal essential region for the activation of the Arp2/3 complex by WASP and WAVE proteins (Machesky et al., 1999; Rohatgi et al., 1999; Yarar et al., 1999). Within the VCA domain, the V region binds G-actin monomers (Miki et al., 1998a), the A region directly binds the Arp2/3 complex (Machesky and Insall, 1998) and the C region drives the conformational changes in the Arp2/3 complex necessary for its activation (Panchal et al., 2003). Branch formation requires the cooperation of VCA, Arp2/3 complex, the first actin monomer, and the mother filament. Concomitant binding of the VCA region to the Arp2/3 complex and actin monomer leads to the formation of a complex that serves as protonucleus for the further addition of

monomer, thus promoting filament elongation (Pollard and Borisy, 2003; Takenawa and Miki, 2001).

The N-terminal parts of WASP and WAVE proteins are significantly divergent. WASP proteins display a common modular organization, which includes a WASP-homology1 domain (WH1), also called Ena/VASP homology 1 (EVH1) domain, a basic region (B) and a GBD (GTPase Binding Domain) domain, positioned next to a proline-rich region (Figure I7). WH1/EVH1 domain of WASP and N-WASP tightly binds to a specific proline-reach sequence of the WASP-interacting protein (WIP) (Volkman et al., 2002), a member of a family of regulators of WASP-mediated actin polymerization (Ramesh et al., 1997) that includes WIP- and CR16-homologousprotein (WICH) and CR16 (Kato et al., 2002; Zettl and Way, 2002). The GBD and B regions associates with GTP-loaded Cdc42 and PtdIns(4,5)P2, respectively, while a plethora of Src-homology (SH)3-containing proteins (Rohatgi et al., 2000; Takenawa and Miki, 2001) associate with the polyproline motifs in the proline-rich region. Moreover, the B and the proline-rich regions have also been implicated in F-actin (Suetsugu et al., 2001) and profilin (Suetsugu et al., 1998; Yang et al., 2000; Yarar et al., 2002) binding, respectively.

The N-terminal region of WAVE proteins contains a WAVE (also known SCAR)-homology domain (WHD/SHD) and a basic region. The basic region is responsible for the binding with PtdIns (3,4,5)P3 that is important for WAVE2 localization (Oikawa et al., 2004). In contrast to WASP and N-WASP, WAVE proteins do not contain GBD motifs, lacking in this way of a surface directly associating Rho GTPases. Alternatively, WAVEs contain a proline-rich region that mediates the association with insulin receptor substrate IRSp53, which has been implicated in physically linking WAVE2 and Rac (Miki et al., 2000) (Figure I7).
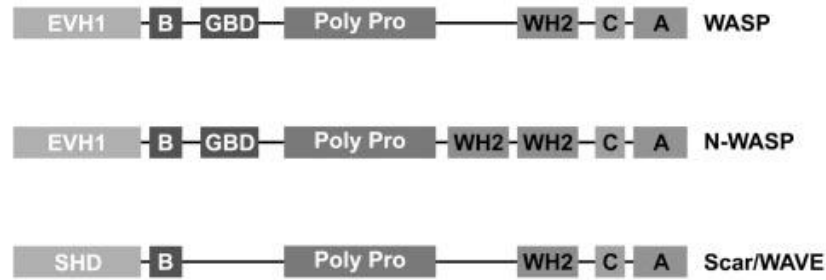
Figure I7: Domain organization of WASP/Scar proteins. *EVH1, Ena/Vasp homology 1 domain; B, basic region; GBD, GTPase-binding domain; Poly Pro, proline-rich region; SHD, Scar homology domain; WH2, verprolin-like or WASP homology 2 domain; C, central or connecting domain; A, acidic domain (Kelly et al. 2006).*

3.4. THE WAVE REGULATORY COMPLEX (WRC)

The WHD/SHD domain of all three WAVE proteins contributes to the formation of a multimeric-complex, first identified for WAVE1 (Eden et al., 2002) and later also for WAVE2 (Innocenti et al., 2004) and WAVE3 (Stovold et al., 2005). This pentameric heterocomplex consists of WAVE, Abi (Abelson-interacting protein), Nap1 (Nck-associated protein 1), Cyfip (p140/Pir121/Sra1) and Brick (HSPC300) proteins (Eden et al., 2002; Gautreau et al., 2004; Innocenti et al., 2004). Nterminus of Cyfip was shown to interact specifically with Rac-GTP, which is a major activator of WRC (Kobayashi et al., 1998).

We now know that RhoGTPase Rac1 stimulates actin branching at lamellipodia by relaying signals to WRC that activates Arp2/3-mediated actin polymerization. Historically, it was the Takenawa group that proposed the critical role of Wave downstream of Rac in actin cytoskeleton remodeling required for membrane ruffling. Dominant-active Rac mutant induces the translocation of endogenous WAVE to membrane ruffling regions (Miki et al., 1998a).

The WHD domain of WAVEs interacts with Abi1/2 and Brick members of the complex (Gautreau et al., 2004). Cyfip and Nap1 interact with WAVE2 and Abi1. Consistently, various WRC subunits was shown to translocate to the protrusion tips after microinjection of constitutively active Rac (Steffen et al., 2004). A series a co-precipitation and gel filtration experiments pointed out the fact that the five subunits of WRC are constitutively and strongly associated. The integrity of the complex is essential for the stability of all its members and for the proper localization of the complex.

The WRC complex composition is conserved, as well as its integrity and its function. For example, in adherent Drosophila cell line, Abi, Cyfip and Kette (Nap1) protect Scar (Wave) from proteasome-mediated degradation and are critical for Scar localization and for the generation of Arp2/3-dependent protrusions (Kunda et al., 2003).

WRC expressed by HeLa cells is composed of Wave2, Abi, Cyfip, Nap1, and Brick. In other cell lines or tissues, WRC may be composed of homologous subunits (WAVE1, WAVE2, WAVE3; Abi1, Abi2) encoded by paralogous genes or by isoforms derived from alternative splicing (for example Abi1 has 10 isoforms) (Gautreau et al., 2004; Innocenti et al., 2004).

3.5. WRC ACTIVATION MECHANISM

While the mechanism of activation of WASP proteins has been largely clarified, the mode through which WAVE proteins are regulated was highly debated and many questions still remain unanswered. However, in both cases, activation occurs via un-masking of the VCA motif which is sequestered by intra-molecular or intra-complex interactions in the basal inactive state.

3.5.1. The case of Wasp

Isolated, full length WASP and N-WASP are autoinhibited due to conformational constrains. The VCA region is masked through the binding of the GBD domain to the C region. This conformation prevents the association of WASP with the Arp2/3 complex (Miki et al., 1998b). The release of autoinhibition and activation of WASP proteins is promoted by proteins or molecules that interact with the N-terminal region of WASP / N-WASP and cause a conformational changes leading to the exposure of the VCA domain (Figure I8). Activated Cdc42 can, for instance, bind to the GBD domain, while phosphatidylinositol-4,5-diphosphate (PIP2) binds a small region of basic residues (B region) close to the GBD domain. Binding of Cdc42 to WASP/N-WASP, is sufficient to activate the protein. Addition of PIP2 increases this activity, in a synergic way. WIP is a protein family (WIP, CR16, and WICH) that bind directly to WASP or N-WASP and cooperate with WASP/N-WASP to form filopodia in fibroblasts (Vetterkind et al., 2002). Additional modulatory roles are also exerted by a plethora of SH3-containing proteins that bind to the proline rich region of WASP/N-WASP and stimulate these NPFs, often acting in a cooperative manner with Cdc42 and PIP2 (Kim et al., 2000; Rohatgi et al., 2000; Takenawa and Miki, 2001). These latter features support to the notion that WASP/N-WASP are the "convergent nodes or coincident detectors" of different signalling inputs leading to de novo actin polymerization.
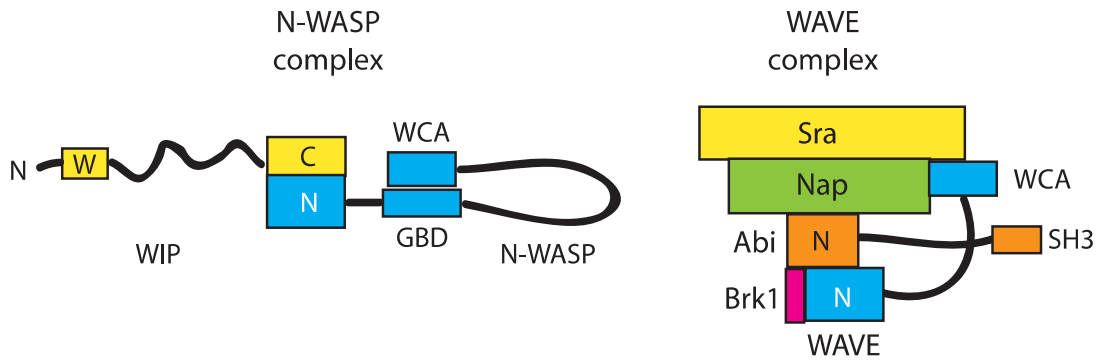
Figure I8: Architecture of N-WASP and WRC at resting state. *The N-WASP complex is dimeric. The WCA domain is intramolecularly masked in N-WASP, but WIP is required for a tightly inhibited state. WIP provides an additional WH2 domain indicated by 'W'. The WAVE complex is pentameric. This complex is also inhibited, but the WCA domain of WAVE is masked by an intermolecular interaction within the complex, most likely with Sra and/or Nap. The linker regions between N-terminal domains and WCA domains of N-WASP and WAVE are rich in prolines, and thus display binding sites for numerous proteins containing SH3 domains. The Abi subunit of the WAVE complex also contains an SH3 domain that has been reported to bind to several proteins. It is not known, however, whether this SH3 domain is free to interact at resting state or masked by an interaction with proline-rich linker regions of WAVE or Abi (Derivery and Gautreau, 2010).*

3.5.2. Multiple signal activation model of WRC

Several events have been proposed to stimulate somehow WRC activity (Rac binding, PIP3 interaction, phosphorylations). However none of these events alone is sufficient for a substantial stimulation of Arp2/3-dependent in vitro actin polymerization. Indeed, it was recently shown that activation of the WRC complex requires simultaneous interactions with prenylated (membrane targeted) Rac-GTP and acidic phospholipids (including PIP3), together with a specific state of phosphorylation. Together these signals promote full activation in a highly cooperative process on the membrane surface, by inducing an allosteric change in the

complex rather than by simple recruitment or by dissociation of the subunits. (Lebensohn and Kirschner, 2009) (Figure I9). Thus, WRC, similarly to WASP, acts as coincident detectors of multiple and converging signaling pathways that controls not only its activity, but also its spatial localization.
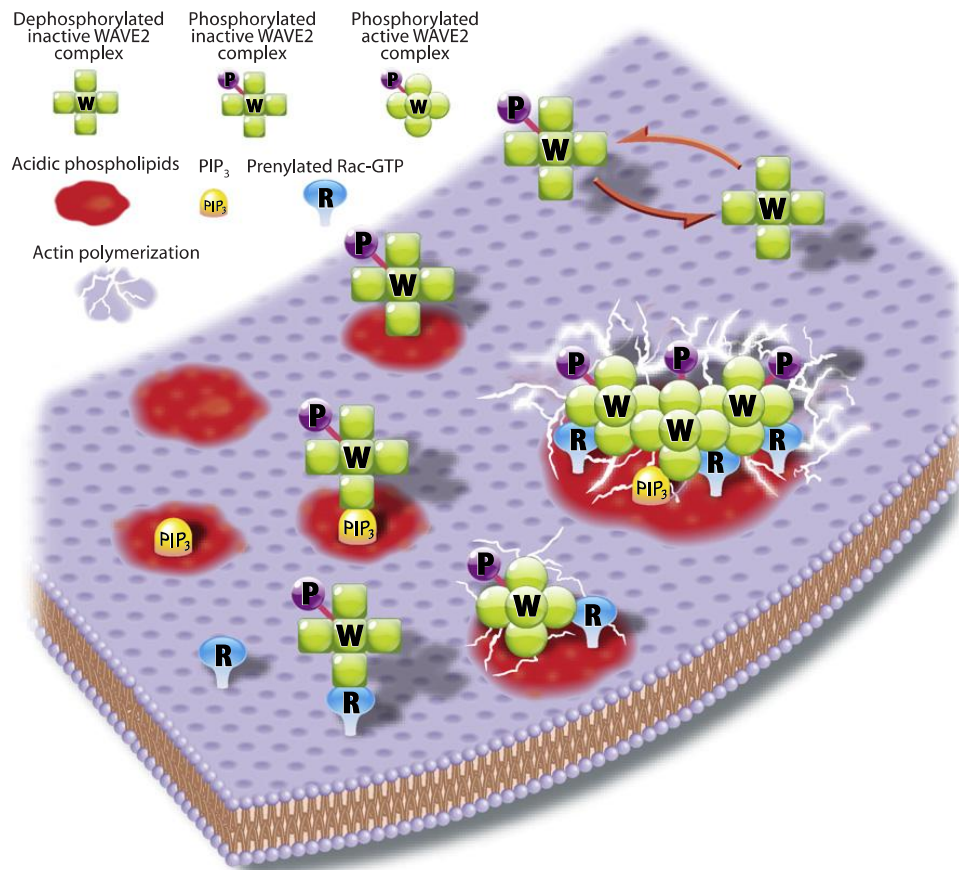
Figure I9: Regulation of SCAR/WAVE proteins. Model for WAVE2 Function Counterclockwise from top right, the WAVE2 complex is intrinsically inactive. Phosphorylated WRC can bind acidic phospholipids, including PIP3, or prenylated Rac-GTP, but binding to either is not sufficient for activation. Binding to both acidic phospholipids (PIP3) and prenylated Rac-GTP activates the WRC. Cooperative association of multiple complexes on the membrane

results in greatly enhanced actin nucleation. (Lebensohn and Kirschner, 2009).

Recently, the crystalization of the Wave complex gave more conformational data to understand the complex activation. Structural and biochemical studies have shown that VCA motif is sequestered by a combination of intra-molecular and inter-molecular contacts within the Wave complex. Phospholipid signaling, Rac and kinases are all required to unlock the inhibited conformation that masks the VCA domain, enabling the latter to associate and activate the Arp2/3 complex (Chen et al., 2010).
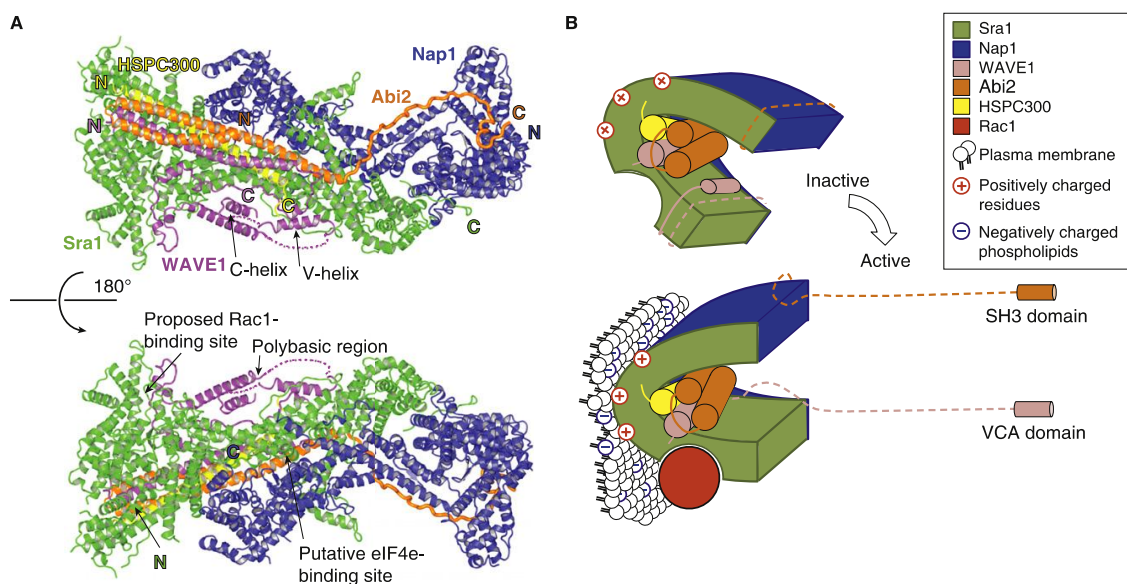
Figure I10: Structure and regulation of the WRC. *(A) Structure of the WRC. Sra1 (green), Nap1 (blue), HSPC300 (yellow), WAVE1 (magenta) and Abi2 (orange). (B) Schematic showing the proposed Wave complex activation mechanism. Unstimulated WRC sequesters the VCA domain of WAVE1, rendering it inactive. Upon binding of the Sra1 subunit to activated Rac1, the entire complex is recruited to the plasma membrane and the VCA domain is released from sequestration. The interaction between the positively charged face of the WRC and negatively charged phospholipids in the plasma*

membrane ensures the VCA domain is oriented in the right way to interact with the actin-polymerizing machinery in the cytoplasm (Davidson and Insall, 2010 ; Chen et al. 2010).

This set of observations highlights the fact that the mechanisms of regulation of this critical machinery are far from being fully comprehended. It is likely that additional modulatory factors, by transiently associating with WRC components, contribute to the switch to a fully active unit. These factors are predicted to be critical to transduce signalling from a variety of cues that must control, in a spatially restricted and temporally defined manner, when and how WAVE becomes active.

3.6. BIOLOGICAL FUNCTIONS OF WASP AND WRC

WASP and WAVE family of proteins are involved in several biological functions that are accompanied by the activation of Arp2/3 complex.

WASP proteins have been reported to be involved in a variety of biological processes: adhesion, phagocytosis, endocytosis, vescicle and organelle motility trafficking within and from Golgi apparatus and exocytosis (Goley and Welch, 2006). WASP family proteins have central roles in membrane trafficking, and are manipulated during infection by intracellular pathogens. Recently, an emerging role for WASPs was found in cytokinesis (Pollitt and Insall, 2008).

WAVE family proteins are the NPFs responsible for activating the Arp2/3 complex in lamellipodia during cell migration and in the formation of macropinocytic structures. Consistent with this function, in mammalian cells all three WAVE isoforms localize to the leading edge of migrating cells (Miki et al., 1998b; Nozumi et al., 2003; Stovold et al. 2005). Analysis of

different cell lines in which the WAVE activities were perturbed by mutations or RNAi, revealed that WAVE2 (Yamazaki et al., 2003; Yan et al., 2003) and WAVE3 (Sossey-Alaoui et al., 2005) are crucial for lamellipodia formation and directed cell migration, whereas WAVE1 is important for formation of dorsal ruffles, which are specialized migratory and endocytic structures detected on the apical surface of mesenchymal and epithelial cells (Buccione et al., 2004), and for stabilization of lamellipodial protrusions (Suetsugu et al., 2003; Yamazaki et al., 2005).

4. SH3BP1

SH3BP1 was isolated through its ability to bind the SH3 domain of the Abl non-receptor tyrosine kinase in a cDNA expression library screen. A short proline-rich segment in the C-terminal tail of 3BP1 was shown to mediate binding to the Abl SH3 (Cicchetti et al., 1992; Cicchetti and Baltimore, 1995). The protein SH3BP1 has a central RhoGAP domains and N-terminal BAR (Bin-Amphiphysin-Rvs) domain that can bind and bend membranes (Figure I11).
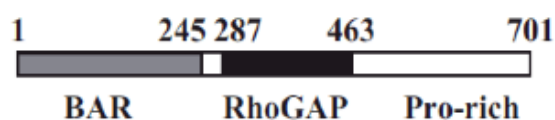
Figure I11: Primary structure of human SH3BP1 (701 amino acids) contains a BAR domain, a RhoGAP domain, and a C-terminal tail with several proline-rich motifs (Parrini et al. 2011).

The Baltimore group (Cicchetti et al., 1995) reported that the central region of SH3BP1 has in vitro GAP activity for Rac and Cdc42, but not for Rho. Moreover in vivo experiments using Swiss

3T3 fibroblasts showed that: i) microinjection of the purified SH3BP1 GAP domain does not inhibit lysophosphatidic acid (LPA)-induced stress fiber assembly, which is mediated by Rho in fibroblasts; ii) microinjection SH3BP1 GAP domain inhibits platelet-derived growth factor (PDGF)-induced membrane ruffling, which is on the contrary mediated by Rac; iii) co-injection of SH3BP1 with an activated mutant of Rac (RacV12) unsensitive to GAPs, does not inhibit RacV12-induced membrane ruffling. Collectively, these results suggest that SH3BP1 down-regulate Rac in vivo.

CHAPTER 2:
REGULATION OF CELL
MOTILITY

1. ACTIN AND MIGRATION

The role of the cytoskeleton is more than simple spatial organization of cell content. Cytoskeleton mediates signals between the cell and the external environment, and plays a mechanical role in cell shape change and in cell motility, in response to these internal or external signals.

The cytoskeleton is a dynamic structure, made of many proteins that can assemble and disassemble. There are three major kinds of protein filaments that make up the cytoskeleton: microtubules, intermediate filaments and actin filaments.

We will focus on the actin because it is the most implicated in cell movement. In fact, actin cytoskeleton is a key regulator of cell migration; actin polymers form polarized structures specific and dynamic architectures capable to assemble into filaments that undergo constant disassembly into monomers; this dynamic polymerization maintains filament length while ensuring polarized growth of their fast growing ends for generation of protrusive forces (Carlier, 1991; Egile et al., 1999; Welch et al., 1997).

Cell movement is a stepwise process that can be generally divided into four phases for the prototype mesenchymal type of motility, which is the most studied since it is typical of cells in the 2D environment of culture dishes. The adhesive steps in the migration cycle (assembly, maturation and disassembly) are tightly coupled to actin polymerization and to actin–myosin contraction, which are in turn regulated by Rho GTPases and PTKs (Vicente-Manzanares et al., 2009) (Figures I12A and I12B).

First step, the cell organizes protrusive structures at the leading edge called lamellipodia, which is the cell portion moving forwards. The historical definition of "Lamellipodium" is a thin region at the leading edge of migrating cells, enriched in actin filaments and free from microtubules (Abercrombie et al., 1970,

Abercrombie et al., 1971) (Figure I12A). This forst sptep is accompagned by formation of new adhesions beneath the lamellipodium near the leading edge. These adhesions stabilize the leading edge through contact with extra cellular matrix (ECM), and generate signals that activate Rac and CDC42, reinforcing the actin polymerization at the leading edge and thus membrane protrusion. Second step, the cell adheres to the substrate via the formation of focal adhesions that anchor it to the extra cellular environment. Next, the nucleus is pushed forward thanks to traction forces generated by the adhesive structures. Finally, the rear of the cell retracts and the whole cell is thus moved forward. Nascent adhesions disassemble as the lamellipodium moves forwards. Actin is involved in every step of the process of cell motility. Protrusive structures could be lamellipodia, but also filopodia, both composed of actin filaments arranged in a network or in bundles respectively. Adhesion to the substrate is achieved through the formation of focal adhesion structures that are connected on one end to the extracellular matrix via transmembrane proteins such as integrins, and to the other side to the stress fibers formed by actin filaments. Retraction of the back of the cell finally occurs through actin retraction fibers and acto-myosin contractility (Mattila and Lappalainen, 2008; Vicente-Manzanares et al., 2009; Parsons et al., 2010).

a

Protrusion

Filopodial adhesion

Nascent adhesion

Actin filament

Disassembling adhesion

Focal complex

Focal adhesion

Dorsal–ventral actomyosin bundle or filament

Nucleus

Filopodium

Lamellipodium

Transition zone
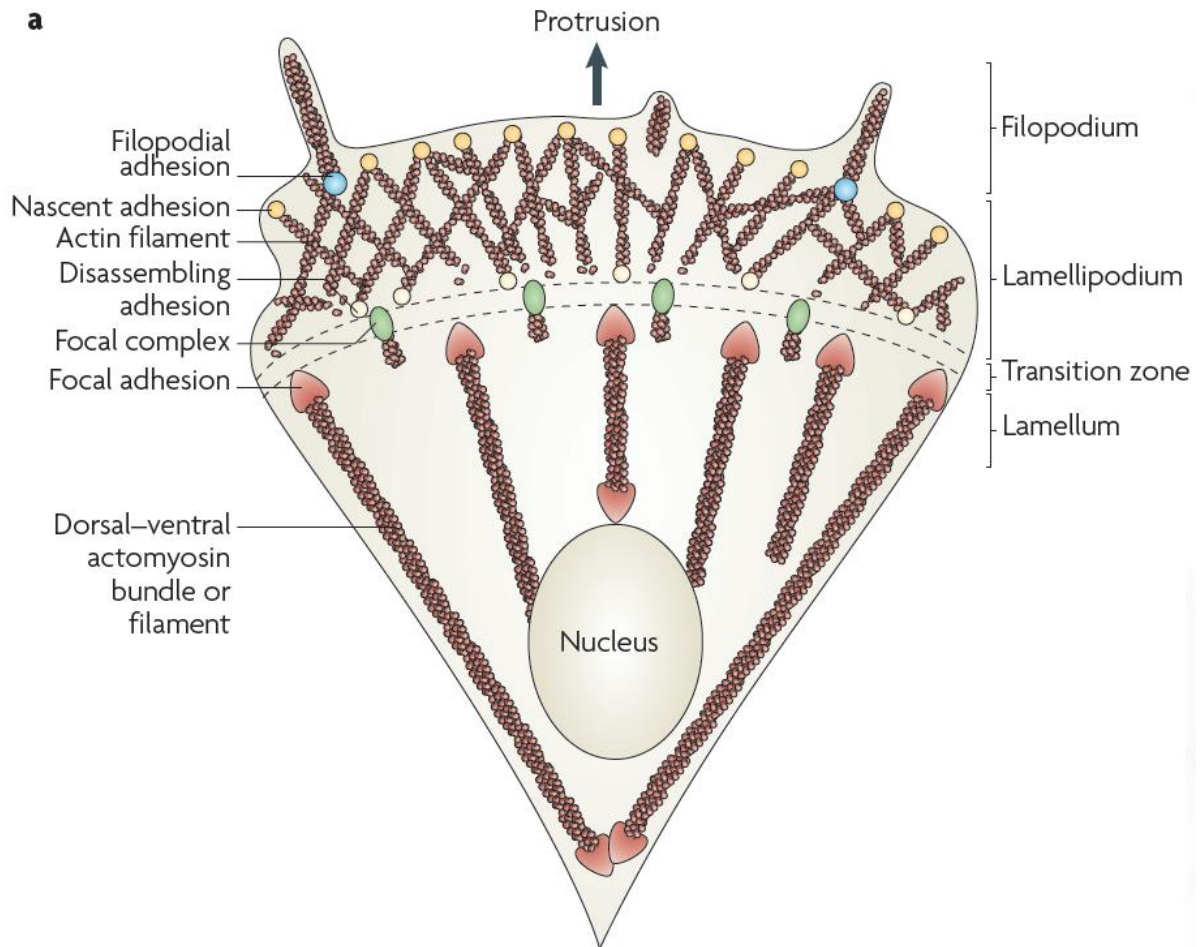
Lamellum

Figure I12A: Structural elements of a migratin cell. Adhesion is closely coupled with the protrusions of the leading edge of the cell (filopodia and lamellipodia). Adhesions (nascent adhesions) initially form in the lamellipodium (although adhesions may also be associated with filopodia) and the rate of nascent adhesion assembly correlates with the rate of protrusion. Nascent adhesions either disassemble or elongate at the convergence of the lamellipodium and lamellum (the transition zone). Adhesion maturation to focal complexes and focal adhesions is accompanied by the bundling and cross-bridging of actin filaments, and actomyosin-induced contractility stabilizes adhesion formation and increases adhesion size (Parsons et al., 2010).
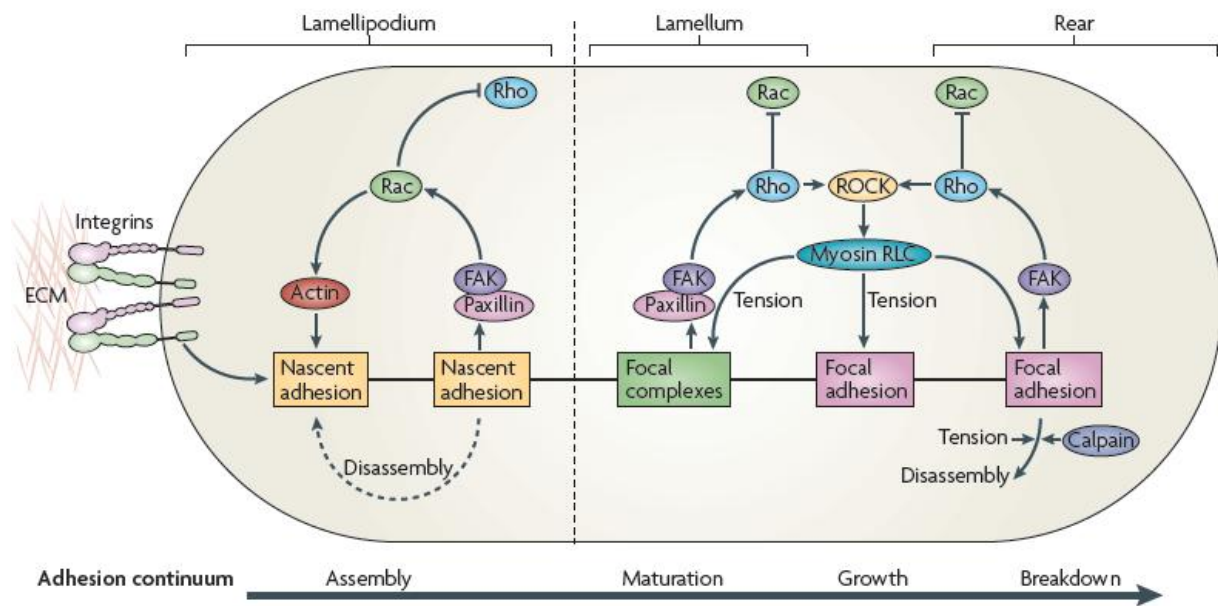
Figure I12B: adhesion maturation and Rho GTPase activation. Nascent adhesion formation and disassembly are coupled with the forward movement of the lamellipodium. Maturation of adhesions is dependent on actomyosin in the lamellum, where adhesions become larger. Adhesion formation and disassembly in the lamellipodium is driven by the activation of Rac, which involves activation of the Tyr-phosphorylated scaffolds, paxillin and focal adhesion kinase (FAK). In the lamellum, adhesion maturation is accompanied by localized activation of Rho, perhaps through FAK-dependent recruitment of Rho guanine nucleotideexchange factors (GEFs) and Rho GTPase-activating proteins (GAPs). Rho activation sustains the activation of myosin II through the action of Rho-associated protein kinase (ROCK), which controls the kinases and phosphatases that regulate its regulatory light chain (RLC) phosphorylation. Myosin II-generated tension sustains adhesion maturation by crosslinking- and tension-induced conformational changes in various adhesion proteins. Disassembly of adhesions at the cell rear is Rho GTPase- and myosin II-dependent, and may also involve the action of proteases, such as calpains, on adhesion-linked proteins. ECM, extracellular matrix (Parsons et al., 2010).

2. Rho GTPase KEY ROLE

Cells may use different motility programs (mesenchymal, amoeboid, collective, etc) according to their intrinsic properties and to their environment. In moving cells, membrane extends differently depending on which motility program involved.

In lamellipodia and filopodia, actin polymerization directly pushes the plasma membrane forward, whereas in invadopodia, actin polymerization couples with the extracellular metalloproteases to create a path through the extracellular matrix. In membrane blebbing, plasma membrane is driving forward using a combination of actomyosin-based contractility.

Each membrane extension type requires the coordination of signaling molecules and cytoskeletal dynamics. Key signalling regulatory proteins in this process are the small Rho GTPases, of which the best characterized are Rac1, CDC42 and RhoA.

Rho proteins (20-30 kD) are small GTPases. Most Rho GTPases switch between an active GTP-bound conformation, which interacts with downstream effectors, and an inactive GDP-bound conformation. Guanine-nucleotide exchange factors (GEFs) promote the GDP\GTP exchange and thus the GTP loading of the protein. GTPase activating factors (GAPs) promote the GTP hydrolysis. Rho GTPases switch capability renders them ideal molecules to control changes in the cytoskeleton dynamics allowing a spatial and timing restricted response to extracellular stimuli (Heasman and Ridley, 2008). The migration process in general, and the formation of cellular protrusions or extensions in particular, are the result of the coordinated activity of Rho GTPases.

Active Rac1, RhoA, and Cdc42 all localize at lamellipodia during protrusion (Machacek et al., 2009). Rho GTPases are activated by different GEFs at the leading edge, depending on the

cell type and extracellular stimulus (Buchsbaum, 2007). Regulation of Rho GTPases localization is important for their function. Rac is known to be recruited to at the leading edge through vesicle trafficking (Donaldson et al., 2009). Endocytic trafficking of Rac is required for Rac activation and for localized Rac-mediated signaling at the plasma-membrane, leading to the formation of actin-based protrusions (Palamidessi et al., 2008).

Many data made strong evidence about Rac role in WRC activation. The first evidence came from the observation that active Rac was shown interacting specifically with WRC via Cyfip subunit (Kobayashi et al., 1998).

Active Rac can recruite WRC complex to the plasmamembrane (Miki et al., 1998; Steffen et al., 2004). Active rac activates WRC complex through Cyfip subunit (Kobayashi et al., 1998). The current activation model is that WRC and is activated by multiple signals: Rac-GTP, acidic phospholipids, and a specific state of phosphorylation (Lebensohn and Kirschner, 2009)

3. RALB/EXOCYST PATHWAY IN CELL MIGRATION

Few recent articles have established the existence of a RalB/exocyst pathway participating in the control of cell migration.

It has been shown that RalA and RalB contribute differently to cell migration in two human cancer cell lines: UMUC-3, a bladder carcinoma line, and DU145, a prostate carcinoma line. RalA depletion had no effect on cell migration, but RalB depletion reduces migration in these cells, using an in vitro Transwell migration assay. Simultaneous depletion of RalA and RalB had no effect on migration. This indicates that RalA and RalB have

nonoverlapping functions in cell motility. The authors proposed the two Ral proteins have antagonist effects, with RalB being promigratory and RalA a motility-inhibitor. This antagonism may reflect the importance of intracellular protein localization in cell motility (Oxford et al., 2005).

Consistently, in our laboratory, it was found that, in non-transformed NRK (Normal Rat Kidney) cells, depletion of RalB, but not RalA, inhibits cell migration using in vitro wound-healing assays. Again, cells depleted of both RalA and RalB migrate normally (Rosse et al., 2006).

In agreement with these in vitro findings, a specific role for RalB in invasion and metastasis was shown in vivo by mouse tail-vein injection assay using a panel of ten genetically diverse human pancreatic cancer cell lines. When RalB was depleted in the injected cells, the formation of metastasis in the mouse lungs was reduced (Lim et al., 2006).

Whereas a role of Ral GTPases in migration was demonstrated, the underlying mechanistic basis has remained elusive. Ral has two well-documented effectors RLIP76/RalBP1 and exocyst, which may link Ral to actin dynamics and membrane traffic. RalBP1, is a Rac/CDC42 GAP implicated in the functional assembly of endocytosis machinery (Jullien-Flores et al., 2000; Nakashima et al., 1999). The exocyst complex regulates exocytosis to regions of rapid membrane expansion (Brymora et al., 2001 ; Sugihara et al., 2001 ; Polzin et al., 2002 ; Moskalenko et al., 2002 ; Moskalenko et al., 2003).

The molecular mechanistic basis for this role of RalB in cell migration has been addressed, and is still under investigation, in our laboratory.

In our system, the RLIP76/RalBP1 effector pathway is not limiting for cell motility, which was somehow surprising since the RhoGAP RalBP1 protein can directly inactivate Rac and Cdc42. In

contrast, the exocyst was found to be required, suggesting that RalB controls cell motility via its exocyst effector. Indeed, RalB was shown both to stabilize the assembly of the full heteromeric exocyst complex and to localize functional exocyst complexes to the leading edge (Rosse et al., 2006).

Cell migration requires de novo plasma membrane addition at the leading edge, and a driving role of vesicle trafficking in directional cell motility has been suggested long time ago (Bretscher and Aguado-Velasco, 1998). Presumably, RalB/exocyst pathway is implicated in the regulation of dynamic membrane expansion in motile cells by coordinating delivery of secretory vesicles to the sites of dynamic plasma membrane expansion that specify directional movement. The secretory vesicles in motile cells may as well carry regulators that are delivered at the leading edge, where they may participate in locally regulating the actin and adhesion dynamics. To this regard, the molecular actors and connectivities are largely unknown.

MATERIALS AND METHODS

1. CELL LINES AND CULTURE

NRK (Normal Rat Kidney), HEK-HT (Human Embryonic Kidney cells stably expressing the early region of SV40 and the catalytic subunit of telomerase hTERT) and human 293T cell lines were grown in Dulbecco's modified Eagle's medium (DMEM, Life Technologies, Inc.) supplemented with 10% fetal bovine serum, 100 units/ml penicillin/streptomycin and 2mM L-Glutamine, at 37°C and 5% CO_2 in humidified incubator on plastic dishes.

High Five (H-5) *Trichoplusia ni* cell line was grown in Express Five medium (Invitrogen) supplemented with 2mM L-Glutamine at 27°C in suspension at 100rpm.

E.coli BL21 cells (Promega) were grown in LB medium at 37° at 200rpm.

2. PLASMIDS AND siRNA OLIGONUCLEOTIDES

2.1. Plasmids

SH3BP1 WT (aa 1–701), DBAR (aa 255–701), DCter (aa 1–466) were expressed using pcDNA3 mammalian expression vector.

YFP-Abi Abi1FL (aa 1-476), YFP-Abi DN (aa 145-476), YFP-AbiN (aa 1-145) were expressed using pCMV mammalian expression vector.

GST-Exo70 and GST-Sec6 were expressed using pGEX4T bacterial expression vector.

GST-Abi1, GST- 535-821 EPS8 and GST-648-821 EPS8 were expressed using pGEX6P1 bacterial expression vector.

2.2. siRNAs

siRNAs were ordered from Eurogentec. Targeted sequences are:

siLuciferase   TACGCGGAATACTTCGA
siUSP9X   CCGCCAGATAGCACAACGATA

siRalB   AAGAGCCCAGTATTCACATTT (Cascone et al., 2006)

siRalA   GACAGGTTTCTGTAGAAGA (Cascone et al., 2006)

siSec5   GGGTGATTATGATGTGGTT (Kashatus et al., 2011)

siSec6   ACCTCCTGAACATGTACCA (Sakurai-Yageta et al., 2008)

siSec8   AATCGACTAGCCGAGTTGT (Sakurai-Yageta et al., 2008)

siExo70   CCAAGATTTCATGAACGTCTA (Misselwitz et al., 2011)

siExo84   GCCACTAAACATCGCAACT

siAbi1   TCTCTAGCTAGTGTTGCTT

siWave2   AGTCACTCAGCTGGATCCC

siCyfip1   GTACTCCAACAAGGACTGC

siSH3BP1-1 Rat GCCTTAGAGATGAGCTGTG (Parrini et al., 2011)

siSH3BP1-2 Rat GAGAAAGGTGGAACAGTGC (Parrini et al., 2011)

siβPIX Rat   GGGTTCGATACGACTGCCA (Parrini et al., 2011)

siRalB Rat   TGACGAGTTTGTAGAAGAC (Parrini et al., 2011)

siSec5 Rat   GGTCGGAAAGACAAGGCAGAT (Parrini et al., 2011)

siSec8 Rat   GGTCCTGATGACAACTTAA (Parrini et al., 2011)

siExo84 Rat   TGGGCATGTTCGTGGATGC (Parrini et al., 2011)

3. WESTERN BLOT

3.1. Preparation of cell lysates

After washing with PBS 1x, cells were lysed directly in the plates using a cell-scraper, in cold lysis buffer (50 mM TrisHCl (pH 7.5), 150 mM NaCl, 1% Triton, 1mM EDTA freshly supplemented with protease inhibitor mixture (Roche) and 1 mM dithiothreitol). Lysates were incubated on ice for 10 minutes and centrifiuged at 13000 rpm for 10 min at 4ºC. The supernatant was transferred into a new tube.

3.2. Electrophoresis, Transfer, Immunoblotting

Desired amounts of proteins were loaded into 10% or 15% 1.5-mm thick polyacrylamide gels for electrophoresis (Biorad).

Proteins were transferred in Western transfer tanks (Biorad) to nitrocellulose membrane (Amersham) in Western Transfer buffer 1x (25 mM Tris, 192 mM glycine, 20% ethanol). Ponceau coloring was used to reveal the proteins transferred on the membrane. Membrane was blocked 1 hour in 5% BSA in TBS 0.1% Tween (TBS-T). After blocking, membrane was incubated with the primary antibody, diluted in TBS-T 1% BSA, for 1 hour at room temperature, or over night at 4°C, followed by three washes of five minutes each in TBS-T and then incubated with the appropriate horseradish peroxidase-conjugated secondary antibody diluted in TBS-T 1% BSA, for 1 hour. After the incubation with the secondary antibody, membrane was washed three times in TBS-T, and the bound secondary antibody was revealed using the ECL (Enhanced Chemiluminescence) method (PerkinElmer).

4. ANTIBODIES

Anti-**Sec6** mouse monoclonal (Stressgen).

Anti-**Sec5** and anti-**Exo84** rabbit polyclonal (gift from Dr Yeaman).

Anti-**RalA**, anti-**Sec8** and anti-**bPix** mouse monoclonal (BD transduction).

Anti-**RalB** rabbit polyclonal (Cell Signalling Technology).

Anti-**Cyfip1** and anti-**Nap** rabbit polyclonal (Upstate)

Anti-**USP9X** mouse monoconal (Abcam).

Anti-**pericentrin** rabbit polyclonal (Covance).

Anti-**Abi1** mouse monoclonal (generated against human Abi1 aa 417-448, C-terminus, Scita group.

Anti-**Wave2** mouse monoclonal (generated against human Wave2 aa 422-498, VCA domain, Scita group.

Anti-**Wave2** rabbit polyclonal (gift from Dr Gautreau).

Anti-**SH3BP1** goat polyclonal (Everest Biotech).

Anti-**SH3BP1** rabbit polyclonal (Atlas).

Anti-**SH3BP1** rabbit polyclonal (gift from Dr Cicchetti).

Anti-**HA** rat monoclonal (3F10) (Roche).

Mouse monoclonal anti-**GST**, anti-**Myc** (E910) and anti-**FlagM2** (IFOM-IEO Campus Antibody facility).

Mouse monoclonal anti-**actin**, anti-**FlagM2**, anti-**GFP** and **beads coupled with FlagM2** antibody (Sigma).

Beads coupled with GFP antibody (ChromoTek).

Western blot secondary antibodies were horseradish peroxidase-conjugated (Jackson ImmunoResearch and Molecular Probes).

Immunofluorescence secondary antibodies coupled with Alexa-488, Alexa-546 or Cy5 (Invitrogen).

5. DNA AND siRNA TRANSFECTIONS

5.1. DNA transfection

Transfections were performed using either calcium phosphate or Lipofectamine Plus reagents (Invitrogen).

5.1.1. Calcium phosphate DNA transfection

293T cells were transfected using the calcium phosphate procedure. In this case DNA (20 μg for a 15-cm dish) was diluted in 878 μl of ddH$_2$O and 122 μl of 2M CaCl$_2$ were added. This solution was added, drop-wise, to 1mL of HBS 2x (50 mM Hepes pH 7.5, 10 mM KCl, 12 mM dextrose, 280 mM NaCl, 1.5 mM Na$_2$HPO$_4$). After 10 minutes incubation, the precipitate was added drop-wise to the cells and removed after 12-16 hours.

This transfection was used for the experiments with the FlagNap/myc-Cyfip subcomplex.

5.1.2. Lipofectamine Plus DNA transfection

At day 0, cells were plated into appropriate dishes (12-wells, 6-cm or 10-cm dishes) in complete DMEM medium. According to manufacturer's instructions, at day 1, two mixtures were prepared and incubated 10 minutes: Mix1 (DNA and Plus reagent in OPTI-

MEM medium) and Mix2 (Lipofectamine in OPTI-MEM medium). Afterwards, these two Mix were mixed together, and incubated additional 10 minutes. Mix1+Mix2 was than added to cells in OPTI-MEM. 3h later, medium was changed to complete medium. At day 2-3, 24-48 hours after transfection, cells are fixed or lysed.

5.2. siRNA transfection

Reverse transfection method was used to transfect cells by siRNA, using Hiperfect (QIAGEN), according to manufacturer's instructions. At day 0, a mix of siRNA at a final concentration of 10nM is prepared in 100uL OPTI-MEM with 6uL Hiperfect reagent. After 10 minutes of incubation at room temperature, the mix is added to freshly plated cells in 12-wells in complete medium. At day 1, medium is changed. At day 3, 72 hours after transfection, cells are used in experiments.

6. IMMUNOFLUORESCENCE

Cells were fixed with 4% paraformaldehyde (in PBS) for 10 minutes, washed with PBS and permeabilised in PBS 0.1% Triton X-100 for 10 minutes at room temperature. To prevent non-specific binding of the antibodies, cells were saturated with PBS supplemented with 10% Fetal Bovine Serum (FBS) for 1 hour and incubated with the indicated antibodies in PBS-FBS 10% for 1 hour. After 3 washes of 5 minutes with PBS, cells were incubated with appropriate secondary antibodies coupled with Alexa-488 or Alexa-546 or Cy5 in PBS-FBS 10% for 1 hour. After 3 washes of 5 minutes with PBS, cells were mounted with Prolong (Invitrogen) and examined by fluorescence microscopy.

7. IMMUNOPRECIPITATION

7.1. Immunoprecipitation buffers

Buffer1: Sec8 and YFP immunoprecipitations (50 mM TrisHCl (pH 7.5), 150 mM NaCl, 1% Triton, 1mM EDTA freshly supplemented with protease inhibitor mixture (Roche) and 1 mM dithiothreitol).

Buffer2: HA immunoprecipitation (20 mM Tris HCl (pH 7.5), 100 mM NaCl, 5 mM MgCl2, 1% Triton, 10% glycerol, freshly supplemented with protease inhibitor mixture (Roche) and 1 mM dithiothreitol).

Buffer3: Flag and V5 immunoprecipitations (50 mM Tris HCl (pH 7.5), 150 mM NaCl, 1% Triton, 0.1% Sodium dodecyl sulfate (SDS), 0.5% Sodium deoxycholate (DOC), 1mM EDTA, 5% glycerol, freshly supplemented with protease inhibitor mixture (Roche) and 1 mM dithiothreitol).

Buffer4: Washing buffer low salt (10 mM Tris HCl (pH 7.5), Sodium dodecyl sulfate (SDS) 0.1%, Sodium deoxycholate (DOC) 1%, EDTA 5mM, glycerol 5%, freshly supplemented with protease inhibitor mixture (Roche) and 1 mM dithiothreitol) and Washing buffer high salt (Low salt buffer + 500 mM NaCl).

7.2. Immunoprecipitation/purification from 293T cells

7.2.1. Sec8 immunoprecipitation (Figure R11 C)

One 10-cm dish of DNA-transfected 293T cells was lysed into 1ml buffer1. Supernatant was incubated 2h rocking at 4°, with 25ul of beads covalently coupled to a mixture of monoclonal anti-Sec8 antibodies (Yeaman et al., 2001). The immobilized immune complexes were washed three times with 1 ml of the same

buffer. Samples were boiled and analyzed by SDS-PAGE. 1.6% input was loaded.

7.2.2. HA immunoprecipitation (Figure R11 D and E)

One 6-cm dish of DNA-transfected 293T cells was lysed in 600ul buffer2. Supernatant was incubated 1h rocking at 4°, with a monoclonal anti-HA antibody (3F10, 1ug). The immobilized immune complexes were washed three times with 1 ml of the same buffer. Samples were boiled and analyzed by SDS-PAGE. 6% input was loaded.

7.2.3. YFP immunoprecipitation (Figure R9)

One 6-cm dish of DNA-transfected 293T cells was lysed in 600ul buffer1. Supernatant was incubated 1h rocking at 4°, with 20ul magnetic beads coupled to GFP antibody (ChromoTek). This "GFP trap" functions also as a YFP trap. The immobilized immune complexes were washed three times with 1 ml of the same buffer. Samples were boiled and analyzed by SDS-PAGE. 1.5% input was loaded.

7.2.4. V5 immunoprecipitation (Figure R6)

I used 5x15-cm dishes per condition. Each 15-cm dish was lysed into 1ml buffer3. Supernatant of 5 dishes was incubated 1h rocking at 4°, with 10ug anti-V5. 1h later, 20ul magnetic G-protein beads (Invitrogen) were added for 1h. The immobilized immune complexes were washed three times in high salt buffer and three times in low salt buffer. Samples were boiled and analyzed by SDS-PAGE. 1% input was loaded.

7.2.5. Flag immunoprecipitation/purification of WRC complex (Figure R4, R5, R7 and R8)

I used 5x15-cm dishes per condition for in vivo association experiments, and 10x15-cm dishes per condition for in vitro interaction assay. Each 15-cm dish was lysed in 1ml buffer3. Supernatant of 5/10 dishes was incubated 2h rocking at 4°, with 20/40ul magnetic beads coupled to FlagM2 antibody (Sigma). The immobilized immune complexes were washed three times in high salt buffer and three times in low salt buffer. For in vivo experiments, samples were boiled and analyzed by SDS-PAGE. 1% input was loaded. For in vitro experiments, beads were kept into buffer5.

7.2.6. Purification of Flag-Nap/Myc-Cyfip subcomplex (Figure R3)

I used 20x15-cm dishes per condition. Each 15cm dish was lysed in 1ml buffer3. Supernatant of 20 dishes was incubated 2h rocking at 4°, with 10ug anti-FlagM2 (Sigma). 1h later, 20ul magnetic G-protein beads (Invitrogen) were added for 1h. The immobilized immune complexes were washed three times in high salt buffer and three times in low salt buffer and kept into buffer5.

8. PROTEIN PURIFICATION FROM BACTERIA OR INSECT CELLS

8.1. Protein production using *E.coli*

8.1.1. Transformation of competent cells

E.coli Top10 cells (Invitrogen) were used for cloning and large scale DNA preparation, while *E.coli* BL21 cells (Promega) were used for protein production. The transformation protocol used was the same for both strains.

50 μl of fresh competent cells were thawed on ice for approximately 10 minutes prior to the addition of plasmid DNA.

Cells were incubated with DNA on ice for 20 minutes and then subjected to a heat shock for 45 seconds at 42°C. Cells were then returned to ice for 2 minutes. Then, 0.4 ml of LB were added and the cells were left at 37°C for 60 minutes before plating them onto plates with the appropriate antibiotic. 200 μl of the transformed bacterial were usually plated. Plates were incubated overnight at 37°C.

8.1.2. Protein expression

A one-day miniculture of transformed *E.coli* BL21 is grown overnight in 1L prewarmed LB with ampicillin selection (100ug/mL) at 37° 200rpm. The overnight culture is diluted 1:50 in ampicillin-LB and grown till OD 0.6. Bacteria are cooled, IPTG added (0.5mM) and grown 4h at 25° 200rpm. Bacteria were pelleted and kept at -80°.

8.1.3. Protein purification buffers

Buffer6: Purification buffer (50 mM Tris HCl (pH 7.8), 500 mM NaCl, 1% Triton, 5% glycerol, freshly supplemented with protease inhibitor mixture (Roche) and 1 mM dithiothreitol).

Buffer7: Purification washing buffer which is purification buffer without Triton.

Buffer8: Dialysis buffer (50 mM Tris HCl [pH 7.5], 150 mM NaCl, 5% glycerol, freshly supplemented with protease inhibitor mixture (Roche) and 1 mM dithiothreitol).

8.1.4. Purified proteins

Pellet is resuspended in buffer6 (20mL for 1L bacteria), sonicated (3x30 seconds) and centrifuged (10000rpm, 45min at 4°). Supernatant is incubated 2h on a rotating wheel at 4° with Glutathione beads (Thermo scientific) (200ul dry beads for 1L bacteria), previously washed 3 times with buffer7. After that, beads are extensively washed with buffer7.

Using this method, the following proteins were produced: GST-Exo70, GST-Sec6, GST-SH3 EPS8 (535-821 EPS8 containing SH3 domain) and GST-Cter EPS8 (648-821 EPS8 C-terminus fragment).

For some experiments the proteins were kept on beads for following binding experiments. When indicated, in order to obtain soluble proteins, elution was performed using three 10-min rounds of incubation in buffer7 supplemented with 50mM Glutathione. pH was adjusted. Overnight dialysis was then performed in buffer8.

While GST-tag EPS8 fragments were abundantly purified (0.5 L bacteria gave about 400-600ug protein); the production yield of GST-Exo70 and GST-Sec6 was poor (1L bacteria gave about 5-15ug protein).

8.2. Protein production using Baculovirus

8.2.1. Transfection of insect cells

Isolation of recombinant DNA:

DH10 MultiBac-YFP electro-competent E.Coli were thawed on ice few minutes prior to the addition of plasmid DNA. Electroporation was performed. Then, 0.9 ml of LB were added and the cells were rotated at 37°C for 4h before plating them onto plates with the appropriate antibiotic. After 48h incubation at 37°C, white colonies (containing DNA of interest) were isolated and

incubated overnight at 37° in new plates. Clones were grown to stationary phase in 2mL LB by shaking at 200rpm and cells were collected by centrifugation. Minipreps were realized (QIAprep Spin Miniprep Kit, QIAGEN).

Transfection of High Five (H-5) cells:

A mix of Bacmid DNA, Express Five medium and INSECTOGENE transfection reagent (Biontex) was prepared and incubated 20 minutes. This mix is added to H-5 cells seeded in the meantime in 6-well plates, and incubated 5h at 27° without shaking. Then, medium is changed and cells are incubated 72h at 27°. Since Bacmid contains the gene for YFP expression, transfection can be checked by fluorescence microscopy. After 10-min centrifugation at 1000rpm, supernatant is the primary viral stock (V0). V0 can be stored in the dark at 4°.

Amplification of primary viral stock (generation of V1 virus):

A shaker flask with 25mL H-5 cells at 0.5×10^5 cell/ml density is prepared. 2mL of V0 is added and cells are cultured for 72h. Cell division stop shows virus infection efficiency. After 10-min centrifugation at 1000rpm, supernatant is the secondary viral stock (V1). V1 can be stored in the dark at 4°.

8.2.2. Protein expression

A shaker flask with 200mL H-5 cells at 0.5×10^5 cell/ml density is prepared. 2mL of V1 is added and cells are cultured for 72h. After 10-min centrifugation at 1000rpm, pelleted cells will be used for protein purification.

8.2.3. Protein purification

Pellet is resuspended in buffer6 (10mL for 1L H-5 cells), sonicated (3x10 seconds) and centrifuged (5000rpm, 45min at 4°).

Supernatant is incubated 2h on a rotating wheel at 4° with Glutathione beads (Thermo scientific) (200ul dry beads for 1L bacteria), previously washed 3 times with buffer7. After that, beads are extensively washed with buffer7.

Abi1 was purified using this method. GST-Abi was produced and cleaved on the beads by addition of GST-PreScission protease (1ug protease for 100ug recombinant protein, overnight on a wheel at 4°). Overnight dialysis is then performed in buffer8. 1L H-5 cells gave 20-50ug cleaved Abi protein.

9. IN VITRO PROTEIN INTERACTION ASSAY

Buffer used in these experiments was In vitro interaction buffer (buffer5) (50 mM Tris HCl (pH 7.5), 150 mM NaCl, 1% Triton, 5% glycerol, freshly supplemented with protease inhibitor mixture (Roche) and 1 mM dithiothreitol).

9.1. Abi - GST-Exo70 (Figure R2)

30ug Abi was incubated in 300 ul buffer5 for 2h rocking at 4°, with 30ug GST-Exo70 or with beads alone, GST-Cter EPS8 or GST-SH3 EPS8 as controls. After, beads were washed three times in high salt buffer and three times in low salt buffer. Samples were boiled and analyzed by SDS-PAGE. 5% input was loaded.

9.2. Flag-tag WRC complex – GST-Exo70/GST-Sec6 (Figure R5)

Bead-bound Flag-tag WRC complex (Flag-HA-Abi, Flag-HA-Cyfip or Flag-HA control) purified from 20x15-cm dishes was incubated in 300 ul buffer5 for 2h rocking at 4°, with 10ug GST-Exo70, GST-Sec6 or GST as control. Afterwards, beads were washed three times in high salt buffer and three times in low salt

buffer. Samples were boiled and analyzed by SDS-PAGE. 5% input was loaded.

9.3. Flag-Nap/Myc-Cyfip subcomplex – GST-Sec6 (Figure R9)

Bead-bound Flag-tag proteins (Flag-Nap/Myc-Cyfip or Flag-Nap and Flag-AEK as control) purified from 30x15-cm dishes were incubated in 300 ul buffer5 for 2h rocking at 4°, with 20ug GST-Sec6 or GST-Exo70 as control. Afterwards, beads were washed three times in high salt buffer and three times in low salt buffer. Samples were boiled and analyzed by SDS-PAGE. 5% input was loaded.

10. WOUND HEALING ASSAY AND TIME-LAPSE MICROSCOPY

Cells were grown to confluence on dishes coated with collagen (type I from rat tail, Interchim) and the monolayer was wounded with a tip. Medium was changed to MEM with 2% fetal bovine serum.

For phase-contrast video microscopy, images were acquired with 10x objective every 15 min.

To track cells, I used Manual Tracking plug-in (developed by Fabrice Cordelières) of the ImageJ software (Rasband, W.S., ImageJ, National Institutes of Health, Bethesda, Maryland, USA, http://rsb.info.nih.gov/ij/, 1997-2003). Persistence of motility was calculated as the D/T ratio, where D is the direct distance from startpoint to endpoint and T is the total track.

RESULTS

CHAPTER 1:
PROJECT

1. PROJECT HYPOTHESIS

In our laboratory, it was established that RalB controls cell motility via the exocyst (see Introduction). The Rac1 GTPase is, on the other hand, a key player in regulating actin dynamics that propels cell motility process (see Introduction).

Therefore, we hypothesize the existence of molecular links connecting the RalB/exocyst and Rac1 pathways. To identify these possible connections, we analyzed the data coming from screening previously performed in the laboratory with the aim to define the Ral pathway interactome.

2. EVIDENCE FOR AN EXOCYST-WRC CONNECTION

Three different screenings previously realized in our group identified molecular connections between the Ral pathway and the WRC complex.

2.1 MOLECULAR SCREENING (YEAST TWO-HYBRID)

A series of two-hybrid screenings using human exocyst subunits as baits, performed in collaboration with the Hybrogenics company, highlighted two potential connections between the exocyst complex and the Wave regulatory WRC complex: the Sec6 exocyst subunit interacted with Cyfip, while the Exo70 exocyst subunit was found to associate with Abi1 (Figure R1 A).

In the case of the Sec6-Cyfip interaction, a 297-745aa fragment of human Sec6 (NCBI, NP_848611.2) was used as bait and the 325-507aa Cyfip (NCBI, NP_055423.1) fragment was recovered from the screening. Notably, this region overlaps with the RacGTP interaction domain of Cyfip (aa 1-407) (Kobayashi et al., 1998) (Figure R1 B).

In the case of Exo70-Abi1 complex, the full length human Exo70 (NCBI, NP_001013861.1) was used to fish out a 36-216aa fragment of Abi1 (NCBI, NP_001012770.1). This latter region encompasses the amino-terminal coiled-coil domain of Abi1 that

was shown to interact directly with Wave2 (aa 1-111) (Leng et al., 2005) (Figure R1 C).
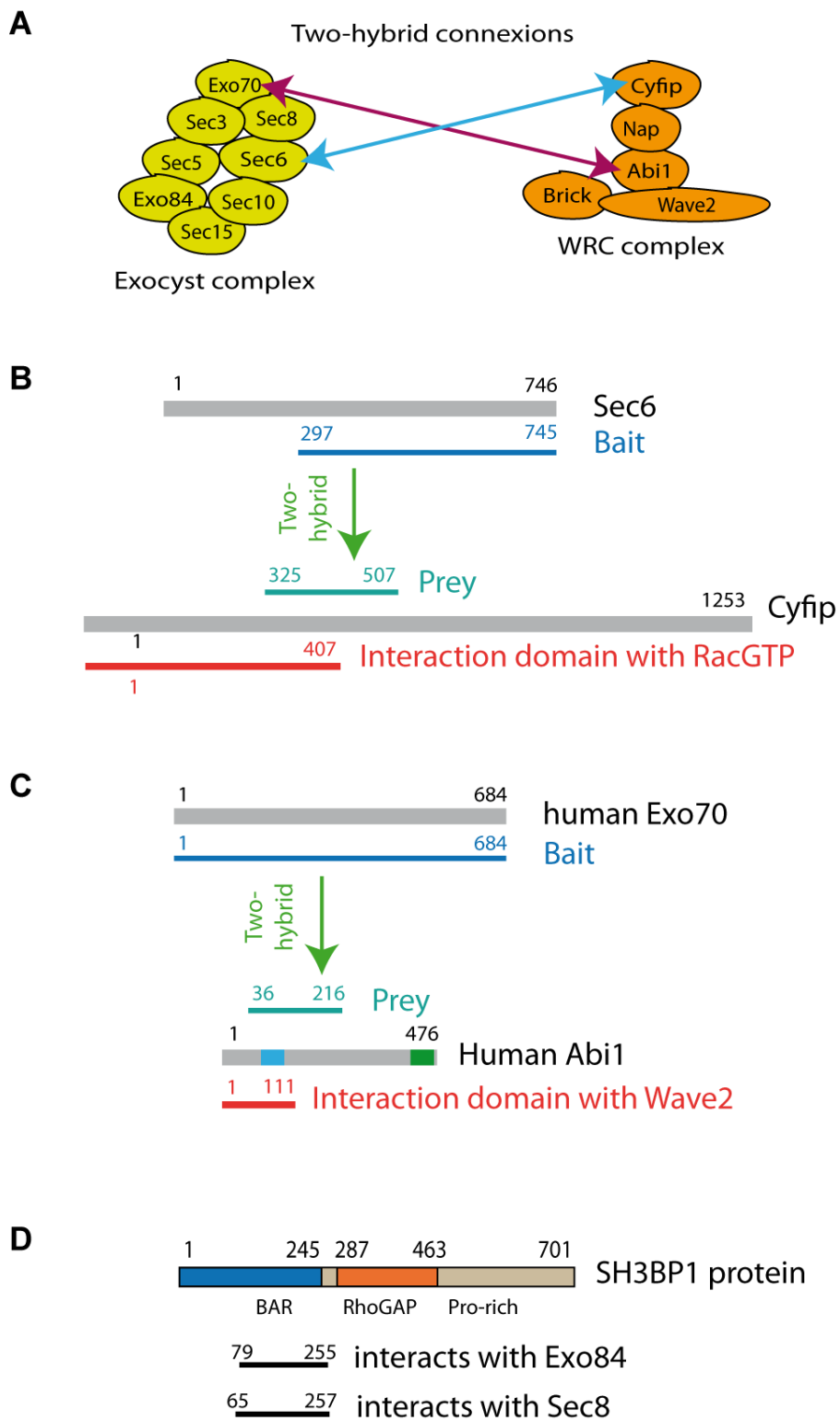
Figure R1: Two-hybrid interaction results. (A) Simplified subunit interactions between exocyst and WRC. Arrows show Exo70-Abi and Sec6-Cyfip interactions. (B) Sec6-Cyfip interaction. Human Sec6 (297-745), used as bait, fished out a Cyfip fragment (325-507). This domain overlaps with the interaction region of Cyfip with RacGTP (1-407). (C) Exo70-Abi interaction. Full length human Exo70, used as a bait, fished out the N-terminal 36-216 Abi fragment, which includes the Wave2 interacting domain of Abi1 (1-111). In Abi1: Blue domain is coiled coil, Green domain is SH3. (D) Primary structure of SH3BP1 and results of two-hybrid. Human SH3BP1 protein is composed of 701 amino acids. It contains an N-terminal BAR domain, a central RhoGAP domain, and a C-terminal tail rich of prolins. Dark lines indicate minimal interaction domains with Sec8 and Exo84 resulting from two-hybrid assay.

2.2 GENETIC SCREEN IN DROSOPHILA

Drosophila melanogaster in vivo model was used to compile a catalogues of the Ral-based network. The fruit fly system provides the advantage with respcet to vertebates to possess a single Ral gene, whose protein product shares 80% of homology with mammalian RalA and RalB. Furthermore, the protein network upstream and downstream of Ral is largely conserved between human and flies (Mirey et al., 2003).

Decreasing Ral activity by overexpression of dominant-negative form of Ral or by using Ral hypomorphic loss-of-function mutations induced a highly penetrant loss-of-bristle phenotype due to post-mitotic cell-specific apoptosis during bristle development (Balakireva et al., 2006). Each wild type bristle, the fly sensory organ, is composed of four cells with different developmental programs. When the activity of Ral is decreased many sensory organs are defective and contain only three cells as a result of the apoptotic death of one of the cells in the sensory

organ lineage. This defect in sensory organ organization leads to Ral-dependent loss-of-bristle phenotype.

This Ral apoptotic loss-of-bristle phenotype was then used to identify new molecular players in Ral signaling. A gain-of-function screen of 1188 *Drosophila* genes was performed in our laboratory, by Claire Beraud and Maria Balakireva, to determine potential Ral interacting partners according to the strategy outlined below: (i) both the dominant negative form of Ral and the wild type form of the protein for each tested gene were co-expressed in the sensory organ cells, (ii) the bristle phenotypes resulting from each Ral genetic interaction were then compared to the control Ral loss-of–bristle phenotype; (iii) suppressors or enhancers of Ral apoptotic bristle phenotype were identified. Both enhancers (577) and suppressors (179) were found as potential Ral partners. Among those, 50 genes are involved in cell cycle, programmed cell death, migration, trafficking or adhesion processes. (Beraud and Balakireva, Camonis group, unpublished data).

Notably, a component of the WRC, Cyfip (which is named Sra in *Drosophila*) was identified as a potential Ral partner since its overexpression enhanced Ral apoptotic phenotype.

2.3. FUNCTIONAL SCREENING ON CYTOKINESIS IN HeLa CELLS

The last step of cell division is called cytokinesis, during which physical separation of dividing daughter cells occurs.

The implication of the exocyst as a Ral effector in the abscission of the intracellular bridge had already been established (Gromley et al., 2005). Moreover, a previous project in our laboratory had showed that depletion of RalA or RalB by siRNAs in three cell lines [HeLa, HBEC (human bronchiolar epithelial cells) and HEK-HT (human kidney epithelial cells)] resulted in

cytokinesis defects, which were different depending on the Ral protein that was interefered. RalA depletion causes the accumulation of binucleate cells. The cleavage furrow is still able to form the intracellular bridge, but the intracellular bridge is no longer stable. Daughter cells are arrested before completion of cytokinesis and fused back to form a single cell with two nuclei. RalB depletion frequently causes, instead, the appearance of cells connected by an intracellular bridge because cells are no longer able to cleave the intracellular bridge (Cascone et al., 2008). Collectively, these findings indicate that RalA and RalB have distinct roles in two different steps of cytokinesis. RalA is in involved in early, while RalB in late cytokinesis steps.

In order to identify new actors of Ral GTPases cytokinesis pathway, a functional screening using interfering RNA was carried out in in HeLa cells, in collaboration with Biophenics Laboratory. 91 genes implicated in proteasome process, cell cycle, cytoskeleton regulation, protein transport, and potentially involved in Ral interactome where targeted by siRNAs. The results showed that depletion of 14 proteins, among the 91 tested, phenocopied the binucleated cell phenotype of RalA, whereas depletion of 8 proteins caused the same defective cleavage of the cytokinetic bridge as RalB-depleted cells (Rasim Selimonglu and Ilaria Cascone, Camonis group, unpublished data).

Abi, a component of WRC, was identified among the latter proteins. Abi depletion caused a significant accumulation of cells that cannot complete abscission and remain connected by intracellular bridges.

3. EVIDENCE FOR AN EXOCYST-SH3BP1 CONNECTION

3.1. SH3BP1 WAS FISHED OUT THROUGH THE EXOCYST TWO-HYBRID SCREENING

In the two-hybrid screening for exocyst partners described above, both Sec8 and Exo84 subunits fished out the SH3BP1 protein, a signaling adaptor possessing a Bar and Rac GAP domains in addition to a prolin-rich C-terminal tail (Parrini et al., 2010) (see Introduction).

SH3BP1 presumably interact with both Sec8 and Exo84 via its Bar domain as suggested by the finding that the smallest fished SH3BP1 fragments encompassed amino acids 65-257 (for Sec8 screen) and 79-255 (for Exo84 screen) (Figure R1 D).

CHAPTER 2:
MOLECULAR AND FUNCTIONAL LINKS BETWEEN EXOCYST AND WRC

1. BIOCHEMICAL STUDIES OF THE EXOCYST-WRC INTERACTION

1.1. WRC DIRECTLY INTERACTS WITH EXOCYST

To confirm the Exo70-Abi1 and Sec6-Cyfip interactions identified by the two-hybrid screening, I performed in vitro interaction assays using purified proteins.

1.1.2. Abi interacts in vitro with Exo70

I purified Abi1 from H-5 insect cells (High 5 cells derived from *Trichoplusia ni*). To this end, I infected H-5 cells with baculo virus expressing GST-tag, full length human Abi1 (isoform a), which was subsequently purified using glutathione-coupled beads and recovered after cleaving Abi1 protein with PreScission protease (see Materials and Methods) (Figure R2 A).

Full-length Exo70 protein was, instead, expressed as GST-fusion in E.coli and purified using glutathione-coupled beads.

As control, I used GST-fused fragments of EPS8 (Epidermal Growth Factor Receptor Pathway Substrate 8) which have been previously shown to either mediated or not the interaction with Abi (Biesova et al., 1997; Scita et al., 2001). More specifically, the EPS8 SH3 domain was identified as the portion mediating the interaction with Abi1 and was therefore used as positive control of the experiment. The EPS8 C-terminus, which was shown to bind actin but not Abi1 was used as negative control of the experiment. An additional negative control is represented by protein-free glutathione beads.

I incubated bead-bound GST-Exo70, GST-SH3-EPS8 and GST-C-ter-EPS8 with GST-cleaved Abi. After 1 hour of incubation of rotatory device at 4º C, (see Materials and Methods), I separated beads by centrifugation before separating the bound proteins by SDS-PAGE followed by western blotting with specific antibodies.

Ponceau red staining of the nitrocellulose membrane shows that similar amounts of pure bead-bound GST-Exo70, GST-SH3 EPS8 and GST-Cter EPS8 were employed.

Immunoblotting with anti-Abi1 antibody shows, instead, that Abi1 binds with similar apparent affinity both GST-SH3 EPS8 and GST-Exo70, but not GST-Cter EPS8 (Figure R2 B).

Thus, Abi1 directly associates with Exo70 with an affinity comparable to that of the Abi1-EPS8 complex.
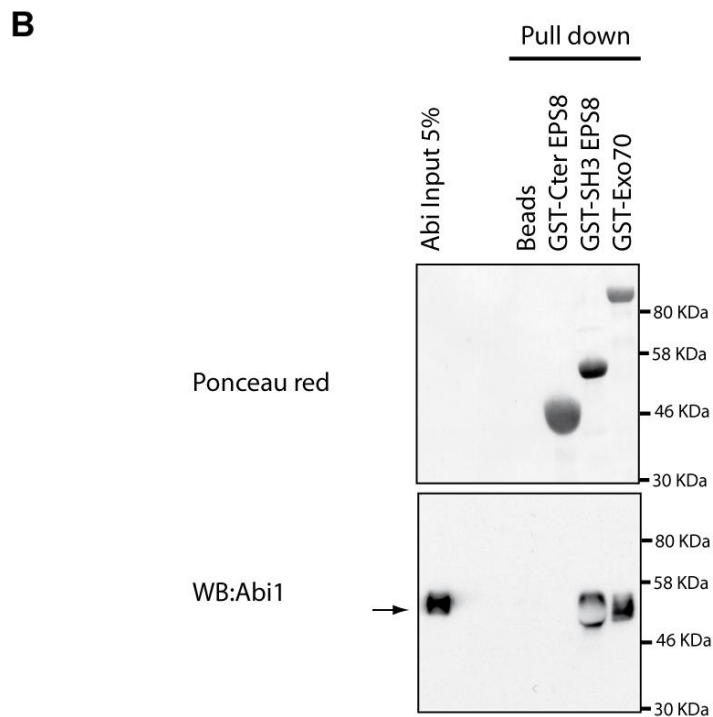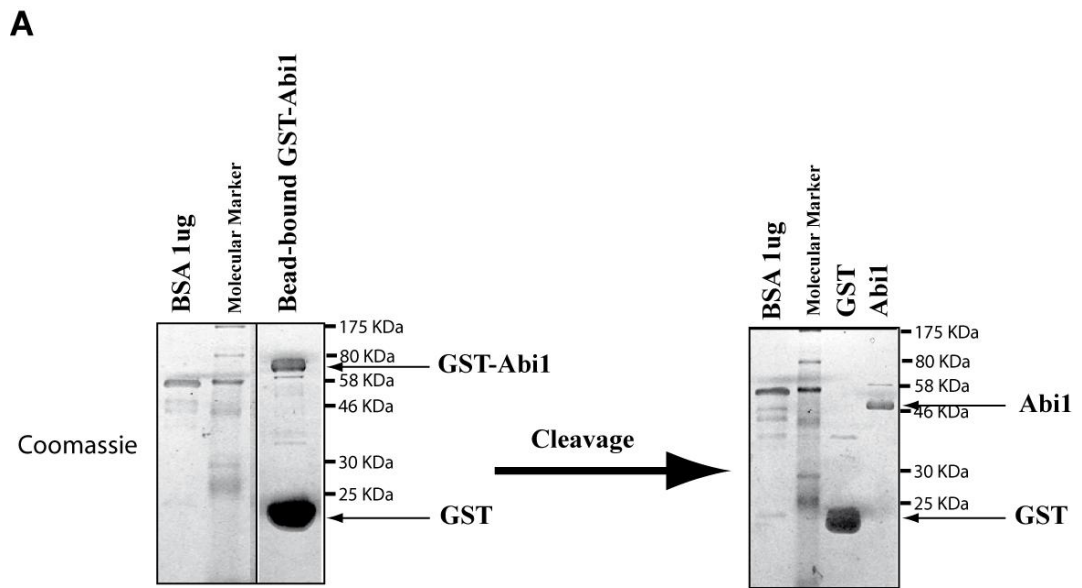
Figure R2. Abi interacts invitro with Exo70. (A) Abi purification. *Coomassie staining showing on the left bead-Bound GST-Abi1 purified from H5 cells, on the right GST alone, and cleaved Abi1.* ***(B) Abi pull down.*** *Abi protein was purified from insect cells; GST-Exo70, GST-Cter EPS8 (negative control) and GST-SH3 EPS8 (positive control) were purified from E.Coli.*

Ponceau red shows GST-tag proteins. Abi was incubated with GST-tag proteins, and then pulled down. Abi1 western blot shows Abi interacting with the positive control and equally well with GST-Exo70. 5% of the Abi input was loaded. The perturbed Abi1 bands pulled down by the SH3 domain of Eps8 is presumably due to the fact the the two proteins runs very closely in SDS-PAGE. Abi1 runs at around 55-65 KDa; and the molecular weight of GST-535-821 fragment of EPS8 that was used is 57KDa (EPS8SH3 31KDa + GST 26KDa).

1.1.3. Cyfip interacts in vitro with Sec6

To validate the Sec6-Cyfip interaction, I had to make sure to preserve the stability and the correct folding of the labile and poorly soluble Cyfip protein. To this end I used an already reported strategy (Innocenti et al., 2004): I coexpressed Cyfip with its major interactor Nap1. The two proteins form a relatively stable subcomplex which is normally incorporated into a large WRC unit.

A Myc-Cyfip expressing vector, together with a Flag-Nap1 expressing vector, were cotransfected in 293T cells. As control, I also transfected Flag-Nap1 vector alone, as well as a non-related Flag-tag protein: AEK (catalytically-dead GEF Arno). I affinity purified Flag-tag proteins using Flag antibody bound onto beads. Purified and soluble GST-Sec6 and GST-Exo70 (which I used as negative soluble control) from E.Coli (see Materials and Methods) were subsequently incubated for 1 hour with immobilized Flag-tag proteins. Bound material, separated by SDS-PAGE, was immunoblotted with specific antibodies

Ponceau red staining of the nitrocellulose membrane shows that similar amounts of pure and soluble GST-Exo70 and GST-Sec6 were used as well as of immobilized Flag-AEK, Flag-Nap1 expressed alone and Flag-Nap1 co-expressed with Myc-Cyfip. The Myc-Cyfip amount is too little to be visible on Ponceau red.

Immunoblotting with anti-Flag antibody enabled to identify Flag-tag proteins, whereas immunoblotting with anti-Myc permitted to assess the presence of Myc-Cyfip in complex with Flag-Nap1.

Immunoblotting with anti-GST antibody shows that GST-Sec6, but not GST-Exo70, specifically associated with Myc-Cyfip (Figure R3).

Thus, Sec6 directly interacts in vitro with Cyfip (but not with Nap).
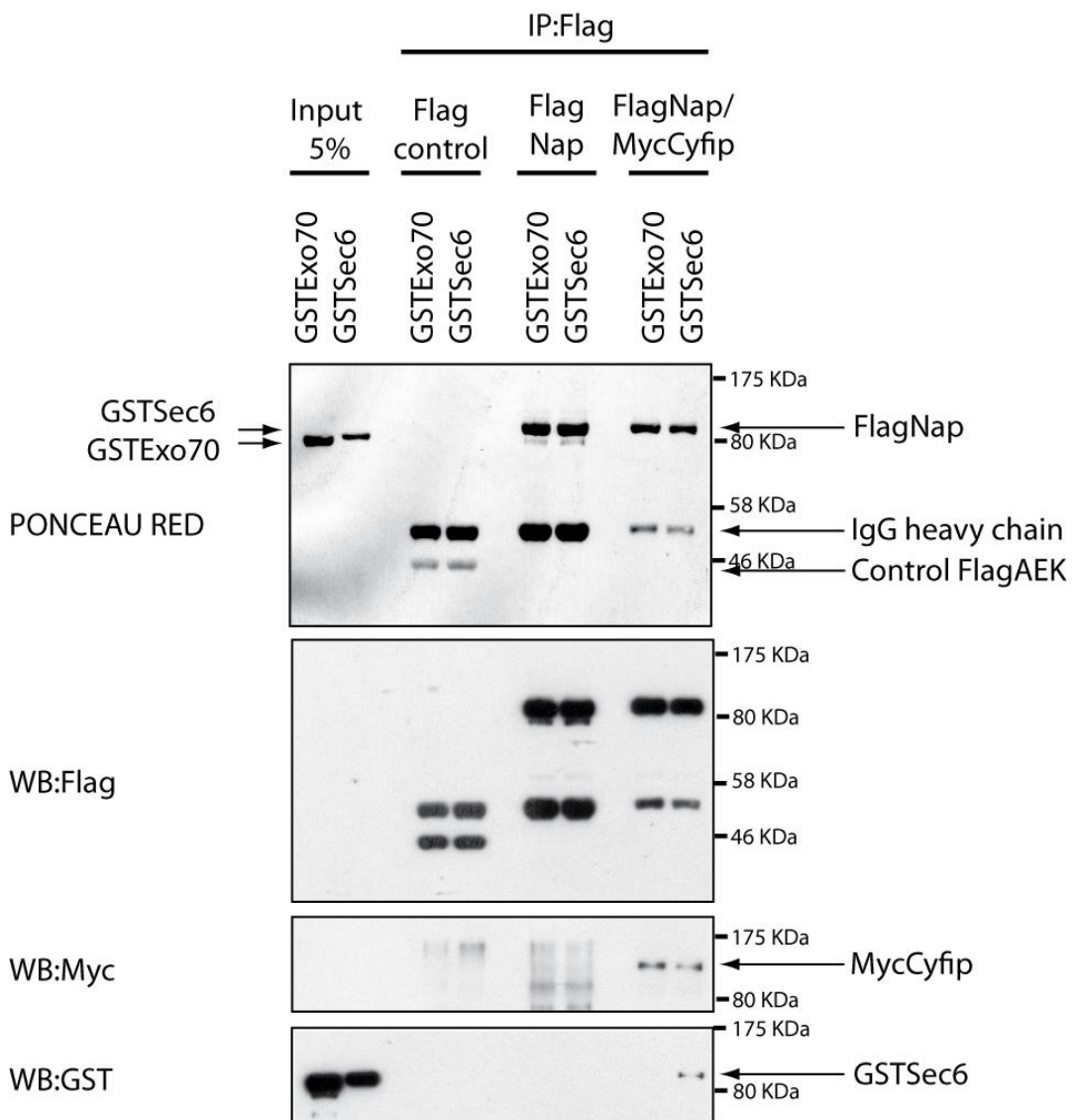
Figure R3. Cyfip interacts invitro with Sec6. GST-tag Exo70 and Sec6 proteins were purified from E.Coli. Flag-tag proteins were purified from 293 cells. As negative control we used flag-tag catalytically inactive Arno GEF (AEK). Immobilized Flag-tag proteins were incubated with soluble GST-Sec6 and GST-Exo70 (soluble protein negative control) and isolated by centrifugation before analyzing bound material by SDS-PAGE. Ponceau red and Flag western blot show Flag-AEK and Flag-Nap. Myc western blot shows MycCyfip complexed with FlagNap. GST western blot shows GST-Sec6 interacting with MycCyfip. 5% of the input was loaded.

1.1.4. WRC interacts in vitro with both Exo70 and Sec6

The previous experiments demonstrated that direct interactions between isolated components of the WRC and exocyst complexes, namely Abi-Exo70 and Cyfip-Sec6, can be revealed using cell-free in vitro system and purified proteins. Next, we asked whether Abi1 and Cyfip can interact with the exocyst subunits also when engaged in the formation of the whole pentameric WRC complex, which represent the physiological relevant and biochemically active multiprotein unit.

In order to achieve purification of the WRC complex, I exploited an efficient method recently published that employs 293T cells stably expressing various double tagged (Flag-HA) subunits of the WRC complex (Derivery et al., 2009).

The steady-state expression level remains relative modest, similar to physiological conditions, because the WRC subunits are quickly degraded when not incorporated in whole WRC complexes. Since the exogenous Flag-HA tagged subunits are expressed at very high rate, they molecularly replace the endogenous ones in the WRC complexes and their excess is cleaned by the degradation cellular machinery. A single-step purification with anti-Flag antibodies allows to quickly obtain a partially pure WRC complex,

with a good stoichiometric ratio of the 5 subunits (Derivery et al., 2009).

I purified the WRC complex using 293T cell lines stably expressing Flag-HA double-tag Abi1 (isoform a) or Cyfip subunit. I incubated the cell lysates from these cell lines with beads coupled to Flag antibody, and I kept the purified WRC complex on beads for the subsequent assays (see Materials and Methods). As control cell line, I used cells expressing the Flag-HA-stop peptide only.

The isolated WRC complex is nearly 90% pure as indicated by the coomassie staining, if we exclude the heavy-chain IgG band (Figure R4). Notably, Cyfip, Nap, Wave2 and Abi proteins are all present in the complex. Brick subunit (6 kDa) could not be detected under the conditions used because it runs out the gel due to its small molecular weight. Since based on previous evidence (Derivery et al., 2009) Brick is also part of the core WRC complex, we would expect Brick to be in the precipitates, but the use of different gels and of specific anti-Brick antibody wound be necessary to unequivocally make such statement.

It is also of note that Abi1 is more abundant in the precipitates when its Flag-HA-tag version is expressed and used for purification of the whole WRC complex. This may be due to the fact that the Flag-HA-Abi1 is expressed at a level slightly exceeding that of the other endogenous components of the complex (Figure R7). The fraction of Abi1 not engaged into the WRC complex is also efficiently immunoprecipitated.

Immunoblotting analysis with specific antibody further confirmed the presence and the identity of the various components of the WRC complex, including Flag-HA-Cyfip/Cyfip, Nap, Wave2 and Abi/Flag-HA-Abi.

Note the difference in the molecular weight between the epitope-tag, exogenous and the endogenous proteins (Figure R4). Endogenous Cyfip runs faster than the double-tagged ectopically

expressed one due to the Flag-HA tags. In the case of Abi, however, endogenous Abi runs slower than the double-tagged one, presumably because a number of different Abi1 spliced isoforms with higher molecular weight are frequently expressed in mammalian cells.
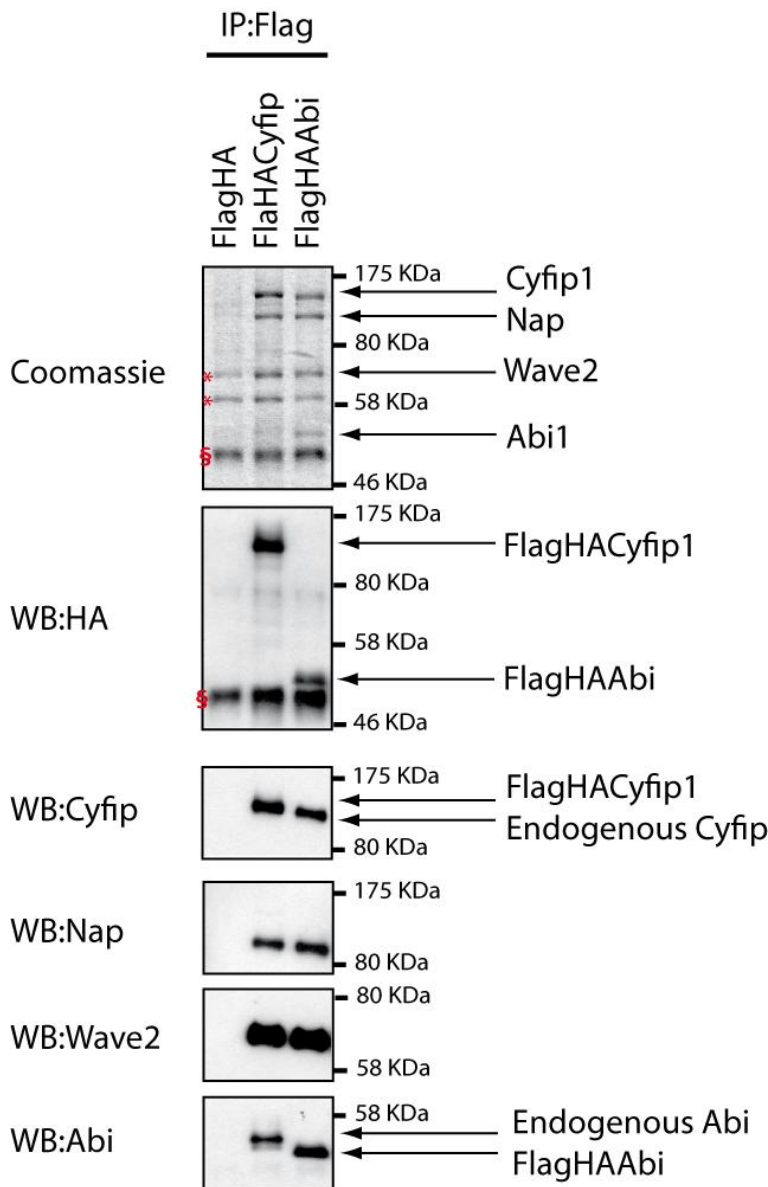

Figure R4. WRC complex purification. WRC was immunoprecipitated with immobilized anti-Flag antitbody from 293 cells either stably expressing Flag-HA-stop as control, or Flag-HA-Cyfip or Flag-HA-Abi. Commassie staining of the

immunopurified complex resolved on SDS-PAGE shows Cyfip (130KDa), Nap (110KDa), Wave2 (70KDa) and Abi1 (55KDa) when the complex is immunoprecipitated using Abi subunit. The IgG heavy chain is indicated by §. Non-specific bands are indicated by *. Immunoblotting with anti-HA antibody shows the HA-tag proteins Cyfip and Abi. Note difference in molecular weight between tagged and untagged proteins in Cyfip and Abi western blots. The western-blots confirmed the presence and the identity of the various bands.

In order to demontrate that GST-tag subunits Sec6 and Exo70 interact with Abi and Cyfip integrated into the WRC complex, I used the WRC complex purified and described upper.

I incubated 1 hour this bead-bound purified WRC complex with soluble GST-Sec6 and GST-Exo70. I used soluble GST as negative control. Both GST-tag exocyst subunits, but not the GST, bound the WRC complex. Notably, the Flag-HA-stop peptide control did not show any binding neither to GST-Tag exocyst subunits, nor to GST (Figure R5).
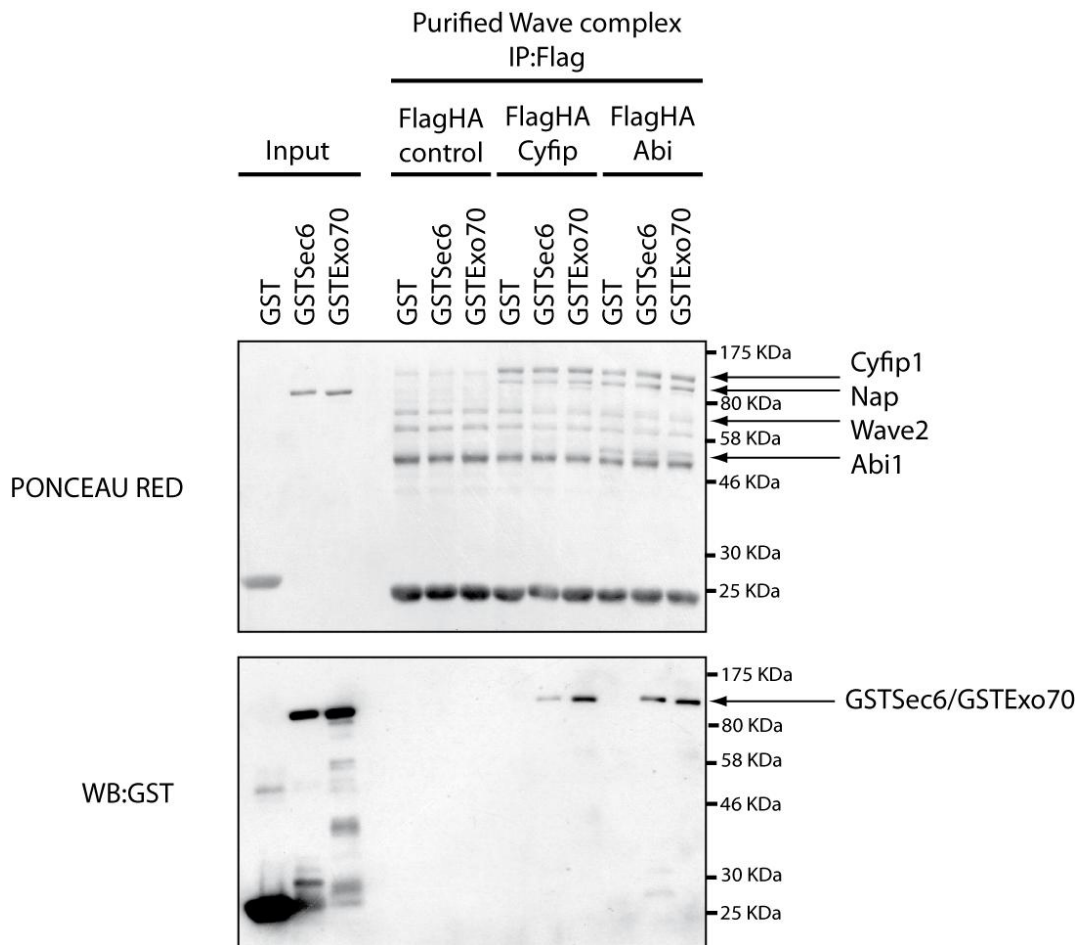
Figure R5. The WRC Complex interacts in vitro with both Exo70 and Sec6. GST-Exo70 and GST-Sec6 proteins were purified from E.Coli, eluted and incubated with the WRC complex immunopurified as described in Figure R4. GST and Flag-HA-stop peptide were used as controls. Immunoblotting analysis with anti-GST antibody shows that GST-Exo70 and GST-Sec6 bind specifically to the Flag-HA immunopurified WRC.

Collectively, these results indicate that the interaction between the WRC and the exocyst complexes is direct and presumably mediated by two independent protein:protein interaction pairs between Abi::Exo70 and Cyfip::Sec6. These interactions can occur either when Abi and Cyfip are isolated or when they are integrated into the whole WRC complex.

98

1.2. WRC INTERACTS WITH EXOCYST IN VIVO

To address whether the exocyst and WRC complexes associate *in vivo*, I performed co-immunoprecipitation experiments using 293T cells stably expressing epitope-tag subunits: Flag-HA-Cyfip1 or Flag-HA-Abi1 for WRC, and His-V5-Sec6 for exocyst. The level of expression of exogenous proteins was comparable to that of the endogenous ones. It was reported (Derivery et al, 2009) that the epitope-tag Cyfip and Abi1 can replace the endogenous subunits in the WRC. I observed that the level of expression of the epitope-tag Sec6 was comparable to that of the endogenous one and that the endogenous Sec6 is not detectable anymore in the whole lysates of cells expressing His-V5-Sec5, suggesting that, also in the case of the exocyst, exogenous Sec6 can molecularly replace endogenous Sec6 and becomes integrated into the endogenous exocyst complex (Figure R6). Based on these considerations, our next strategy consisted in immunoprecipitating the exogenous, epitope-tag subunits, which are presumably incorporated into the corresponding complexes and test for proteins binding to these multimolecular units by immunblotting.

1.2.1. Endogenous Cyfip co-immunoprecipitates with the exocyst complex

I performed exocyst complex immonoprecipitation from 293 cells stably expressing His-V5-Sec6. Immunoprecipitation with anti-V5 antibody pulled down, together with the most abundant epitope-tagged Sec6, other exocyst subunits, including Sec8, Sec5 and Exo70. In fact, all the exocyst subunits we could test with available antibodies were present in the immunoprecipitates (Figure R6). The finding that the stoichiometry of the exocyst subunits is different from the expected one unit of each component per complex after Sec6-based purification is not surprising, considering that the exocyst is not a stable complex,

but its composition changes with spatio-temporal dynamics which are largely unknown (White and Camonis, 2005).

I used two negative controls: anit-V5 immunoprecipitation from lysate of not-transfected 293 cells and immunoprecipitation with control IgG.

Immunoblotting with anti-Cyfip antibody indicated that endogenous Cyfip protein specifically co-immunoprecipitates with the exocyst complex (Figure R6).
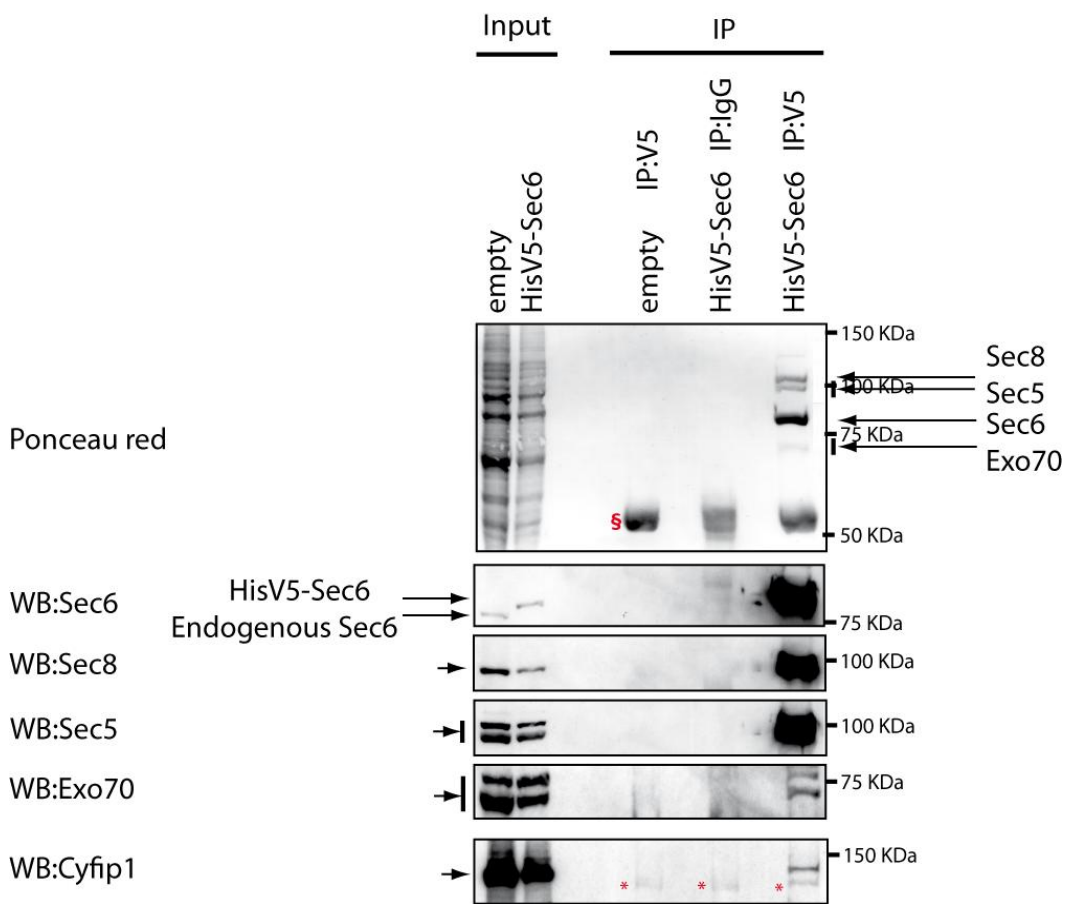
Figure R6. Endogenous Cyfip co-immunoprecipitates with the exocyst. *Exocyst V5 immunoprecipitation in 293 cells stably expressing His-V5-Sec6. The exocyst complex was immunoprecipitated with anti-V5 antibody as shown by Red Ponceau of proteins resolved by SDS_PAGE and the anti-Sec6, anti-Sec8, anti-Sec5 and anti-Exo70 immunostaining. Two*

*negative controls: V5 immunoprecipitation from not-transfected cells and IgG immunoprecipitation from His-V5-Sec6-expressing 293 cells. Cyfip Western Blot shows a fraction of endogenous Cyfip co-precipitated with the exocyst complex. § These bands are the IgG heavy chains. * Non-specific bands.*

1.2.2. Endogenous Exo70 co-immunoprecipitates with the WRC complex

As previously described, I purified the WRC complex by performing anti-Flag immunoprecipitations from 293 cells stably expressing one epitope-tag subunit, either Flag-HA-Abi1, or Flag-HA-Cyfip.

Ponceau red staining of SDS-PAGE-resolved immunoprecipitates clearly shows the individal subunits of the WRC complex: Cyfip, Nap1, Wave2 and Abi (Brick exited from gels because of its small molecular weight). In these series of experiments, the stoichiometry of WRC complex resulted well preserved throughout the purification, with each subunit being present roughly at an equal molecular ratio.

The staining with ponceau red revealed also the presence of non-specific bands at about 75 kDa and 55 kDa (the latter corresponding to IgG heavy chain)

Immunoblotting analysis with specific antibodies enable to identify the various subunits of the WRC complex, Cyfip, Nap1, Wave2, Abi and Flag-HA-Abi (Figure R7), and Flag-HA-Cyfip (Figure R8).

Remarkably, I found that endogenous Exo70 co-immunoprecipitated with the WRC complex obtained either from Flag-HA-Abi or from Flag-HA-Cyfip expressing cells, but not from control Flag-HA expressing cells.

Note that on whole cells lysates two bands of around 75 kDa are recognized by anti-Exo70 antibodies. Both bands, which

associate to the WRC complex, are specific since they disappeared after treatment with siRNA against Exo70 (Figure R10 B).

The results of this set of experiment strongly suggest that Exo70 can interact with Abi even when this protein is integrated into into the WRC complex.
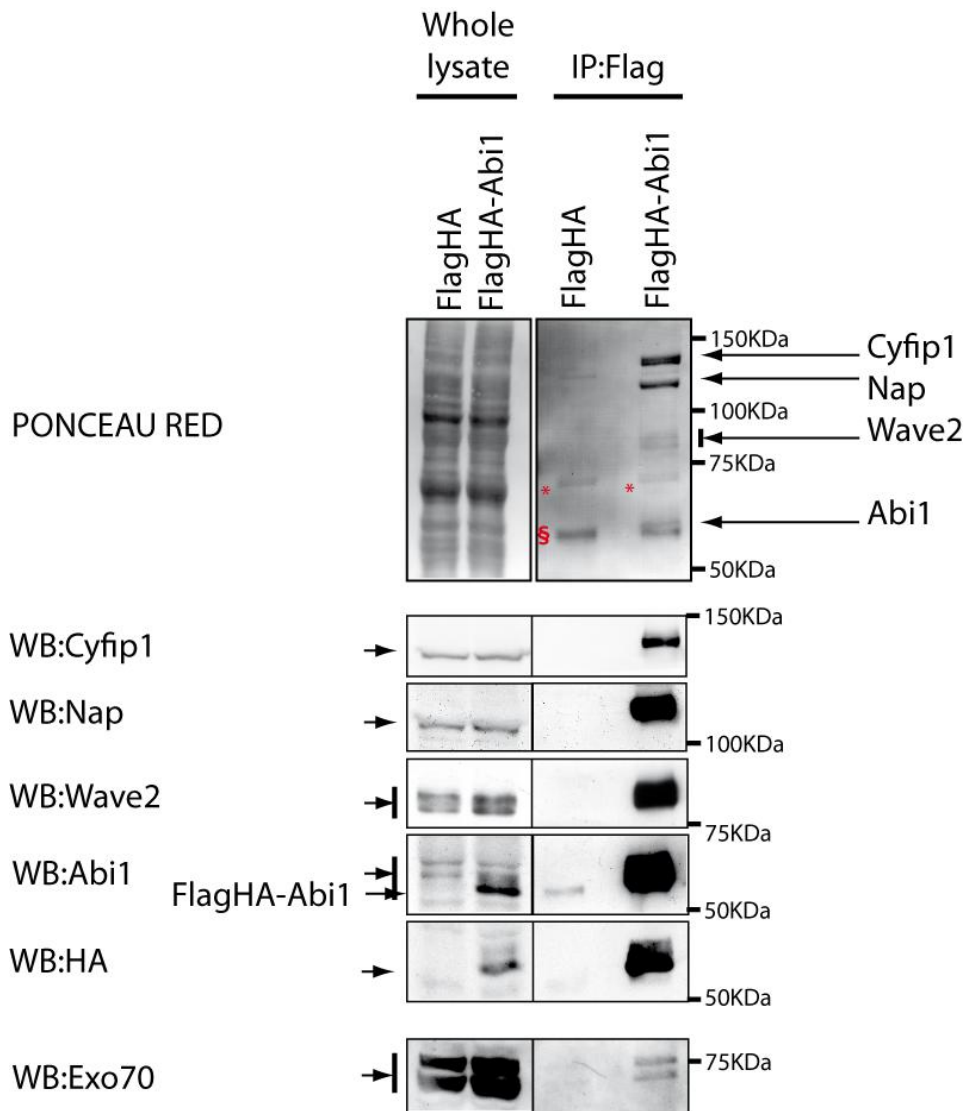
Figure R7. Endogenous Exo70 co-immunoprecipitates with the WRC complex. Co-immunoprecipitation Flag-HA-Abi - Exo70. *The WRC complex was purified by anti-Flag immunpecipitation as previously described. Ponceau red and westrern blots show the WRC complex subunits. Exo70 Western blot shows that endogenous Exo70 interacts specifically with*

the WRC complex. The IgG heavy chain is indicated by §. Non-specific bands are indicated by *.
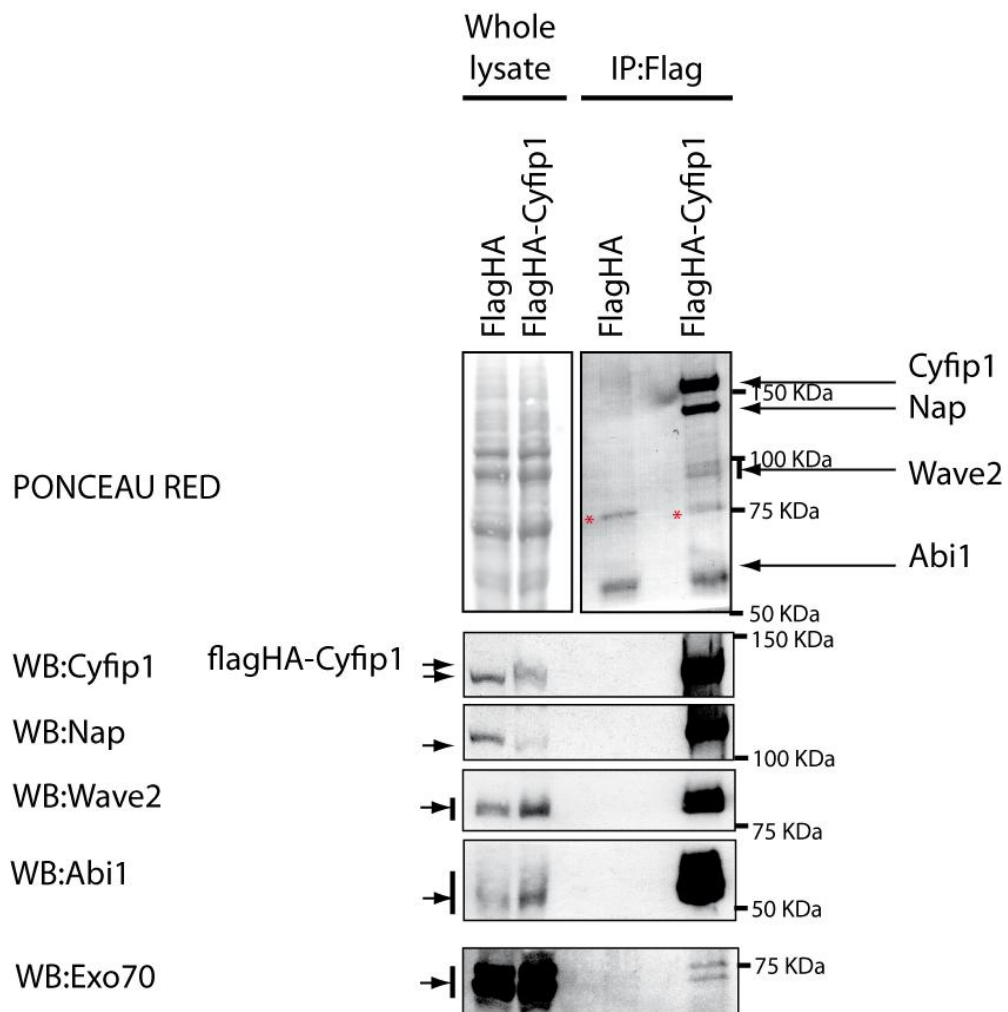

Figure R8

Figure R8. Endogenous Exo70 co-immunoprecipitates with the WRC complex. Co-immunoprecipitation Flag-HA-Cyfip - Exo70. The WRC complex was purified by anti-Flag immunpecipitation as previously described. Ponceau red and westrern blots show the WRC complex subunits. Exo70 Western blot shows that endogenous Exo70 interacts specifically with

103

1.2.3. The N-terminus of Abi1 mediates the interaction with Exo70

The two-hybrid assay suggested that the N-terminus of Abi was responsible for the association with Exo70. In order to characterize which region of Abi1 interacts with Exo70 in vivo, I overexpressed HA-Exo70 alone or together with YFP-Abi full-length (Abi1FL, 1-476), YFP-Abi lacking N-terminus (Abi1DN, 145-476, or YFP-Abi N-terminus (Abi1N, 1-145) (Figure R9 A) in 293 cells. Next, I performed an immunoprecipitation using anti-YFP antibody and analyzed pulled-down proteins by anti-YFP and anti-HA immunoblotting.

The different YFP proteins, including YFP alone that I used as control can be evidenced by immunoblotting with anti-YFP antibody. Immunoblotting with anti-HA antibody shows that HA-Exo70 strongly associated with full-length Abi1, but more weakly with the Abi N-terminus. The very faint band detectable with AbiDN is comparable to the YFP control, indicating that AbiDN cannot interact with Exo70. These results indicate that the N-terminus of Abi1 is required for binding to Exo70 and that the N-terminus alone is sufficient for binding to Exo70, albeit with reduced affinity as compared to full-length Abi1 (Figure R9 B).

A

B
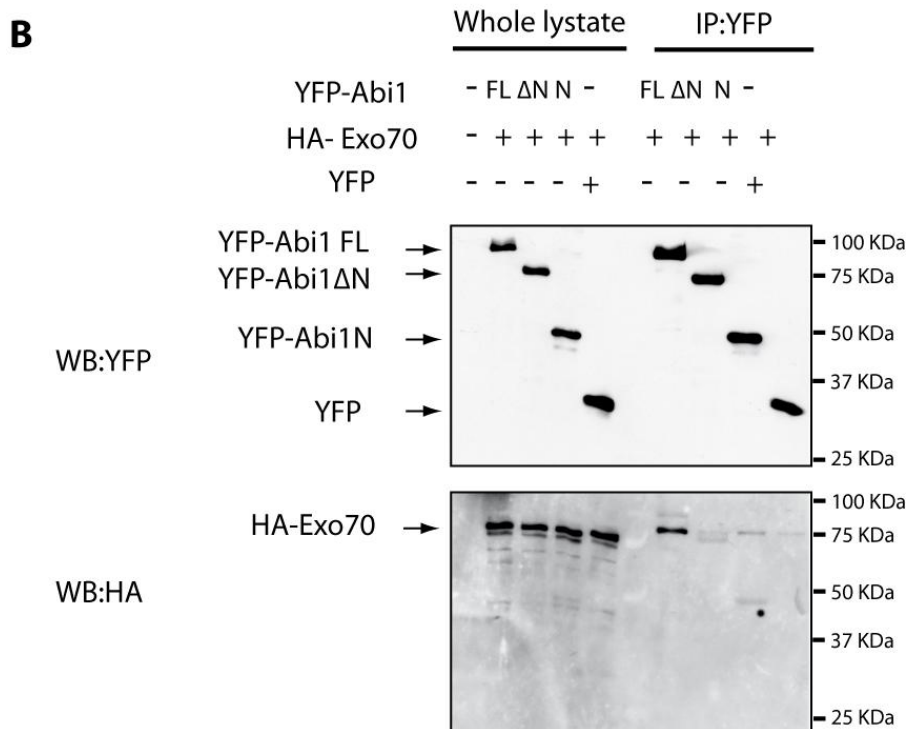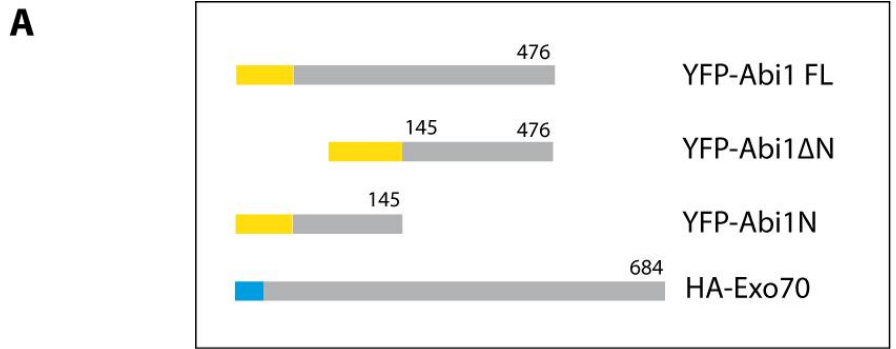
Figure R9. The N-terminus of Abi1 is required for binding to Exo70. (A) Diagram representing the various Abi1 and Exo70 constructs. *HA-Exo70 and different YFP-Abi1 fragments were used: full-length YFP-Abi1 (FL), YFP-Abi1 deleted of its N-terminus (DN), and YFP-Abi N-terminus (N).* **(B) Co-immunoprecipitation YFP-Abi – HA-Exo70.** *Vectors expressing HA-Exo70 and YFP-Abi (FL, DN, N) or YFP as control, were cotransfected as indicated, then immunoprecipitation against YFP was performed.*

2. FUNCTIONAL ROLE OF THE EXOCYST-WRC INTERACTIONS

2.1. DEPLETION OF THE WRC OR EXOCYST SUBUNITS INHIBITS CELL MOTILITY OF HEK-HT CELLS IN WOUND-HEALING ASSAY

Our biochemical results show that WRC and exocyst complexes can associate in vivo, but also indicate that a minor fraction of the total complexes is engaged in the binding since only small amounts of Exo70 (Figure R7 and R8) and Cyfip1 (Figure R6) are recovered in the immunoprecipitations.

We reasoned that the two complexes may interact in a temporal-limited and spatially-confined manner, and that their dynamic interactions may play some important roles in the regulation of cell motlity. We thus focus our investigation in trying to understand the function relevance of exocyst-WRC association in motile cells.

To this end we used HEK-HT cells as motility model (Hahn et al., 1999). By performing wound-healing assays and single-cell tracking analysis, I firstly confirmed that both the WRC and exocyst complexes are required for HEK-HT motility. Depletion of all tested WRC (Abi1, Wave2, Cyfip1) or exocyst (Sec5, Sec6, Sec8, Exo70, Exo84) subunits inhibited cell (Figure R10), under conditions in which no effects could be detected when RNAi oligos against unrelated proteins, such siLuc and siUSP9X (ubiquitin specific peptidase 9, X-linked) were used.

An interesting implication of RalA in this cell line was surprising. In fact, RalB but not RalA was shown implicated in migration (Lim et al., 2006; Oxford et al., 2005; Rossé et al., 2006). This can be explained by cell specific effect, or 2D migration effect, or finally by a lower threshold in exerimpent results.
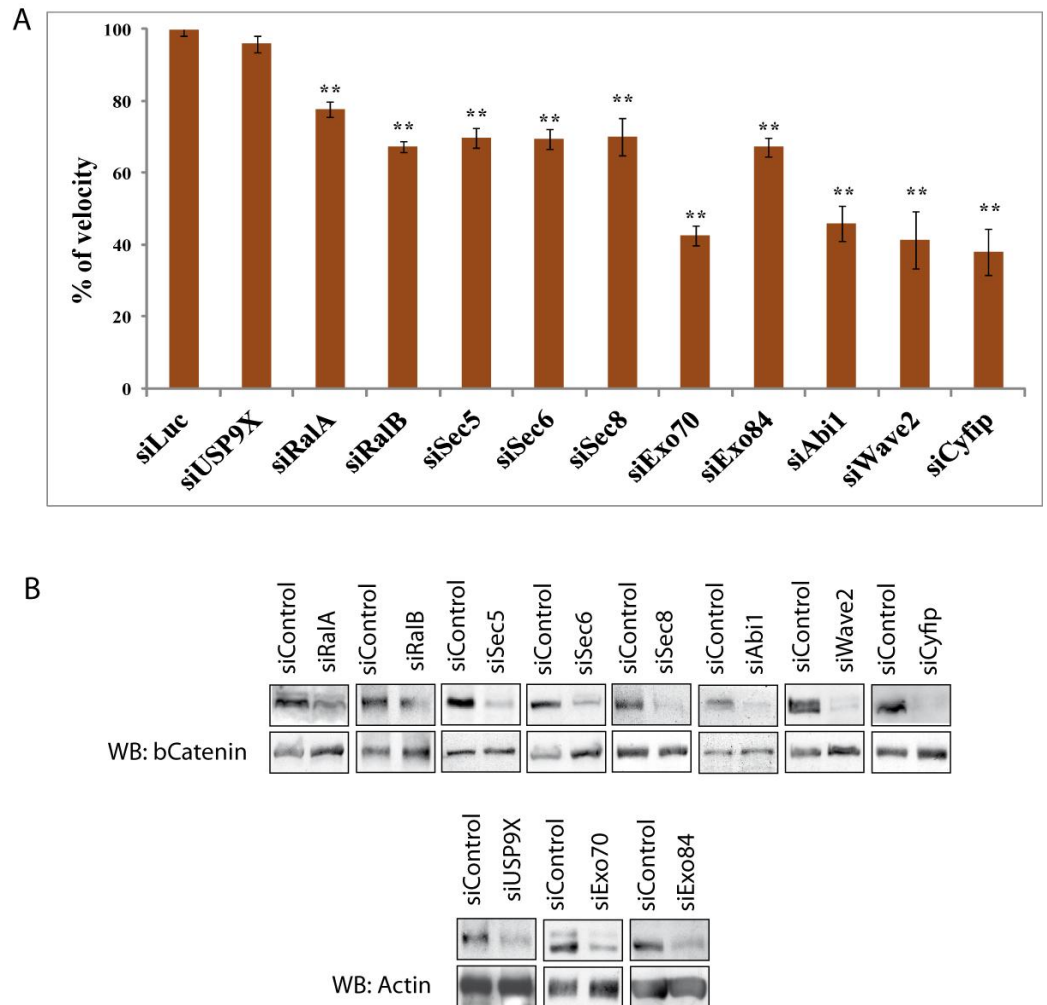
Figure R10. Depletion of WRC complex or the exocyst inhibits cell motility of* HEK-HT *cells in wound healing assay. (A) Depletion of Rals, exocyst or WRC inhibits wound healing cells motility. *Graph is percentage of velocity reported to siLuc control. Depletion of RalA, RalB, Sec5, Sec6, Sec8, Exo70, Exo84, Abi1, Wave2, Cyfip1 inhibits cell migration in wound healing assay. Data from six independent experiments, from 20 to 125 cell per condition. Error bar is SEM. Student test **<0.001.* ***(B) Validation of protein depletions.***

2.2. THE EXOCYST IS REQUIRED FOR THE LOCALIZATION OF THE WRC COMPLEX AT THE LEADING EDGE OF MIGRATING CELLS

Localization of the WRC complex at the leading edges of lamellipodia to nucleate actin is crucial for migration. We therefore asked whether the exocyst is important for the localization of WRC complex at the leading edge of migrating cells by depleting individually various exocyst subunits (Sec5, Sec6 or Exo70). For these experiments we used random motile HEK-HT cells on fibronectin substrate.

In control siLuc-treated cells, Wave2 is prominently and specifically localized at the tips of lamellipodia, which occupy the majority of the cell periphery (Figure R11 A).

To quantify Wave2 recruitment at the leading edges, I used Image J software to manually draw and measure the total cell outline (a) and the outline portions positive for Wave2 staining (b). The b/a ratios represent the "% of cell outline with Wave2".

71% of the outline of motile control cells presented recruitment of Wave2. However, When I depleted exocyst subunits (Sec5, Sec6 or Exo70), the percentage significantly decreased (Figure R11 B). Importantly, the depletion of these exocyst subunits did not change the total cell outline (Figure R11 C).

These results support the hypothesis of a critical role of the exocyst in the recruitment of the WRC complex to the leading edge of cell protrusions.

A

IF:Wave2

siLuc

siSec5

siSec6

siExo70

B

C
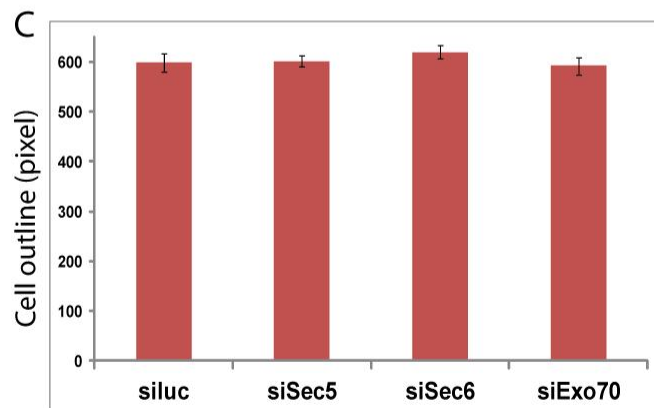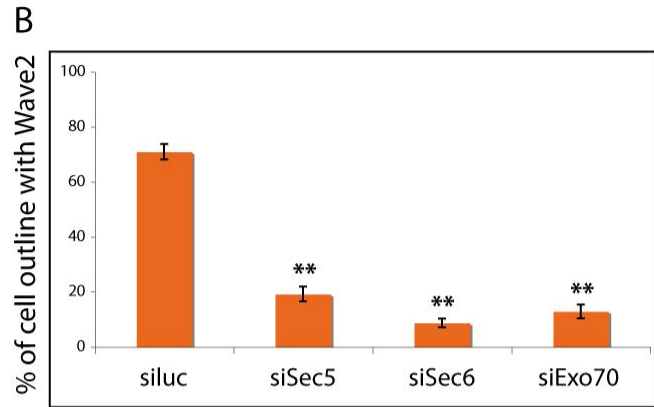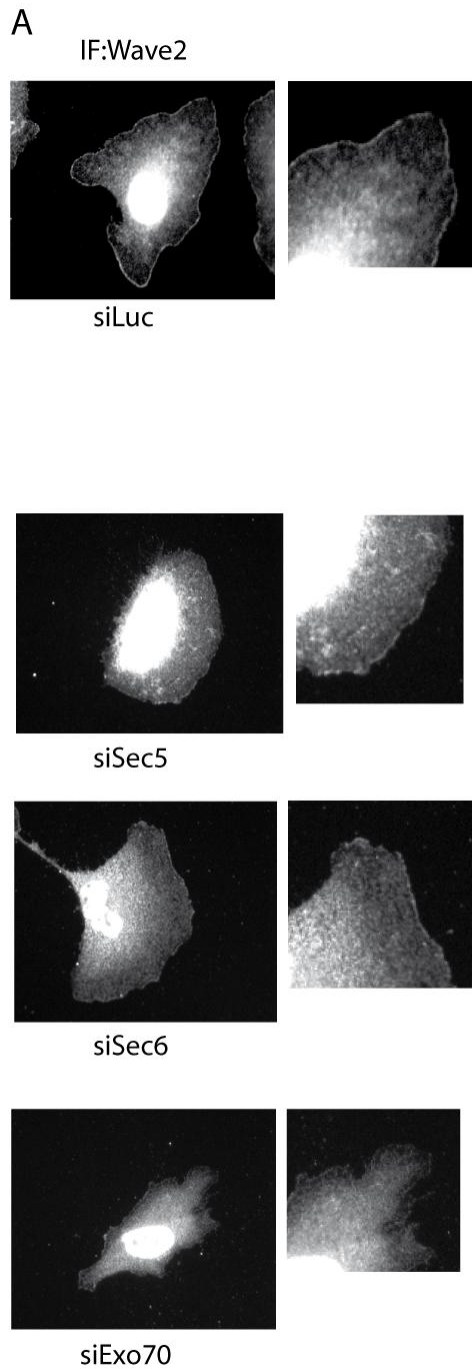
Figure R11. Functional studies of exocyst-WRC complexes interaction.
(A) Exocyst is required for Wave2 localization at the front of migrating cells. (A) Wave2 immunofluorescence on random-motile HEK-HT cells. Representative photos of

*Wave2 staining of migrating HEK-HT cells, depleted or not of exocyst subunits. **(B) Quantification of Wave2 recruitment at the cell outline.** The percentage of perimeter of the cell with positive staining for Wave2 was measured. Data from three independent experiments, ten cells per condition. **(C) Quantification of the cell outline of cells lacking the exocyst.** Error bar is SEM. Student test **<0.001.*

CHAPTER 3:
MOLECULAR AND FUNCTIONAL LINKS BETWEEN EXOCYST AND RAC VIA SH3BP1

1. THE RHOGAP SH3BP1 ASSOCIATES WITH THE EXOCYST

The two-hybrid screening had suggested a potential interaction between the N-terminal BAR domain of SH3BP1 and two exocyst subunits, Sec8 and Exo84. In order to verify whether SH3BP1 indeed associated in vivo with exocyst, I used a co-immunoprecipitation approach from 293T cells.

Since I could not succeed in co-immunoprecipitating endogenous exocyst subunits with endogenous SH3BP1, I had to overexpress at least one partner.

Overexpressed full-length SH3BP1 co-immunoprecipitated with endogenous Sec8. This interaction resulted to be mediated by BAR domain. In fact, when I used SH3BP1 deleted of the BAR domain, the interaction was abolished (Figure R12 B). This result is coherent with the two-hybrid data.

Moreover, by overexpressing Sec8 or Exo84 with full-length SH3BP1 or with SH3BP1 truncated of its C-terminus, I could show an interaction of both exocyst subunits with both SH3BP1 forms. Overexpressed Sec8 or Exo84 did not interact with SH3BP1 lacking the BAR domain (Figure R12 C and D).

In conclusion, both two-hybrid screen and co-immunoprecipitation experiments demonstrated that SH3BP1 binds to Sec8 and Exo84, and that this interaction is mediated by SH3BP1 BAR domain.
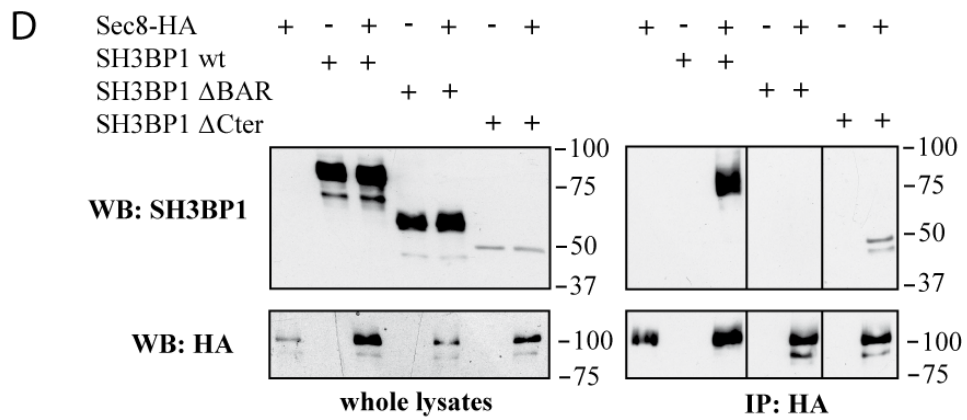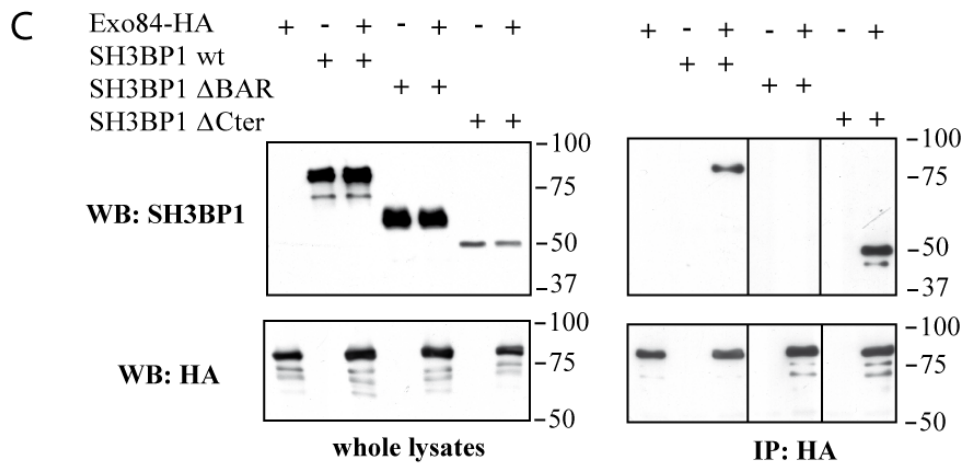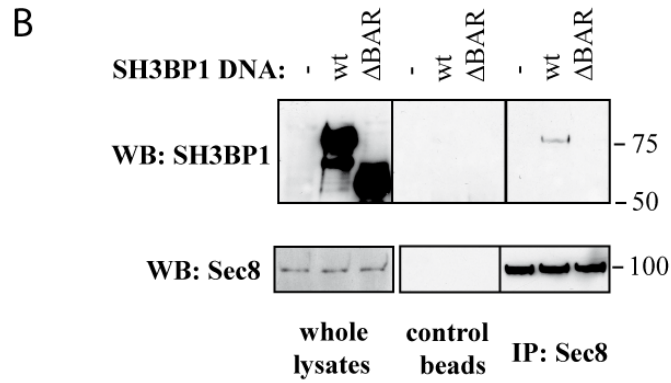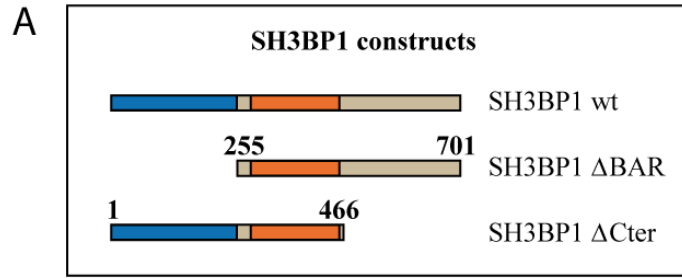
Figure R12. The RhoGAP SH3BP1 associates with the exocyst. (A) The three DNA SH3BP1 constructs used. Full-length wild-type SH3BP1 (wt), SH3BP1 lacking BAR domain (DBAR) and lacking C-terminus (DCter). (B) Endogenous exocyst interacts in vivo with SH3BP1. Vectors expressing SH3BP1 wt or SH3BP1 DBAR were transfected in 293T cells. Endogenous Sec8 was co-immunoprecipitated with anti-Sec8 antibodies covalently linked to beads. Upper western blot shows associated SH3BP1. (C) SH3BP1 co-immunoprecipitates with Exo84. Vectors expressing HA-tagged Exo84 and SH3BP1 (wt, DBAR, or DCter) were transfected into 293T cells. Exo84-HA was immunoprecipitated with anti-HA antibodies, and associated SH3BP1 was detected by western blotting. (D) SH3BP1 co-immunoprecipitates with Sec8. Vectors expressing HA-tagged Sec8 and SH3BP1 (wt, DBAR, or DCter) were transfected into 293T cells. Sec8-HA was immunoprecipitated with anti-HA antibodies, and associated SH3BP1 was detected by western blotting.

2. SH3BP1 LOCALIZES AT THE EDGE OF MIGRATING CELLS, TOGETHER WITH THE EXOCYST

2.1. SH3BP1 LOCALIZES AT THE LEADING EDGE

We were interested about localization of SH3BP1 in motile cells. I used normal rat kidney (NRK) cells in immuno-fluorescence experiments. Cell motility was induced by producing with a pipette tip a scratch in the confluent cell monolayer (wound-healing assay). By wide-field microscopy, I found that SH3BP1 localized at the advancing front of lamellipodia in control cells. This staining at the leading edge was specific because it disappeared in cells depleted of SH3BP1 and it was reproducible using three different antibodies (Figure R13 A). This localization of SH3BP1 at the front by immuno-fluorescence was also confirmed by confocal microscopy (Figure R13 C).

2.2. SH3BP1 COLOCALIZES AT THE LEADING EDGE WITH THE EXOCYST

We then studied the colocalization of SH3BP1 and exocyst. I performed double staining on NRK cells: SH3BP1 and Sec8 or Exo84. Confocal analysis showed that SH3BP1 is enriched at the same cellular locations as Sec8 or Exo84: the leading edges of lamellipodia (Figure R13 C).

2.3. SH3BP1 AND EXOCYST LOCALIZATIONS AT THE FRONT ARE MUTALLY DEPENDENT

We studied the effect of depletion of exocyst on SH3BP1 localization at the front, and viceversa. On one side, depletion of Sec8, Exo84 and Sec5 subunits by RNAi reduced SH3BP1 localization at the leading edge of migrating NRK (Figure R13 B). On the other side, depletion of SH3BP1 reduced recruitment of exocyst to the leading edge, Sec8 subunit in this experiment (Figure R13 D). This indicates that both SH3BP1 and exocyst are important for the localization of each other at the front of migrating cells.

2.4. THE BAR DOMAIN OF SH3BP1 IS REQUIRED FOR ITS RECUITEMENT TO THE FRONT

Exogenous full-length SH3BP1 localized at the front as the endogenous SH3BP1 (Figure R13 E). SH3BP1 lacking the BAR domain was not recruited to the front (Figure R13 E and F). This suggests that the BAR domain, presumably via its interaction with the exocyst, is important to the transport of SH3BP1 to the front. These results all together are supporting the notion that SH3BP1 associates with the exocyst at leading edge of migrating cells, where SH3BP1 may play a role locally in the regulation of migration.
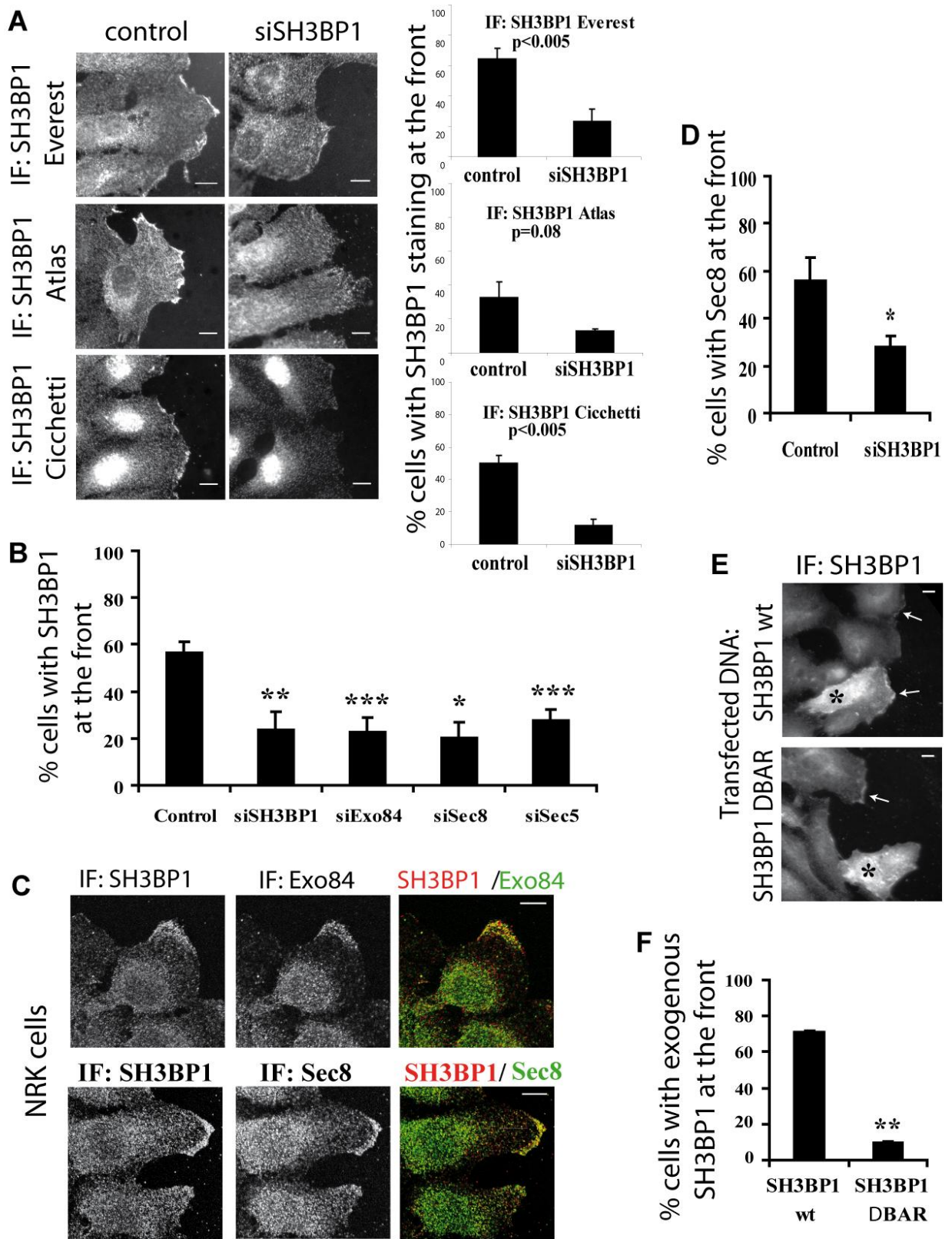
Figure R13. SH3BP1 Localizes at the Front of Motile Cells, Together with the Exocyst.

(A) SH3BP1 localizes at the front. Immuno-fluorescence staining for SH3BP1 was made on motile control or SH3BP1-depleted NRK cells. NRK cells were fixed during migration, and stained with one of three different antibodies against SH3BP1 (two commercial antibodies were bought from Everest Biotech and Atlas Antibodies; one home-made antibody was a gift from Dr. P. Cicchetti). Representative images show the result of 3 to 4 independent experiments. Graphs on the right show quantification of these experiments (mean percentages of cells showing SH3BP1 signal at leading edge; 100 cells per condition per experiment). Control is siRNA targeting Luciferase. Cicchetti antibody gives nonspecific nuclear signal. *(B) Effect of exocyst or SH3BP1 depletion on SH3BP1 recruitment to the front.* NRK cells were treated with siRNA targeting SH3BP1 (siSH3BP1-2) or exocyst subunits, fixed during migration and stained for SH3BP1. Graph shows percentage of cells having signal at the front. This quantification comes from 2 to 6 independent experiments (100 cells per condition per experiment). *(C) SH3BP1 colocalizes with Exo84 and Sec8.* Migrating NRK cells were costained for SH3BP1/Sec8 and SH3BP1/Exo84. On the right confocal microscopy merged images, generated using ImageJ software (NIH). *(D) SH3BP1 depletion disturbs exocyst localization.* Migrating NRK cells were depleted of SH3BP1 and stained for Sec8. Graph shows quantification of 3 independent experiments. *(E) BAR domain is required for SH3BP1 localization at the front.* Vectors expressing SH3BP1 wt or SH3BP1 DBAR were transfected into NRK cells, cells were stained for SH3BP1. Stars indicate transfected cells overexpressing SH3BP1 proteins. Arrows indicate endogenous or exogenous SH3BP1 signal at the front. *(F) Quantification of experiments in (E).* Quantification of three independent experiments. Bars on images indicate 10 um. Bars on graphics represent SEM. * indicates $p < 0.05$, **$p < 0.01$, and ***$p < 0.001$ (Student's t test).

3. SH3BP1 REGULATES CELLS MOTILITY

We investigated the functional implication of SH3BP1 in cell migration using wound healing assay. For quantitative read out of the role of SH3BP1 in migration, we used single cell-tracking analysis. In NRK cells, I efficiently depleted SH3BP1 via two independent siRNAs (Figure R15 C) and measured single cell velocity. Cell-tracking analysis showed that the speed of cell migration during wound closure was reduced by 30%–45%. It revealed also a slight but significant (10%–15%) decrease in persistence of migration (Figure R14).

We tested another in vitro migration assay, the Boyden chamber. Consistently with wound-healing assay results, it showed that cells lacking SH3BP1 cannot migrate. This migration defect was corrected by overexpressing the human form of SH3BP1 that is resistant to the SH3BP1 siRNA (see Supplemental article, Figure 3D).

This rescue of normal migration phenotype was obtained also in wound healing assay, by tracking cells expressing cherry-fused alleles of SH3BP1, in a SH3BP1-depleted or normal context. Cells depleted of endogenous SH3BP1 and expressing a siRNA-resistant SH3BP1 could migrate normally. But expression of a SH3BP1 R312A mutant, which impairs the GAP activity of SH3BP1, did not rescue migration. This indicates that the GAP activity of SH3BP1 is required for its function in regulating cell migration. Interestingly, neither the expression of SH3BP1 DBAR rescued cell migration. This shows that also the BAR domain is important for SH3BP1 function in cell migration (see Supplemental article, Figure 3E).

	n cells	velocity (μm/h)			persistence		
		mean	SEM	p value	mean	SEM	p value
control	85	44.96	1.24		0.89	0.01	
siSH3BP1-1	60	25.22	1.14	$<10^{-23}$	0.76	0.01	$<10^{-12}$
siSH3BP1-2	53	31.03	0.99	$<10^{-15}$	0.81	0.01	$<10^{-7}$

Figure R14. SH3BP1 regulates cell motility. Single cell-tracking analysis. Cell velocity and migration persistency were measured by cell tracking from 3 independent wound healing experiments, using ImageJ software. (p values are results of Student's t test).

4. RALB, EXOCYST AND SH3BP1 DO NOT CONTROL ORIENTATION OF MICROTUBULES ORGANIZING CENTER

It was shown by in vitro assays that RhoGAP domain of SH3BP1 has a GAP activity on Cdc42 and Rac1, but not RhoA (Cicchetti et al, 1995). We wanted to know whether in vivo, in migrating cells, SH3BP1 has a GAP activity on Rac or Cdc42 or both. During migration, microtubule-organizing center (MTOC) and Golgi apparatus reorient to face the wound. This phenomenon is controlled by Cdc42 (Ridley et al, 2003, Etienne-Manneville, 2004). Depletion of the RhoGEF b-Pix, a well-known activator of Cdc42 (but also of Rac in some circonstances), inhibits this reorientation of MTOC (Osmani et al, 2006).

I performed MTOC repositioning experiments in migrating cells. Depletion of b-Pix inhibited MTOC reorientation, as expected. However depletion of either RalB, different exocyst subunits (Sec5, Sec8, Exo84) or SH3BP1 did not disrupt MTOC positioning face to the wound (Figure R15 A). This shows that the RalB/exocyst/SH3BP1 pathway does not regulate cell migration by controlling MTOC reorientation, and that it does not control Cdc42 activity in migrating cells.

Moreover, overexpression of SH3BP1 DBAR, that cannot bind exocyst, did not disturb MTOC reorientation (Figure R15 B), meaning that interaction with exocyst is not the determinant for SH3BP1 to choose Rac instead of Cdc42. As positive controls in this experiment, I expressed dominant-negative (N17) or dominant-active (V12) Cdc42 mutants, which both perturbed MTOC positioning as expected.
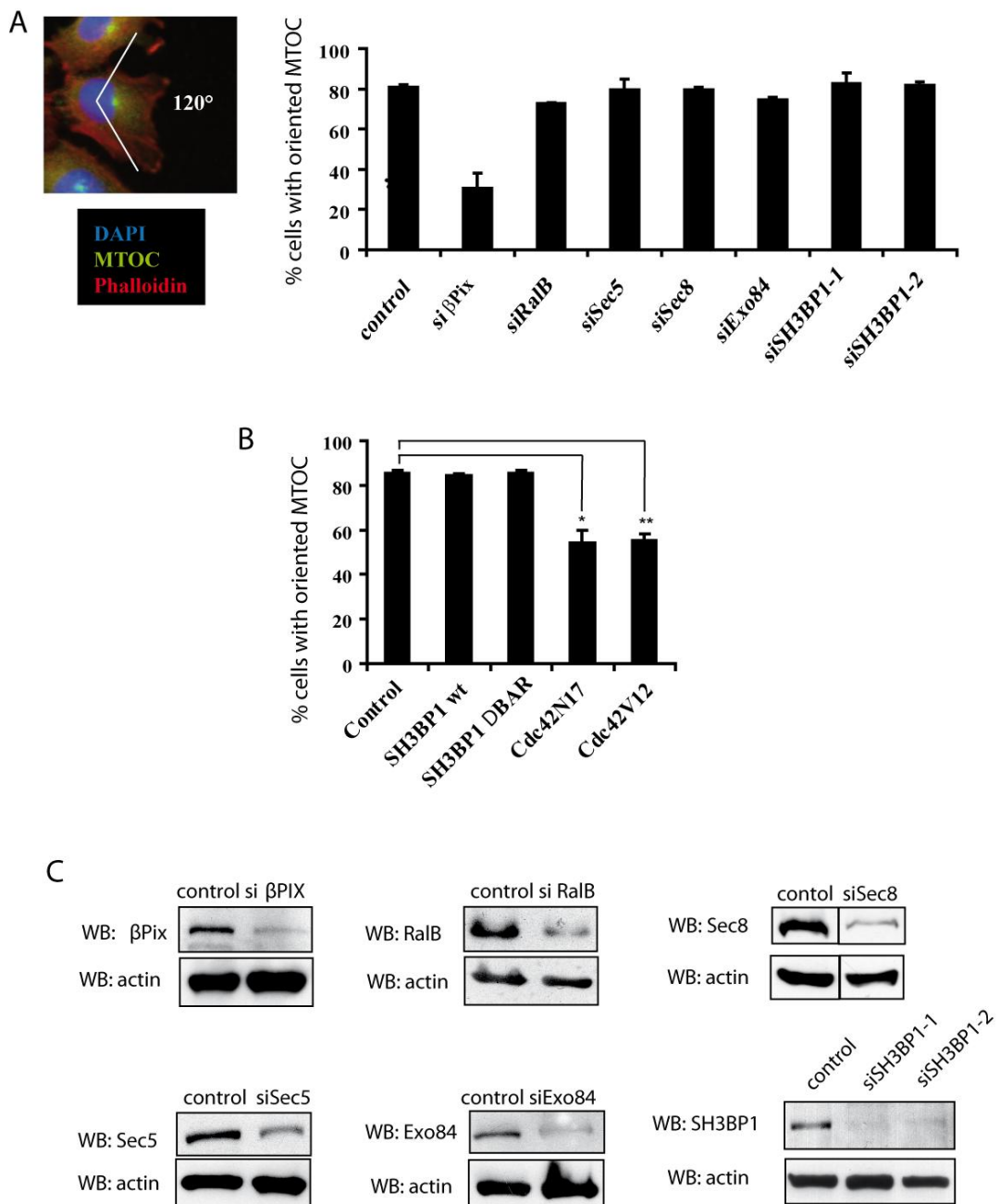
*Figure R15. RalB, exocyst or SH3BP1 do not control Microtubule-Organizing Center orientation during migration. (A) RalB, exocyst or SH3BP1 depletions do not disturb Microtubule-Organizing Center orientation. On the left, a representative photo of well oriented MTOC in a migrating cell (MTOC should be into an angle of 120 degrees). The MTOC was stained with anti-pericentrin antibodies, the nucleus with DAPI, and the actin fibers with phalloidin. On the right, quantifiation of MTOC orientation in migrating cells depleted with siLuc (control), sibPix, siRalB, siSec5, siSec8, siExo84, siSH3BP1-1, or siSH3BP1-2. 3 independent experiments, 100 cells per condition per experiment). (B) Expression of wild-type SH3BP1 or DBAR mutant does not perturb MTOC orientation. Exogenous wild-type SH3BP1 (wt), SH3BP1 DBAR, dominant-negative Cdc42N17 or dominant-active Cdc42V12 were expressed into NRK cells. Quantification was only on cells expressing exogenous proteins, which were identified by costaining with anti-SH3BP1 or anti-Cdc42 antibodies. Error bars represent SEM. ** indicates $p < 0.01$ (Student's t test). (C) Validation of Protein depletions. NRK cells were treated with the indicated siRNA (siLuc, siSH3BP1-1, siSH3BP1-2, siβPIX, siRalB, siSec5, siSec8 or siExo84). A portion of cells were used for wound-healing or MTOC experiments, the rest were lysed and analyzed by western blot with the indicated antibodies.*

5. SH3BP1 CONTROLS THE ORGANIZATION OF CELL PROTRUSIONS BY INACTIVATING RAC AT THE FRONT

A series of additional experiments performed in our group showed that the target of SH3BP1 in migration is Rac.

A FRET approach with Raichu biosensors (tools to monitor the spatiotemporal activation of Rac1 in living cells) was used to study the gradient of Rac activity at the front of motile cells (see Supplemental article, Figure 5A and Movie S2). Quantification of

Rac activity along a line in the direction of cell movement, from the nucleus to the leading edge, showed that the Rac1 gradient is significantly up-regulated when SH3BP1 is depleted (see Supplemental article, Figure 5C). We concluded that SH3BP1 is required to inactivate Rac1 at the front.

Since Rac1 activity regulates the formation of protrusions (Pankov et al, 2005; Raftopoulou and Hall, 2004; Ridley et al, 2003), we asked whether abnormally up-regulated Rac1 activity has an impact on protrusion dynamics in SH3BP1-depleted cells. Visualization of cell outlines of migrating cells showed that depletion of SH3BP1 induced delocalized and more numerous lamellipodia, leading to an efficient migration (see Supplemental article, Figure 6A and Movie S3). Computer-assisted analysis of morphodynamics demonstrated that the protrusions of migrating cells lacking SH3BP1 developed more rapidly but were more unstable, as compared to those of control cells (see Supplemental article, Figures 6C-H). We concluded that SH3BP1 is necessary for the spatiotemporal organization of protrusions during cell migration.

Importantly, both Rac activity up-regulation and protrusion disorganization in SH3BP1-depleted cells could be rescued by expression of siRNA-resistant wild-type SH3BP1, but not of the R312A GAP-defective mutant, strongly supporting the function of SH3BP1, via its GAP activity on Rac, in the spatiotemporal regulation of protrusions during cell motility.

Cells expressing GTP-hydrolysis-deficient RacG12V presented defects in motility and morphodynamics (see Supplemental article, Figures 7A-C). So, overexpression of active Rac1 mimics depletion of SH3BP1. Inactivation of Rac at the right moment and at the right place is crucial for formation of efficient lamellipodia.

DISCUSSION

DISCUSSION

RalB/exocyst pathway participates to cell migration (Lim et al., 2006; Oxford et al., 2005; Rossé et al., 2006). WRC complex is an important actor in cell migration by promoting downstream of Rac actin branch elongation and thus generating dendritic network supporting lamellipodia extension (Amann and Pollard, 2001; Takenawa and Miki, 2001). However, how RalB/exocyst and Rac/WRC pathways are coordinated during cell migration was still elusive at the beginning of my PhD.

To shed light on this question, I have studied the molecular and functional links between RaB/exocyts and Rac/WRC, which emerged from screenings previously performed in our laboratory.
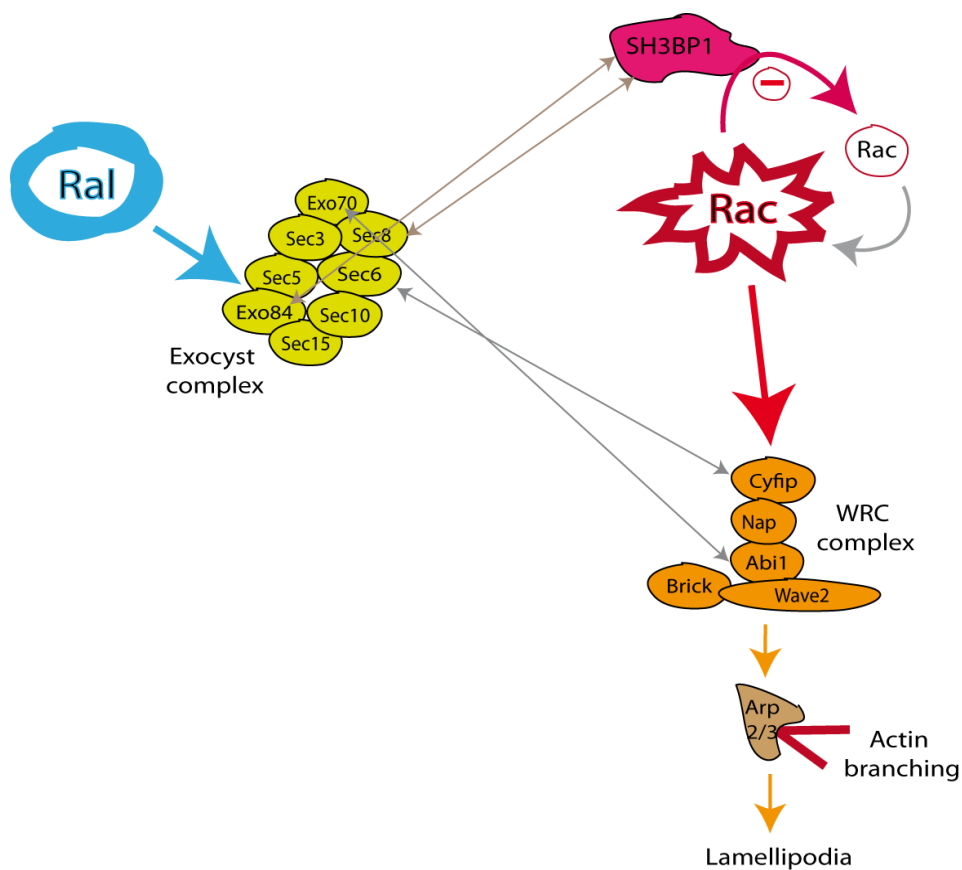
Figure D1: Summary of the cross-talk between Ral and Rac pathways in the control of cell migration.

1) THE SH3BP1 LINK

We demonstrated by several biochemical approaches that the exocyst associates with SH3BP1 and that this interaction is mediated by SH3BP1 BAR domain, confirming and validating the two-hybrid screening data.

In motile NRK cells, SH3BP1 is localized at the leading edge of cell protrusions (Figure R12 A and C), where also Sec8 or Exo84 are present (Figure R12 C). More relevantly, SH3BP1 localization depends on exocyst and conversely exocyst localization depends on SH3BP1 (Figure R12 B), indicating the importance of the interaction between SH3BP1 and the exocyst for their recruitment at the front of migrating cells.

Depletion of SH3BP1 decreases cell velocity (Figure R14 A and Figure R15 C), a defect that can be rescued by the Expression of a wild-type SH3BP1 form resistant to siRNAs, but not by the expression of GAP-deficient or BAR-deleted SH3BP1 (see article, Figure 3 D and E). This latter finding indicates that the GAP activity and the BAR domain of SH3BP1 are both important for migration.

The BAR domain is necessary for SH3BP1 binding to exocyst, for the localization of SH3BP1 at the front (Figure R13 E and F) and for SH3BP1 function in motility regulation. Thus, the BAR domain by its binding to exocyst, plays a critical role in SH3BP1 recruitment to the cell leading edge.

We proposed a model in which the exocyst recruits the RhoGAP SH3BP1 to the extending lamellipodia, where it may act locally as a GAP on RhoGTPases, to regulate cell migration.

Next, we had to identify the Rho-family target of SH3BP1 in motile cells.

Previous in vitro works had shown that the RhoGAP domain of SH3BP1 has GAP activity toward Cdc42 and Rac1, but not RhoA (Cicchetti et al, 1995). The fact that front-rear polarity, assessed

by the study of microtubule-organizing center (MTOC), is not perturbed by depletion of SH3BP1 (Figure R15 A), suggested that Cdc42 is not the likely target of SH3BP1 gap activity, leaving Rac1 as the most probable SH3BP1 substrate.

Interestingly, Ral/exocyst/SH3BP1 pathway regulates migration not by regulating cell polarity, but by controlling the directionality of migration. In fact, SH3BP1-depleted cells have persistency defects (Figure R14).

The final proof that Rac1 is indeed the target of SH3BP1 in motile cells came from the direct observation of localized Rac activity using a FRET-based Rac1 biosensor. I found that in SH3BP1 depleted cells, Rac1 activity is significantly up-regulated at the leading edge (see article, Figure 5C), but not in other parts of the cell. This result indicates that SH3BP1 is required to inactivate Rac1 at the leading edge.

Collectively, our data led us to propose the following model: the exocyst complex interacts with the RhoGAP SH3BP1 in order to transport it to the leading edge of lamellipodia where SH3BP1 may encounter and inactivate its target Rac1-GTP (Figure D2).

Many GEF proteins, have been proposed to mediate Rac activation at the leading front of migrating cells, these include bPIX (ten Klooster et al., 2006), DOCK3 (Sanz-Moreno et al., 2008), Asef (Itoh et al., 2008), and Tiam1 (Palamidessi et al., 2008). In particular, this latter work proposed that Rac activation may occur on endosomes. Endosome-localized and activated Rac may than translocate to the plasmamembrane via recycling contributing to spatial restriction and polarization of Rac signaling.

The presence of a GAP at the front is somewhat counterintuitive since activation rather than inactivation of this GTPases is expected to be critical to initiate and/or sustain signaling, leading to actin polymerization. However, this finding can be conceptualized assuming that a constant and spatially-

restricted turnover of Rac activity is required to properly regulate the dynamics of protrusions and adhesions during migration. Indeed, a number of reports indicates that the expression of constitutive active Rac promotes isotropic extension of lamellipodia and stabilizes focal adhesion, but inhibit directional motility, lending support to the notion that temporal and polarized activation of Rac is the critical event to sustain cell locomotion. Within this context, SH3BP1 may be an intrinsic component of a Rac built-in regulatory system aimed at promoting successive cycle of activation of Rac through localized delivery of both guanine nucleotide exchange factors as well as of GAP.
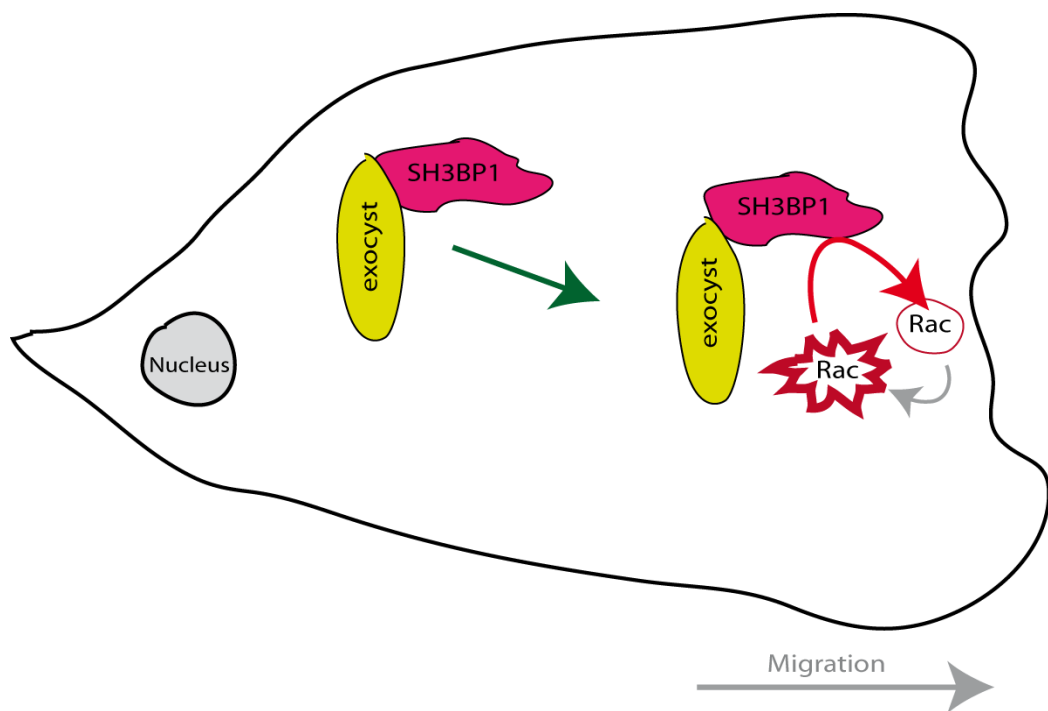
Figure D2: Model of exocyst-mediated recruitment of SH3BP1 to the leading edge, and inactivation of Rac at the front.

1) EXOCYST AND WRC BIOCHEMICAL INTERACTION

We found that two protein::protein interactions, Abi1::Exo70 and Cyfip::Sec6, mediate a direct association between the WRC and the exocyst complexes. Abi and Cyfip were found to interact with exocyst components both as free isolated proteins (Figure R2 B and R3) and as subunits integrated into the WRC complex (Figure R5).

We could roughly map the putative Exo70-binding interface on a region encompassing amino acid 36-145 of Abi by combining two-hybrid and co-immunoprecipitation data, However, the isolated N-terminus domain alone of Abi1 (aa 1-145) interacted with an apparent very low affinity with Exo70. This result suggests that other portions of the Abi protein likely contribute to Exo70 binding, or that additional Abi1-binding partners facilitate interaction with Exo70.

We further demonstrated the in vivo relevance of the interaction between exocyst and WRC by using cell lines stably expressing, at physiological level, an epitope tagged component of the WRC complex (Figure R7, R8 and R9). In the case of WRC complex, the immunoprecipitation shows the presence of all five components because the WRC complex is constitutive and stable (Gautreau et al., 2004), whereas the immunoprecipitation of the exocyst complex does not show all the subunits because the exocyst is much more dynamic, it is composed of at least two subsets, one on secretory vesicles and one as a secretion target on the plasma membrane (Guo et al., 2000; Guo et al., 1999 ; Guo et al., 1999b, Moskalenko et al,. 2003). This explains the

2) FUNCTIONAL ROLE OF EXOCYST-WRC INTERACTION

We found that Ral proteins, exocyst and the WRC complex are all implicated in migration of HEK-HT cells (Figure R10 A).

The implication of RalA in the migratory properties of this cell line was surprising. In fact, using other cell models, RalB but not RalA was shown to affect cell migration in other cell types (Lim et al., 2006; Oxford et al., 2005; Rossé et al., 2006). This could be due to a cell type specific effect.

The inhibitory effect on cell velocity (roughly 30 %) was similar for depletion of RalB and of most of exocyst subunits, with the notable exception of Exo70 the depletion of which resulted in a more marked inhibition of cell motility. Importantly, these effects were observed despite exocyst depletions was significant (~ 50 %), but never complete, suggesting that the amount of the core exocyst components is limiting for migration. It is of note that we could not assess whether exocyst is absolutely required for cell migration since the complete silencing of exocyst led to cell toxicity.

The impact of WRC and Exo70 depletion was stronger (roughly 60 % velocity inhibition). The more drastic inhibition of cell migration observed after Exo70 depletion might be due the fact that this protein, which is not part of the core exocyst complex, was shown to directly interact with Arp2/3 complex (Zuo et al., 2006) and/or with Abi. Notably, in yeast, Exo70p does not seem to be associated to vesicles, but it is stably localized at the plasmamembrane (Boyd et al., 2004). The stable position of the subunit Exo70 of the exocyst suggests that it may act as docking device for the delivery of vesicles. A similar situation may also occur in mammalian cells. In this system, thanks to its interaction with Phosphatidylinositol, Exo70 is crucial for the docking and fusion of post-Golgi secretory vesicles to the plasma membrane

(Liu et al., 2007). These peculiar features may account for the more essential role exerted by Exo70 on cell migration as compared to other exocyst components.

We studied the relation between exocyst and WRC localization at the leading edges of lamellipodia. It is generally accepted that if WRC is present at the edge this means that it is active. The molecular mechanisms accounting for the activation of WRC at this location have been recently clarified using biochemical Lebensohn and Kirschner, 2009) and structural approaches (Chen et al., 2010). The emerging model indicates WRC activity is the result of a set of integrated protein::protein and protein::lipid interactions, which concur in the proper modulation of WRC activation. Within this context binding of WRC to active Rac, its phoshorylation as well its association with plasma membrane localized PIP3 appears to act in synergy in promoting full, but spatially restricted activation of the complex at the plasmamembrane. Conversely, little remains known about the molecular mechanisms that bring the WRC complex to the plasmamembrane. Even though it has been proposed that active Rac may be sufficient to recruit the WRC complex to the plasmamembrane to promote actin branching (Miki et al., 1998; Steffen et al., 2004), other factors are very likely involved. Consistently, we found that the recruitment of Wave2 at the leading edge of random migrating cells is impaired in the absence of the exocyst (Figure R11 A and B), suggesting a role of exocyst, beside Rac, in directing the WRC at the sites of its action. We are currently repeating these experiments in a context of Rac activation (cells expressing RacV12), both in non migrating cells (HeLa) and in random motile cells (HEK-HT), in order to better characterize the respective contribution of Rac-GTP and of exocyst in WRC recruitment.

Overall our results are consistent with the model of exocyst working as carrier of WRC: the exocyst complex interacts with the WRC in order to transport it to the leading edge of lamellipodia where WRC can meet its activator Rac1-GTP (Figure D3).
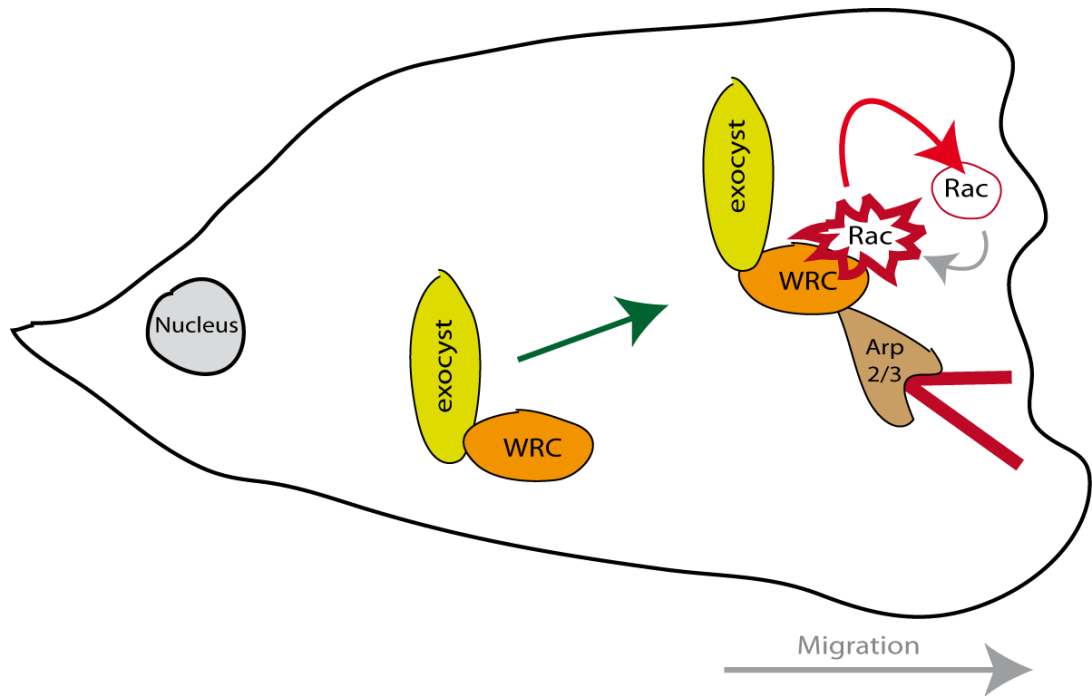
Figure D3: Model of exocyst mediated recruitment of WRC complex to the leading edge, in order to be activated by Rac-GTP and to promote actin branching.

According to this simple, yet speculative model, the exocyst may contribute to drive WRC to the leading edge, where it can bind to and become activated by Rac (via Cyfip). Activated, GTP-loaded Rac may subsequently trigger the dissociation of the exocyst-WRC interaction, freeing the exocyst for another round of transport. If the model if correct, we would expect that the WRC complex is unable to interact at the same time with both exocyst and active Rac. To validate this prediction, we are currently performing in

vitro competition experiments with purified proteins. Most specifically, we are testing whether the WRC-GSTSec6 association can be disrupted by adding purified active RacV12, but not inactive RacN17.

To further validate the relevance of our model, we also plan to perform live imaging experiments with fluorescent constructs of exocyst (Cherry-Exo70, Cherry-Sec6) and of WRC complex (GFP-Wave2, GFP-Abi1, GFP-Nap1 and GFP-Cyfip1). On one side, fast-acquisition video-microscopy will provide us with spatial-temporal information about the coordinated dynamics of these proteins. On the other side, fluorescence-lifetime imaging microscopy (FLIM) will be used to try to directly visualize in live motile cells the molecular interactions between exocyst and WRC complexes.

2) EXOCYST, AN ORGANIZER OF RAC PATHWAY

Our data add on the a set of emerging evidence which indicates that the exocyst complex is involved in many biological processes that require the targeting and tethering of vesicles to specific plasma membrane domains (Whyte et al., 2002; Lipschutz et al., 2002). One example is protrusion formation during migration. In fact, migrating cells need to establish a leading front, enriched by trafficked components important for lamellipodia extension (Hertzog and Chavrier, 2011).

The exocyst may be more than a structural multi-molecule entity helping the transport of vesicles to the plasmamembrane, it might be actively implicated in signaling by recruiting to lamellipodia important regulatory molecules, thus impacting on migration.

Strikingly, the exocyst appears to be linked to both downstream and upstream Rac pathways, acting on the one hand

on a Rac negative regulator, such as SH3BP1, a GAP specific for Rac at the cell leading edge, and on the other hand on a Rac effector (WRC complex). Exocyst may be essential to orchestrate a regulatory loop centered on Rac: activated Rac will switch on the WRC complex to promote actin branching and it will be inactivated by SH3BP1 (Figure D4).
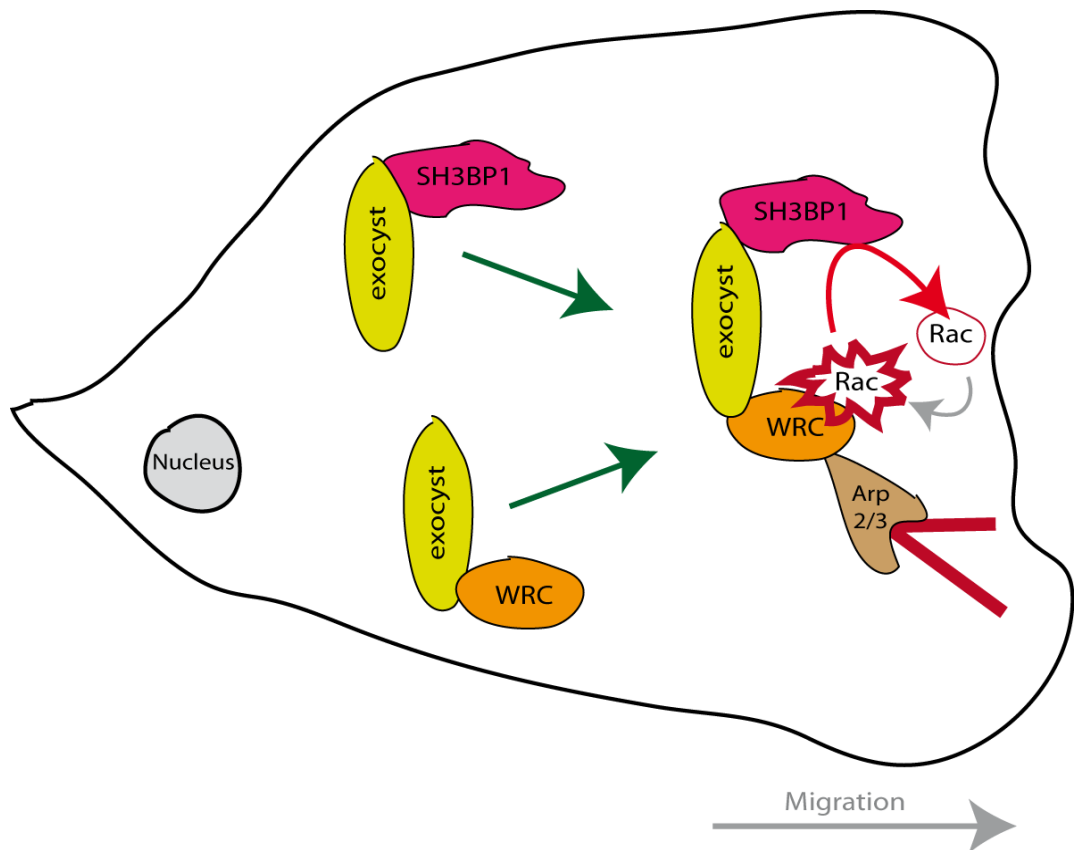
Figure D4: Integrative model of exocyst-mediated double recruitment of Rac regulator (SH3BP1) and Rac effector (WRC complex) to control motility at the leading edge.

5) PERSPECTIVES

This PhD work established the existence of a direct association between a major complex regulating exocytosis, the exocyst, and a major complex regulating actin dynamics, the WRC complex. In order to investigate in more detail the relevance of this novel association, in a variety of cellular functions, a very powerful tool would be the availability of mutants that disrupt specifically protein::protein association without perturbing the integrity and functionality of the whole complex.

Among the two complexes, the exocyst does not seem to be a good candidate in order to search for WRC-binding-deficient mutations. The exocyst is a dynamic complex, having different subunit composition depending on the biological process. Furthermore, crystal structures are solved only for portions of some of the subunits, but we are still far from the solution of the tertiary structure of whole exocyst complex. Conversely, the WRC complex seems to be a better candidate to identify specific mutation impairing the biding to the exocyst. The WRC complex is constitutive, very stable, and its crystal structure has been recently solved (Chen et al., 2010).

It remains to be established whether we need to identify interaction-impaired mutant of Cyfip or Abi1. Cyfip is a high molecular weight protein, relatively unstable. Furthermore, Cyfip minimal interaction domain with Sec6 defined by two hybrid assay is rather extended. Abi1 instead is a better characterized protein, relative stable even when isolated from the complex, and easier to manipulate than Cyfip. Moreover, Abi1 interaction domain with Exo70 was better defined both by two-hybrid assay and by co-immunoprecipitation experiments: it is the N-terminus region comprising the aa 36-145.

Furthermore, the structure of almost the entire Exo70 subunit, the Abi partner, is solved. In fact, structures of 62–623aa and 58–543aa yeast Exo70 (Dong et al., 2005; Hamburger et al., 2006) and of 85–653aa mouse Exo70 Moore et al., 2007) are available. In mutation design and analysis, we will need to keep in mind that Exo70 has distinct cell behavior comparing to the other exocyst components. Exo70 localizes at plasmamembrane (Boyd et al., 2004; He et al., 2007), and interacts with the PIP2 (Liu et al., 2007), and even Arp2/3 complex (Zuo et al., 2006), beside Abi.

By carefully comparing the Abi and Exo70 structures and by modeling potential binding interfaces, we plan to rationally design several mutations of Abi residues that interfere with Abi binding to Exo70 but not with its incorporation into the WRC complex. If the in silico analysis cannot be narrow enough to identify single aminoacid but only sequences, random mutagenesis by error-prone DNA polymerase may be performed on selected Abi sequences.

Thus, this Exo70-binding-deficient Abi mutant should still incorporable into WRC complex but should not bind anymore the exocyst complex.

The candidate mutations will be tested as follows. First, we will test by two-hybrid assay whether the Exo70-binding-deficient Abi mutants can bind Wave2, but not Exo70. Second, we will test the incorporation of the Exo70-binding-deficient Abi mutants in the WRC by co-immunoprecipitation strategies similar to those shown in Figures R6, R7 and R8.

The availability of Exo70-binding-deficient Abi mutants will allow us to ask important questions on the role of exocyst-WRC association.

In the context of cells depleted of endogenous Abi, we will able to compare the functional effect on migration, and also on other biological processes, of expression of a Exo70-binding-

deficient Abi mutant   with respect to the expression of wild-type Abi.

We will construct GFP-fusion of this Abi mutant, whose localization will be compared to that of GFP-Abi wild-type. This construct will be also used in two parallel live imaging approaches: fast-acquisition video-microscopy and fluorescent life time imaging microscopy (FLIM). By combining the use of this Abi mutant molecular tool together with powerful imaging techniques, we are expected to learn a lot on when, where, how and why the exocyst and WRC complexes meet inside the cells.

SUPPLEMENTAL ARTICLE

SH3BP1, an Exocyst-Associated RhoGAP, Inactivates Rac1 at the Front to Drive Cell Motility

Maria Carla Parrini,[1,2,*] Amel Sadou-Dubourgnoux,[1,2] Kazuhiro Aoki,[6] Katsuyuki Kunida,[6] Marco Biondini,[1,2] Anastassia Hatzoglou,[1,2,9] Patrick Poullet,[1,3,5] Etienne Formstecher,[4] Charles Yeaman,[7] Michiyuki Matsuda,[6] Carine Rossé,[1,2,8,10] and Jacques Camonis[1,2,8,*]
[1]Institut Curie, Centre de Recherche, Paris F-75248, France
[2]Inserm U830, Analysis of Transduction Pathways Group, Paris F-75248, France
[3]Inserm U900, Paris F-75248, France
[4]Hybrigenics Services SAS, Paris 75014, France
[5]Mines ParisTech, Fontainebleau Cedex F-77305, France
[6]Laboratory of Bioimaging and Cell Signaling, Graduate School of Biostudies, Kyoto University, Kyoto 606-8501, Japan
[7]Department of Anatomy and Cell Biology, Carver College of Medicine, University of Iowa, Iowa City, IA 52242-1109, USA
[8]These authors contributed equally to this work
[9]Present address: CNRS UMR5088, University of Toulouse, Toulouse 31062 Cedex 09, France
[10]Present address: UMR144, Institut Curie, Paris 75248 Cedex 05, France
*Correspondence: parrini@curie.fr (M.C.P.), jcamonis@curie.fr (J.C.)
DOI 10.1016/j.molcel.2011.03.032

SUMMARY

The coordination of the several pathways involved in cell motility is poorly understood. Here, we identify SH3BP1, belonging to the RhoGAP family, as a partner of the exocyst complex and establish a physical and functional link between two motility-driving pathways, the Ral/exocyst and Rac signaling pathways. We show that SH3BP1 localizes together with the exocyst to the leading edge of motile cells and that SH3BP1 regulates cell migration via its GAP activity upon Rac1. SH3BP1 loss of function induces abnormally high Rac1 activity at the front, as visualized by in vivo biosensors, and disorganized and instable protrusions, as revealed by cell morphodynamics analysis. Consistently, constitutively active Rac1 mimics the phenotype of SH3BP1 depletion: slow migration and aberrant cell morphodynamics. Our finding that SH3BP1 downregulates Rac1 at the motile-cell front indicates that Rac1 inactivation in this location, as well as its activation by GEF proteins, is a fundamental requirement for cell motility.

INTRODUCTION

Cell motility is a highly coordinated cellular process that relies on the precise spatiotemporal integration of various pathways (Ridley et al., 2003), and understanding the connections among migration-regulating molecular machineries is a major challenge in cell biology. Recent studies have identified a migration-regulatory pathway that emanates from the RalB GTPase and its downstream effector complex known as the exocyst (Lim et al., 2006; Oxford et al., 2005; Rosse et al., 2006). The exocyst is comprised of eight subunits and tethers secretory vesicles to the plasma membrane (He and Guo, 2009). Although RalB is known to control the assembly and localization of exocyst subunits at the leading edge of motile cells (Rosse et al., 2006), how the exocyst in turn controls migration remains uncertain. One contributing mechanism was revealed recently when the exocyst complex was shown to regulate the dynamics of cell-matrix adhesion by coordinating the activities of atypical protein kinase C (aPKC) and Jun N-terminal kinase (JNK) (Rosse et al., 2009). The exocyst is also thought to contribute to polarized delivery of regulatory molecules to the migration front, but clear experimental evidence for this is lacking.

The small GTPases of the Rho family (Cdc42, Rac, Rho) regulate cell motility by controlling the dynamics of the actin cytoskeleton (Raftopoulou and Hall, 2004). Specifically, Cdc42 is crucial for establishing front-rear polarity, Rac1 for producing networks of polymerized actin at protrusions, and RhoA for inducing actomyosin contractility. We reasoned that there should exist some regulatory mechanisms connecting the Ral/exocyst signaling pathway to the action driven by Rho family GTPases. In pursuing this possibility, we identified a molecular link for the coordination between Ral and Rac during migration: the RhoGAP SH3BP1, which partners with the exocyst complex to spatially restrict Rac1 activity. Specifically, SH3BP1 inhibits Rac1 activity by promoting the hydrolysis of bound GTP to GDP, and failure of this Rac1 inactivation leads to anarchic protrusions and ineffective migration.

RESULTS

The RhoGAP SH3BP1 Associates with the Exocyst Complex

SH3BP1 (SH3-domain binding protein 1, also known as 3BP-1; NP_061830) was identified in a series of yeast two-hybrid screens aimed at identifying partners of the eight subunits of the exocyst complex; it was found to bind to both the Exo84 and Sec8 subunits. SH3BP1 contains an N-terminal BAR
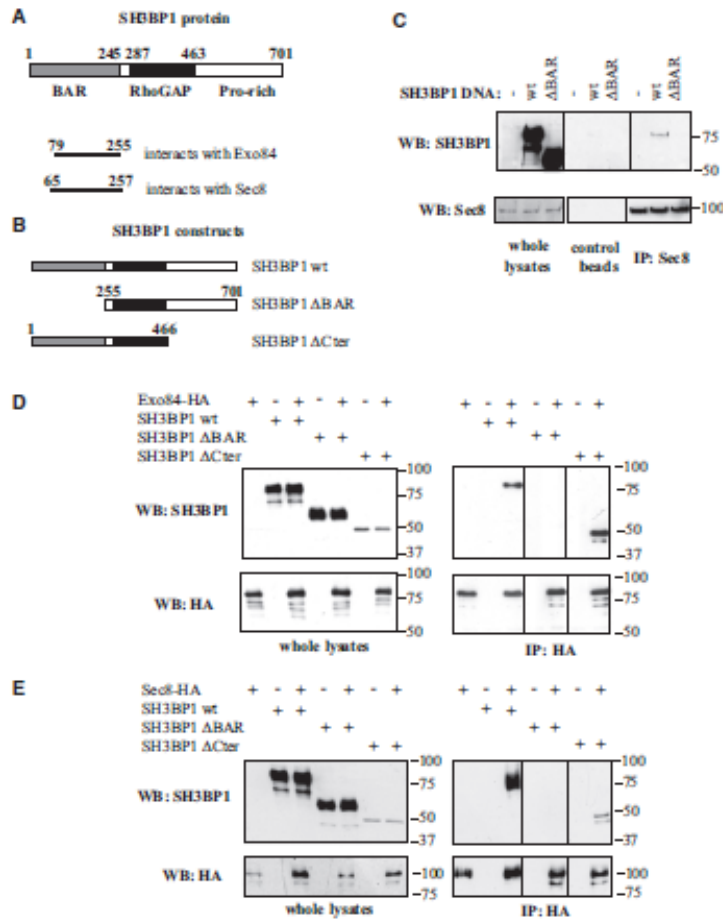
Figure 1. The RhoGAP SH3BP1 Associates with the Exocyst Complex

(A) Primary structure of SH3BP1 and two-hybrid results. The human SH3BP1 protein (701 amino acids) contains a BAR domain, a RhoGAP domain, and a C-terminal tail with several proline-rich motifs. The domains that are minimally required for the interactions with Exo84 and Sec8, as defined by two-hybrid screening, are shown.

(B) Constructs of SH3BP1 used in this work.

(C) Endogenous exocyst interacts in vivo with SH3BP1. 293T cells were transfected with vectors expressing wild-type (wt) or ΔBAR SH3BP1. Endogenous Sec8 was immunoprecipitated with anti-Sec8 antibodies covalently linked to beads. Associated SH3BP1 proteins were detected by western blotting with anti-SH3BP1 antibodies.

(D) Coimmunoprecipitation of Exo84 and SH3BP1. 293T cells were transfected with vectors expressing Exo84-HA and SH3BP1 (wild-type, ΔBAR, or ΔCter). Exo84-HA was immunoprecipitated with anti-HA antibodies, and associated SH3BP1 proteins were detected by western blotting.

(E) Coimmunoprecipitation of Sec8 and SH3BP1. 293T cells were transfected with vectors expressing Sec8-HA and SH3BP1 (wild-type, ΔBAR, or ΔCter). Sec8-HA was immunoprecipitated with anti-HA antibodies, and associated SH3BP1 proteins were detected by western blotting.

domain was deleted, this association was abolished, confirming that this domain is required for the interaction between SH3BP1 and the exocyst (Figure 1C). In these experiments, only a small fraction of SH3BP1 associated with the endogenous exocyst, possibly because of the large excess of overexpressed SH3BP1 or because of the highly regulated nature of the interaction. In addition, by overexpressing Exo84 or Sec8 along with various SH3BP1 forms (Figures 1B),

(Bin-Amphiphysin-Rvs) domain (putatively involved in protein-protein interactions and in binding to curved membranes), a central RhoGAP domain, and a C-terminal tail with several proline-rich sequences (Cicchetti et al., 1992). The smallest fragments of SH3BP1 recovered from the screens were amino acids 79–255 for the Exo84 interaction and amino acids 65–257 for the Sec8 interaction; thus the putative exocyst-interacting domain is in the N-terminal BAR-domain of SH3BP1 (Figure 1A). The SH3BP1-exocyst interaction appears to be specific since (1) SH3BP1 was the only BAR-containing protein identified in the exocyst screens, in spite of the fact that ten other BAR-containing proteins have been identified in other screens of the same library, and (2) the same SH3BP1 region was found in only one other screen, although more than 1200 screens have been performed on the same library with unrelated bait proteins (data not shown).

We demonstrated an association in vivo between SH3BP1 and the exocyst by showing that overexpressed full-length SH3BP1 coimmunoprecipitated with endogenous Sec8. When the BAR

we found that both of these exocyst components can interact with full-length SH3BP1 and with a SH3BP1 form lacking the C-terminal tail, but not with a SH3BP1 form lacking the N-terminal BAR-domain (Figures 1D and 1E).

Thus, both yeast two-hybrid and coimmunoprecipitation studies indicate that SH3BP1 binds to Exo84 and Sec8, and that these interactions are mediated by the SH3BP1 BAR-domain. We did not succeed in coimmunoprecipitating endogenous exocyst subunits with endogenous SH3BP1. We reason that if the two proteins interact only very locally, such an association would be masked by the vast excess of nonassociated exocyst and SH3BP1.

SH3BP1 Localizes at the Front of Motile Cells, Together with the Exocyst

We studied the localization of SH3BP1 in migrating cells. In normal rat kidney (NRK) cells, endogenous SH3BP1 was most prominently localized at the leading edge of motile cells (Figure 2A).

139
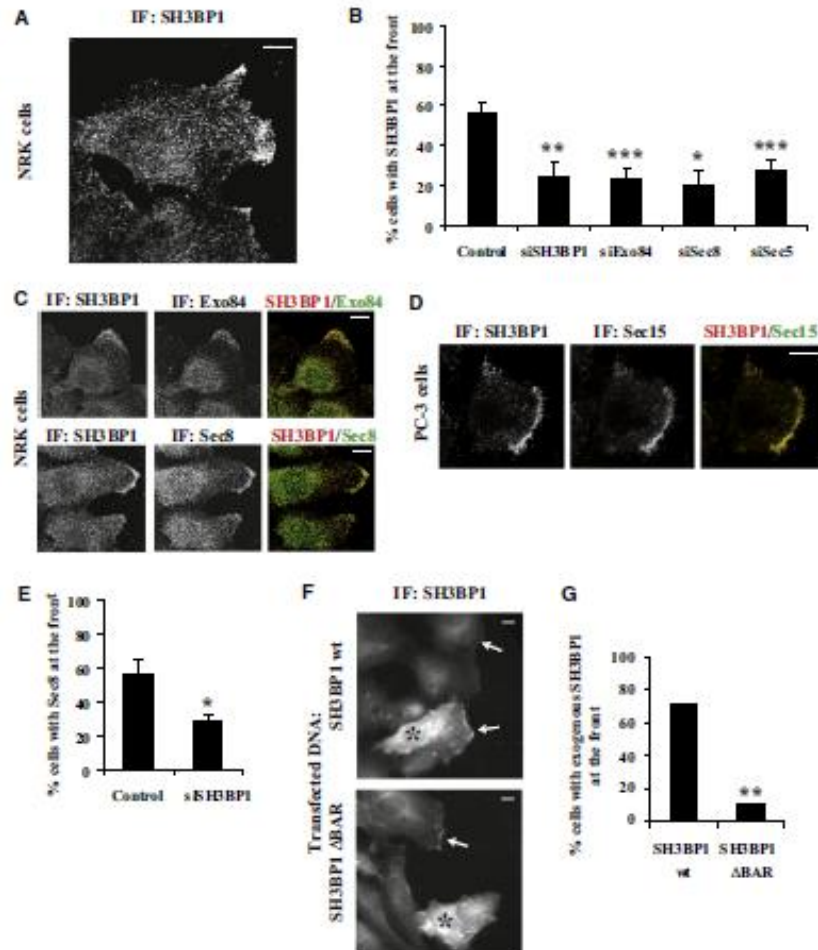
Figure 2. SH3BP1 Localizes at the Front of Motile Cells, Together with the Exocyst

(A) Localization of SH3BP1 at the front. NRK cells were fixed during migration, stained with an anti-SH3BP1 antibody (EverestBiotech), and observed by confocal microscopy.

(B) Effects of SH3BP1 or exocyst depletion on SH3BP1 recruitment to the front. NRK cells were treated with control siRNA targeting Luciferase (control), siRNA targeting SH3BP1 (siSH3BP1-2) or exocyst subunits, fixed during migration and stained for SH3BP1. Cells with a fluorescent signal at the leading edge were counted (at least 100 cells per condition per experiment) in two to six independent experiments per siRNA. The mean percentages of positive cells and the standard error of the mean (SEM) are shown.

(C) Colocalization of SH3BP1 with Exo84 or Sec8. NRK cells were costained for SH3BP1/Exo84 and SH3BP1/Sec8. Confocal microscopy merged images on the right were generated using ImageJ software (NIH).

(D) Colocalization of SH3BP1 with Sec15 at the leading edge of migrating prostate tumor PC-3 cells. Confluent PC-3 cell layers were wounded and allowed to heal for 6 hr. Cells were fixed and costained with anti-SH3BP1 and anti-Sec15 antibodies.

(E) Depletion of SH3BP1 affects exocyst localization. Motile NRK cells, treated with siLuc (control) or siSH3BP1-2, were stained for Sec8. Quantification was performed for three independent experiments.

(F) BAR domain is required to localize SH3BP1 at the front. NRK cells were transfected with vectors expressing SH3BP1 WT or SH3BP1 ΔBAR and stained for SH3BP1. Stars indicate transfected cells overexpressing the SH3BP1 proteins. Arrows indicate regions with endogenous or exogenous SH3BP1 at the front.

(G) Quantification of experiments in (F). Quantification was performed for three independent experiments. Notice that cherry-fused SH3BP1 WT and ΔBAR localized as their nontagged versions (data not shown).

Bars on images indicate 10 μm. Bars on graphics represent SEM. *indicates p < 0.05, **p < 0.01, and ***p < 0.001 (Student's t test). All cell images of this article were rotated such as motility direction is horizontal and rightward.

140

C

	n cells	velocity (µm/h)			persistence		
		mean	SEM	p value	mean	SEM	p value
Control	85	44.96	1.24		0.89	0.01	
siSH3BP1-1	60	25.22	1.14	$<10^{-23}$	0.76	0.01	$<10^{-12}$
siSH3BP1-2	53	31.03	0.99	$<10^{-15}$	0.81	0.01	$<10^{7}$

E

#	siRNA	DNA	n cells	velocity mu/h		p value	
				mean	SEM	versus # 1	versus #6
1	siLuc	cherry	17	31.07	2.22		0.31 ns
2		cherry-SH3BP1 wt	40	28.73	1.42	0.19ns	0.36 ns
3		cherry-SH3BP1 R>A	37	28.54	1.15	0.16 ns	0.32 ns
4		cherry-SH3BP1 ΔBAR	15	28.78	2.27	0.24 ns	0.39 ns
5	siSH3BP1-2	cherry	16	24.12	1.92	0.01 *	0.08 *
6		cherry-SH3BP1 wt	21	29.62	1.97	0.31 ns	
7		cherry-SH3BP1 R>A	28	24.58	1.12	0.01 *	0.02 *
8		cherry-SH3BP1 ΔBAR	42	25.58	1.18	0.02 *	0.04 *

Figure 3. SH3BP1 Regulates Cell Motility

(A) Depletion of SH3BP1 inhibits cell migration in wound-healing assay. NRK cells were transfected with siLuc (control) or siSH3BP1-2. Time-lapse acquisitions of a representative experiment are shown. See Movie S1 for the entire video sequence.

(B) Validation of SH3BP1 protein depletion. Efficiency of SH3BP1 depletion by two siSH3BP1s (siSH3BP1-1, siSH3BP1-2) was verified by western blotting.

(C) Cell-tracking analysis. Individual cells from three independent wound-healing experiments were tracked using the ImageJ software. P values are results of a Student's t test.

(D) Depletion of SH3BP1 inhibits cell migration, which is rescued by wild-type SH3BP1, but not by GAP-deficient SH3BP1. NRK cells were transfected with siRNAs (Luc or SH3BP1-2) and with DNAs (empty vector [–], wild-type SH3BP1 [WT], and R312A SH3BP1 [R > A]). 75,000 cells were added to the upper chamber and allowed to migrate for 6–12 hr, with the exact time varying from one experiment to another. Representative fields of crystal violet-stained cells that had migrated to the lower surface of the porous membrane are shown for control (Luc, –) and SH3BP1-depleted (SH3BP1, –) cells (left panel). Motility was expressed as a percentage of treated cells, relative to control cells (Luc, –), that had migrated to the lower chamber (right, upper panel). Mean motilities were calculated from four independent experiments. Bars represent SEM. * indicates p < 0.01, **p < 0.001, and ns (not significant) p = 0.1 (Student's t test). The level of exogenous SH3BP1 was roughly 10-fold that of the endogenous protein (right, lower panel).

(E) Wild-type SH3BP1, but neither GAP-deficient SH3BP1 nor ΔBAR mutant, rescues the migration defect of SH3BP1-depleted cells in wound-healing assay. NRK cells were transfected with siRNAs (Luc or SH3BP1-2) and with plasmids expressing either cherry alone or cherry-fused SH3BP1 WT, cherry-fused SH3BP1 R > A or cherry-fused SH3BP1 ΔBAR. Fluorescence images showed that expression levels of cherry constructs were similar. Red fluorescent cells were tracked during wound closure as described in (C).
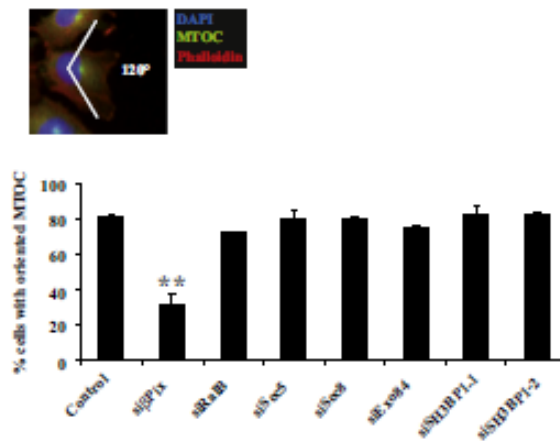
Figure 4. Depletion of RalB, Exocyst, or SH3BP1 Does Not Perturb the Orientation of the Microtubule-Organizing Center

NRK cells were treated with siLuc (control), siβPix, siRalB, siSec5, siSec8, siExo84, siSH3BP1-1, or siSH3BP1-2 and subjected to wound-healing experiments. The MTOC was stained with anti-pericentrin antibodies, the nucleus with DAPI, and the actin fibers with phalloidin. The mean percentage of correctly oriented cells, i.e., those in which the MTOC faced the wound (within a 120° angle) was calculated from at least three independent experiments for each siRNA. At least 100 cells per condition per experiment were counted. Error bars represent SEM. ** indicates p < 0.01 (Student's t test).

This staining at the leading edge was specific, was reproducible using three different antibodies (see Figure S1 available online), and was strongly reduced in cells depleted of SH3BP1 by RNAi (Figure 2B and Figure S1). Confocal microscopy analysis of cells costained for SH3BP1 and Exo84 or Sec8 showed extensive regions of colocalization at the leading edges of migrating cells, but not elsewhere in the plasma membrane or in the cytoplasm (Figure 2C). We confirmed that SH3BP1 also colocalized with the exocyst (Sec15 subunit) at the leading front in a second model for cell motility: wound healing in cultures of the human PC-3 prostate tumor cell line (Figure 2D). Depletion of exocyst components (Exo84, Sec8, Sec5) by RNAi reduced recruitment of SH3BP1 to the leading edge (Figure 2B) and, conversely, depletion of SH3BP1 reduced recruitment of the exocyst (Sec8 subunit) to the leading edge (Figure 2E), indicating that localization is mutually dependent. Taken together, these results are consistent with SH3BP1 and the exocyst being associated at the leading front, where SH3BP1 might contribute to the molecular machinery that is responsible for migration. While exogenously expressed full-length SH3BP1 localized to the front as does endogenous protein, the SH3BP1 ΔBAR construct was not recruited to the leading edge (Figures 2F and 2G), suggesting that the BAR domain and potentially the interaction with exocyst are required to transport SH3BP1 to the front.

SH3BP1 Regulates Cell Motility via Its GAP Activity

We assessed the contribution of SH3BP1 to cell migration by selectively depleting the SH3BP1 product via an RNAi approach. We first carried out wound-healing assays using NRK cells, and found that SH3BP1 depletion (>85%, with two independent

siRNAs) (Figure 3B) strongly inhibited wound closure (Figures 3A and Movie S1). Cell-tracking analysis indicated that average speed of cell migration during wound closure was reduced by 30%–45% in this context, and also revealed a slight but significant (10%–15%) decrease in persistence of migration (Figure 3C). SH3BP1 depletion also resulted in robust inhibition of wound closure in other cell lines, including HEK-HT (human embryonic kidney) and RPE1 (human retinal pigment epithelial) cells (data not shown), suggesting that the role of SH3BP1 in regulating cell migration is general and conserved.

Consistent with the wound-healing assays, Boyden chamber assays revealed that cells treated with a siRNA against SH3BP1 were defective in migration (Figure 3D). This defect was corrected by subsequent DNA transfection with a vector expressing a human form of SH3BP1 that is resistant to the SH3BP1 siRNA. In contrast to the expression of wild-type SH3BP1, expression of the R312A SH3BP1 mutant, whose GAP activity is impaired due to substitution of the critical "arginine finger" in the GAP domain (Bos et al., 2007) (Figure S2A), did not lead to the rescue of normal motility (Figure 3D). We confirmed these results by tracking cells expressing cherry-fused alleles of SH3BP1 in the context of a wounded monolayer where endogenous SH3BP1 had been depleted or not by RNAi. Speeds of cells in the different genetic contexts are listed in Figure 3E. Cells where endogenous SH3BP1 was depleted, but which expressed a siRNA-resistant SH3BP1, migrated as fast as control cells. This was not the case when a siRNA-resistant SH3BP1 R312A mutant was expressed, confirming the requirement of the GAP activity of SH3BP1. When the SH3BP1 ΔBAR allele was expressed, SH3BP1-depleted cells did not recover normal speed, pointing out the importance of the BAR domain for SH3BP1 function during migration.

RalB, the Exocyst Complex, and SH3BP1 Do Not Control the Orientation of the Microtubule-Organizing Center

The isolated RhoGAP domain of SH3BP1 displays GAP activity toward Cdc42 and Rac1, but not toward RhoA (Cicchetti et al., 1995), in vitro. We obtained similar results in vivo by expressing the full-length SH3BP1 protein together with FRET-based Raichu probes (Nakamura et al., 2006) (tools with which to monitor the activity of Cdc42, Rac1, and RhoA; Figures S3A and S3B). Consistent with the results of previous pull-down studies (Lu and Mayer, 1999), we observed a small preference for Rac1 rather than Cdc42 as substrate.

We questioned whether the physiological target of SH3BP1 in motile cells is Cdc42, Rac1, or both. Reorientation of the microtubule-organizing center (MTOC) and Golgi apparatus in front of the nucleus serves as a landmark of cell polarization during migration and is controlled by Cdc42 activity (Etienne-Manneville, 2004; Ridley et al., 2003). We confirmed that, as in previous studies (Osmani et al., 2006), the depletion of RhoGEF β-PIX strongly inhibited MTOC orientation in our cells under our experimental conditions. MTOC repositioning in front of the nucleus was not affected by the depletion of RalB, exocyst components (Sec5, Sec8, Exo84), or SH3BP1 (Figure 4). Western blot analysis confirmed that each of the tested proteins was efficiently depleted (Figure S3C and Figure 3B). Moreover, expression of SH3BP1 ΔBAR mutant, which is defective in

exocyst binding, did not perturb the MTOC orientation (Figure S3D), indicating that interaction with exocyst is not sufficient for SH3BP1 to select Rac over Cdc42 as substrate.

We conclude that the RalB/exocyst/SH3BP1 pathway does not regulate cell migration by controlling MTOC reorientation, and that it does not control Cdc42 activity in motile cells. It remains unclear how SH3BP1 constrains its biochemical activity on Rac1 in the context of cell motility.

SH3BP1 Is Required to Inactivate Rac1 at the Front

We directly tested the hypothesis that Rac1 is the SH3BP1 target relevant to cell migration, using a FRET approach with Raichu biosensors to monitor the spatiotemporal activation of Rac1 in living motile cells. In analyzing the first row of motile NRK cells that express Raichu-Rac1 (KRasCter; targeted to the plasma membrane via the K-Ras C-terminal tail) (Itoh et al., 2002; Nakamura et al., 2006) (starting acquisition and analysis 3 hr postwounding), we observed that Rac1 was activated in a dynamic gradient that grew more intense toward the leading edge, as previously reported for other cell types (Itoh et al., 2002; Kraynov et al., 2000). Control nonfunctional Raichu probes did not present a FRET gradient pattern and did not show any variation upon SH3BP1 silencing (Figure S4A). In cells treated with siSH3BP1, Rac1 appeared to be activated more strongly and across a broader area (Figure 5A and Movie S2). We quantitatively compared FRET signals on the total cellular area in control cells (n = 33) and SH3BP1-depleted cells (n = 28). The average Rac1 activity was only slightly higher in SH3BP1-depleted cells than in control cells (p = 0.07, Student's t test) (Figure 5B), indicating that the loss of SH3BP1 did not significantly affect the global levels of active Rac1. However, when we compared FRET signals spatially along a line going from the nucleus to the leading edge, we found that the average Rac1 gradient was significantly upregulated in siSH3BP1-treated cells compared to control cells (Figure 5C). These measurements indicate that SH3BP1 loss induced a localized, rather than global, defect in Rac1 activity. We obtained very similar results with another probe, Raichu-Rac1 (Rac1Cter), which includes the C terminus of Rac1 and therefore better reflects the localization of endogenous Rac1 (Figures S4B–S4D). Importantly, the spatial defect in Rac1 activity of SH3BP1-depleted cells was rescued by expression of wild-type SH3BP1, but not of the R312A GAP-defective mutant (Figure 5D). The action of SH3BP1 at the leading edge appears rather specific, since silencing of two other GAP proteins, p190RhoGAP and RLIP76/RalBP1, acting on Rac1 (Cantor et al., 1995; Jullien-Flores et al., 1995; Ligeti et al., 2004), did not perturb the Rac1 activity gradient (Figure 5E), despite their efficient depletion (Figure 5F).

Taking these results together, we conclude that the GAP SH3BP1 is required to locally downregulate Rac1 at the leading front.

Depletion of SH3BP1 Dramatically Perturbs the Organization and Dynamics of Cell Protrusions

Since Rac1 activity intimately regulates the formation of protrusions (Pankov et al., 2005; Raftopoulou and Hall, 2004; Ridley et al., 2003; Wu et al., 2009), we asked whether abnormally upregulated Rac1 activity has an impact on protrusion dynamics

in SH3BP1-depleted cells. We addressed this question by using a membrane-targeted fluorescent RFP protein (RFP-CAAX) to visualize movement of the cell periphery, and comparing videos of migrating SH3BP1-depleted and control cells (Figure 6A and Movie S3). Visual inspection of several movies revealed that the large majority of control cells had only one dynamic, well-defined lamellipodium toward the front. The protruding front in siSH3BP1-transfected cells was longer than that in control cells (average distance between nucleus and leading edge, 27.5 μm, SEM = 1.6 μm versus 21.3 μm, SEM = 1.3 μm; p < 0.005, Student's t test) and was often discontinuous, forming multiple subprotrusions. As a consequence, the average number of active protrusions per cell was higher in SH3BP1-depleted cells than in control cells (1.59 versus 1.17; p < 0.005, Student's t test), and the percentage of ectopic protrusions (those not within the 120° angle facing the wound) increased from 12% in control cells to 22% in SH3BP1-depleted cells (Figure 6B).

To objectively examine the role of SH3BP1 in plasma membrane morphodynamics, we performed a computer-assisted analysis of time-lapse images. We first measured velocities of movements at the cell edge, generating velocity maps for control and SH3BP1-depleted cells (Figures 6C and 6E). Edge fractions were classified into three categories: retracting, when velocity was lower than −2.5 μm/10 min; static, when velocity was between −2.5 μm/10 min and +2.5 μm/10 min; and protruding, when velocity was higher than +2.5 μm/10 min. We found significant increases in both the retracting and protruding edge fractions in siSH3BP1-treated cells, indicating that the leading edges of SH3BP1-depleted cells moved faster than those of control cells (Figure 6G).

We also quantified the stability of membrane dynamics at the cell edge by using the mathematical tool of autocorrelation analysis as previously reported (Dobereiner et al., 2006; Maeda et al., 2008). Autocorrelation is the spatiotemporal cross-correlation of the signal (the edge velocity in our case) with itself. We generated autocorrelation maps of the edge velocity as a function of time (minutes of the videos of the moving cells) and of space (along the cell periphery). Whereas control cells exhibited an ordered pattern as expected for typical directional migration (Figure 6D), SH3BP1-depleted cells showed a much less ordered pattern (Figure 6F), indicating that protrusion formation during migration of the latter cells is random and instable. Plotting temporal cuts of autocorrelation maps (ΔCell periphery = 0 degrees; broken white arrows in Figures 6D and 6F) revealed that, although autocorrelation coefficients were fairly stable over time in the case of control cells, they decayed rapidly in the case of SH3BP1-depleted cells (Figure 6H). Thus, the persistence of protrusion and retraction dynamics in SH3BP1-depleted cells was significantly reduced compared to those in control cells. We could correct the morphodynamics defect of SH3BP1-depleted cells by expressing wild-type SH3BP1, but not the R312A GAP-defective mutant, as shown by an analysis of the autocorrelation coefficients at Δt = 10 min (Figure 6I and Figure S5). This rescue result strongly supports a direct role of SH3BP1 GAP activity in the stability of membrane dynamics of motile cells.

Since in comparison to protrusions in control cells those in SH3BP1-depleted cells are more numerous, partially delocalized,

143
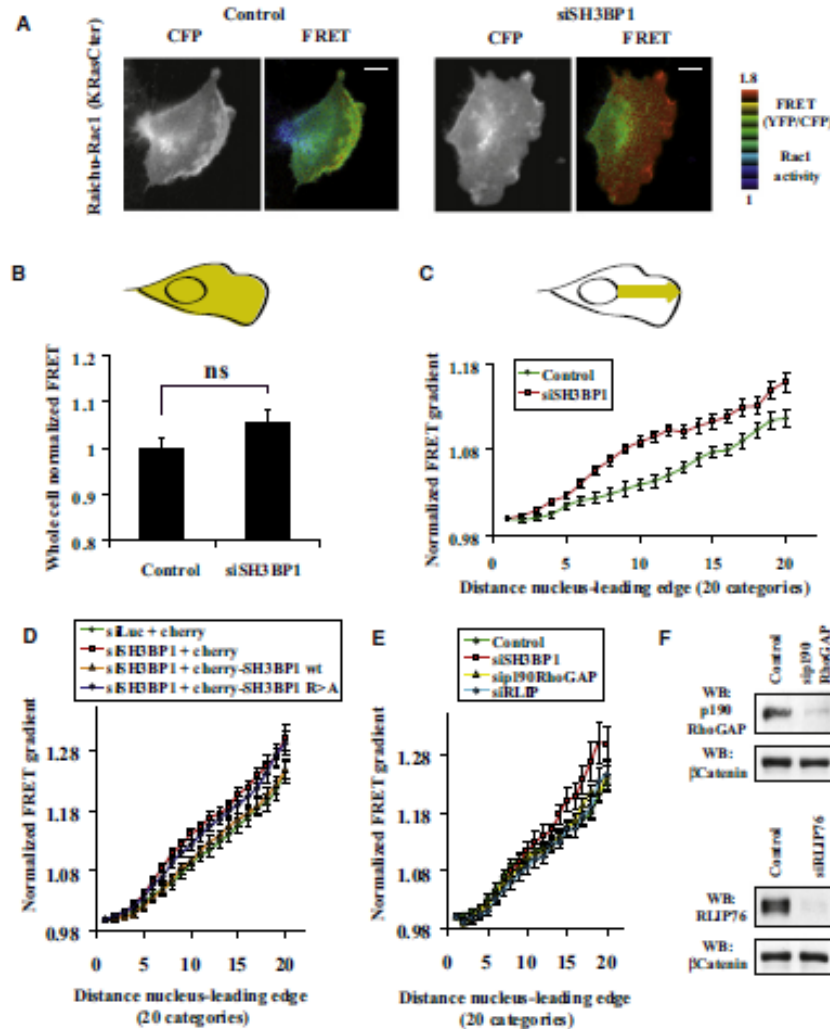
Figure 5. Spatial Regulation of Rac1 Activity in Motile Cells Requires SH3BP1

(A) Visualization of Rac1 activity by FRET. NRK cells were transfected with siLuc (control) or siSH3BP1-2, 24 hr later transfected with plasmid expressing Raichu-Rac1 (KRasCter), 2 days later wounded, and visualized live by FRET microscopy. Scale bars, 10 μm. See also Movie S2.

(B) Whole-cell Rac1 activity. YFP and CFP images were acquired for each motile NRK cell, and mean intensities were measured for the entire cell surface (area in yellow in the cell drawing). Single-cell FRET = YFP/CFP ratios (indicators of Rac1 activity) were calculated for each experiment and were normalized against the average FRET values for siLuc-treated cells. n = 33 for control siLuc and n = 28 for siSH3BP1, from three independent experiments. Bars represent SEM. Note that the difference between the two cell populations is not significant (p = 0.07, Student's t test).

(C) Gradients of Rac1 activity. We used the line-scan function of the MetaMorph software to measure FRET (i.e., Rac1 activity) along 4 μm wide strips, starting from the nucleus and ending at the leading edge following the direction of cell motility (yellow arrow in the cell drawing). Details of the normalization procedure are described in the Experimental Procedures. The resulting FRET curves represent the averaged gradient of Rac1 activity at the front of several cells in three independent experiments. n = 45 for control siLuc and n = 34 for siSH3BP1. Bars represent SEM. Note that the difference between the two curves is highly significant: p < 0.01 for categories 4, 6, 17, 19, and 20; p < 0.001 for categories 7, 8, 9, 10, 11, 12, 13, 14, 15, and 16 (Student's t test).

(D) Wild-type SH3BP1, but not GAP-deficient SH3BP1 mutant, rescues the spatial Rac1 activity in SH3BP1-depleted cells. NRK cells were transfected with siLuc or siSH3BP1-2 and 24 hours later cotransfected with plasmids expressing Raichu-Rac1 and the indicated cherry constructs. Red fluorescent cells were analyzed by FRET microscopy as described in (C). Curve slopes in (D) and (E) are slightly different from (C) because cell culture conditions and illumination settings were not identical. Number of cells (n) analyzed per condition was between 34 and 46. The highly significant difference between the curves of siLuc-treated and siSH3BP1-treated cells was confirmed when cherry only was expressed (siLuc + cherry versus siSH3BP1 + cherry): p < 0.05 for categories 6 and 20; p < 0.01 for categories 7, 11, 14, 15, 16, 17, 18 and 19; p < 0.001 for categories 8, 9, 10, 12, 13 (Student's t test). The curve of siSH3BP1-treated cells expressing cherry-SH3BP1 WT is

144

and developed more rapidly but with a shorter persistence, we conclude that SH3BP1 is necessary for the spatiotemporal organization of protrusions during cell migration.

Expression of Active Rac1 Mimics Depletion of SH3BP1

If inactivation of Rac1 at the front by SH3BP1 is required to organize protrusions and to drive efficient directional motility, cells expressing GTP-hydrolysis-deficient RacG12V should present defects in motility and morphodynamics. We tested this prediction by expressing RFP-fused wild-type or constitutively active mutant G12V Rac1 in motile NRK cells. Cells expressing RacG12V were severely impaired in motility, while cells expressing wild-type Rac1 migrated as control cells (untransfected or RFP-only transfected) (Figures 7A and 7B).

RacG12V-expressing cells displayed a much more rapid drop of the autocorrelation coefficients, as compared with wild-type Rac-expressing cells, indicating that GTP hydrolysis is necessary for the persistence of membrane dynamics (Figures 7C). The fast-cycling F28L mutant showed a similar but milder phenotype, with inhibition of motility (Figure 7B) and perturbation of morphodynamics (Figures 7C). Since RacG12V is always loaded with GTP, while RacF28L constitutively cycles between GDP- and GTP-bound states, their different phenotype strength could simply reflect their different GTP-loading levels. Moreover, since RacF28L-expressing cells presented abnormalities, we can conclude that GDP/GTP cycling per se is not sufficient to drive efficient protrusion organization. It seems that Rac not only needs to cycle but needs to cycle at the right place and with the right kinetics, as spatiotemporally dictated by GEF and GAP proteins.

Thus, expression of constitutively active Rac1 mutants mimicked the phenotype of SH3BP1 depletion, clearly pointing out the importance of inactivating Rac1 during the motility process.

DISCUSSION

We report here that SH3BP1 is a GAP that stimulates the GTPase activity of Rac1 during migration. However, several GEF proteins, including βPIX (ten Klooster et al., 2006), DOCK3 (Sanz-Moreno et al., 2008), Asef (Itoh et al., 2008), and Tiam1 (Palamidessi et al., 2008), have been proposed to activate Rac1 at the leading edge by replacing bound GDP with GTP. Thus, the presence of a Rac1-specific GAP at the leading edge—where Rac1 needs to be active—may seem surprising. One might have expected to instead find a RacGAP at the back of the cell in order to maintain the back-to-front Rac1-GTP gradient. However, current evidence supports the concept that unlike the prototype Ras, which needs to be locked into the GTP-bound state to execute its biological functions, other small

GTPases require GDP/GTP cycling (Barale et al., 2006; Lin et al., 1997; Miller and Bement, 2009). This could explain why transformation induced by GEFs specific to Rho family GTPases is much more efficient than transformation induced by constitutively active Rho family GTPases, and also why GTPase-defective Rho/Rac/Cdc42 mutants have never been found in human tumors (Karlsson et al., 2009; Sahai and Marshall, 2002; Schmidt and Hall, 2002). Together with the RacGEFs, SH3BP1 might promote continuous GDP/GTP cycling of Rac1 at the migrating front of the cell, and this cycling may be necessary for the turnover of protrusions and adhesions during directional motility. The combined action of local RacGEFs and local RacGAP SH3BP1 would allow Rac1 to undergo a "GTPase flux" at the protruding front, similarly to what was proposed for RhoA GDP/GTP cycling during cytokinesis (Miller and Bement, 2009). Perturbing this fine-tuned balance of GEF/GAP activities on Rac1 may produce drastic alterations in the dynamics underlying motility—a notion consistent with the "membrane anarchy" we have observed in cells lacking SH3BP1.

We propose that in motile cells the exocyst complex (acting as effector of Ral proteins) participates in the transport and recruitment of regulatory molecules, including SH3BP1, to the front and only the front (Figure 7D). We show that the Ral/exocyst/SH3BP1 signaling pathway does not control the polarity of motile cells, i.e., orientation of the MTOC. Rather, it defines the site where the front protrusion forms and, accordingly, impacts the directionality of movement, as shown by the fact that SH3BP1-depleted cells have a persistence defect (Figure 3C). Therefore, the exocyst seems to be responsible for delimiting the cell region where Rac1 cycling is effective in driving cell migration. To this regard, it is worth mentioning that the ΔBAR SH3BP1 mutant, defective for binding to exocyst, did not rescue the migration defect of SH3BP1-depleted cells in wound healing assay (Figure 3E), consistently with our model, but puzzlingly it appeared to be able to stimulate the passage of SH3BP1-depleted cells through the porous membrane in a Boyden chamber (data not shown). Discrepancies between Transwell and wound-healing motility assays are not rare, maybe because the motility programmes of cells passing through the 3D porous membrane of a Transwell are likely different from those of cells closing a wound on a 2D dish. In our case, the discrepancy suggests that the localization of SH3BP1 at the front is required for the mesenchymal-type 2D motility, but not for the 3D motility through a pore.
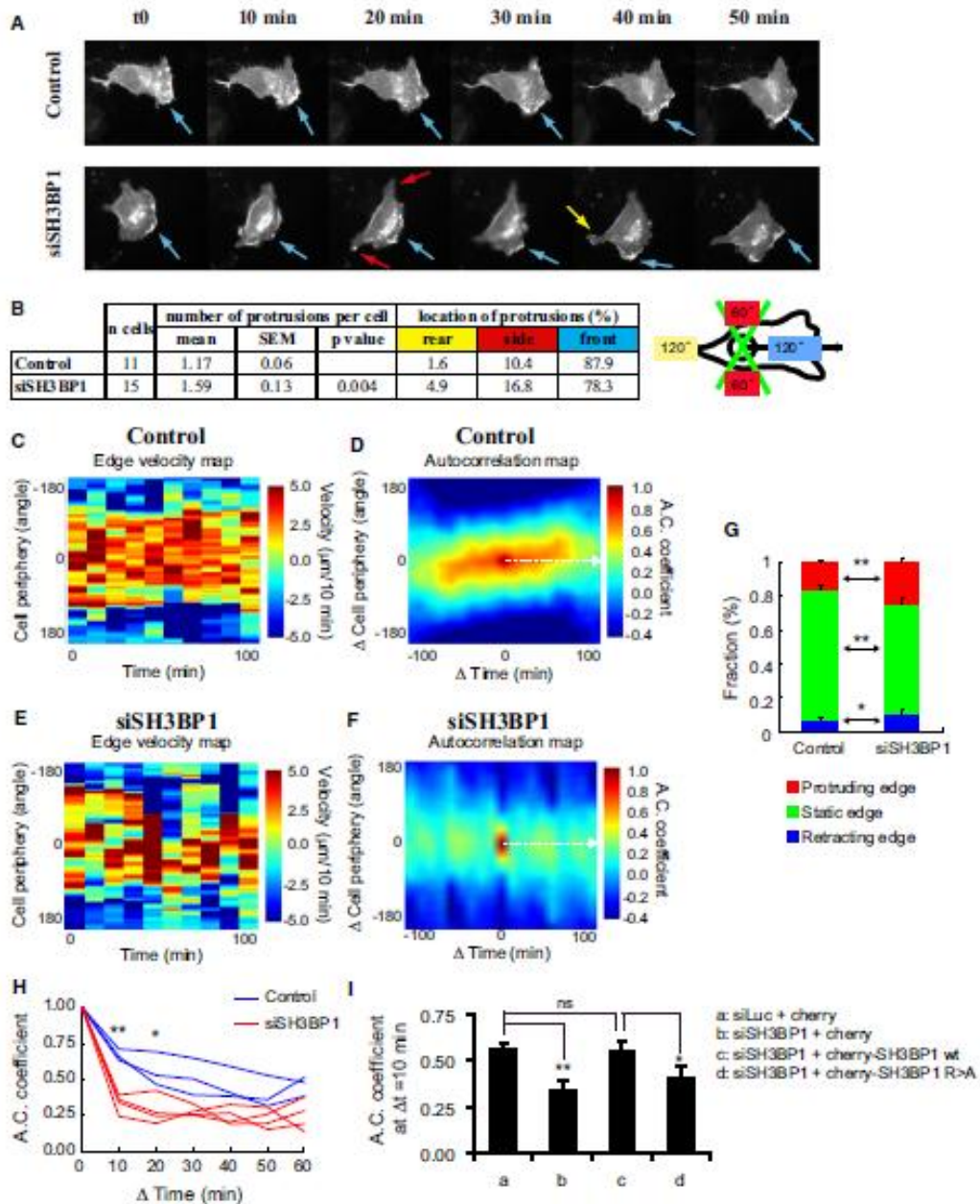
The precise timing of these activating and inactivating events, as well as the identities of the subcellular compartments where they occur, remains unclear. Rac1 cycling could take place at specific subdomains of the leading-edge plasma membrane, and the various positive and negative regulators could be supplied by membrane trafficking. Alternatively, Rac1

145

Figure 6. Protrusion Dynamics in SH3BP1-Depleted Cells Is Disordered and Unstable

(A) SH3BP1-depleted cells display defects in morphodynamics. NRK cells were treated with siLuc (control) or siSH3BP1-2, transfected with a plasmid expressing membrane-targeted RFP-CAAX, wounded, and visualized live by fluorescence microscopy. A selection of time-lapse acquisitions from a representative experiment is shown. See also Movie S3 for the entire video sequence. Arrows point to the protrusions, and their color indicates protrusion locations according to the code defined in (B).

(B) Visual analysis of morphodynamics. The number and location of the protrusions were recorded by visually inspecting the images sequences. Eleven movies of siLuc-treated cells and 15 movies of siSH3BP1-treated cells were analyzed. Protrusion location was classified in three categories: front, when protrusions were

147

may be activated at endosomes, by the GEF Tiam1, and then translocated via recycling to the plasma membrane (Palamidessi et al., 2008) where it would encounter SH3BP1.

In summary, we have found that the SH3BP1 GAP protein links vesicle trafficking and the exocyst complex, of which migration-promoting activity is under the control of Ral, to local modulation of the Rac pathway, and that it thereby plays a crucial role in integrating the molecular machineries and pathways that regulate cell migration.

EXPERIMENTAL PROCEDURES

Cell Culture, Transfections, and Plasmids

NRK, human 293T, and monkey COS-7 cells were grown in Dulbecco's modified Eagle's medium supplemented with 2 mM glutamine, antibiotics (penicillin and streptomycin), and 10% fetal bovine serum. Human PC-3 prostate tumor cells were maintained in Ham's F12 medium supplemented with 10% fetal bovine serum, penicillin, streptomycin, and kanamycin. Transient DNA and siRNA transfections were carried out with Lipofectamine Plus Reagent (Invitrogen) and Hyperfect (QIAGEN), respectively. Expression vectors for SH3BP1 WT (amino acids 1–701), ΔBAR (amino acids 255–701), ΔCter (amino acids 1–466), and R > A (R312A) were generated by cloning human cDNAs encoding full-length SH3BP1 protein and the respective truncated and mutated versions into pcDNA3. Notice that human SH3BP1 is resistant to the two siRNAs against rat SH3BP1 used in the present study in NRK cells. In order to generate cherry-fusion constructs, the SH3BP1 alleles were inserted by PCR techniques into pCherry-C1, obtained from Dr Tsien. pRaichu-Rac1, pRaichu-Cdc42, pRaichu-RhoA (Nakamura et al., 2006), pcDNA3-Exo84-HA and pcDNA3-Sec8-HA (Sakurai-Yageta et al., 2008), and pCXN2-mRFP-Rac1 (Kurokawa et al., 2004) were reported previously. pCAGGS-mRFP-X and pCAGGS-GFP-X express mRFP and GFP fluorescent proteins, respectively, fused to the membrane-targeting signal of K-Ras.

Wound Healing and Time-Lapse Microscopy

For wound-healing assays, cells were grown to confluence on coverslips or glass-bottom dishes coated with collagen (type I from rat tail, Interchim #207050357, 120 μg/ml in H$_2$O for ≥1 hr 37°C). The monolayer was wounded with a pipette tip, at which point the medium was changed to MEM with 2% fetal bovine serum. For phase-contrast video microscopy, a 10× objective was used and images were acquired every 15 min. The Manual Tracking plug-in (developed by Fabrice Cordelières) of ImageJ software was used to track cells, after which data were exported to Excel for mathematical and statistical analysis. Persistence of motility was calculated as the D/T ratio, where D is the direct distance from startpoint to endpoint and T is the total track.

The FRET of the Raichu-Rac1 biosensor was measured as the YFP/CFP ratio and represented using an eight-color scale code, as shown to the right of time-lapse figures, with the upper and lower limits indicated. For time-lapse video, images were acquired every 10 min. For single time point, whole-cell measurements, the background-subtracted images were thresholded to define the whole-cell surface. The mean cell fluorescence intensities (CFP and YFP) were then measured and the YFP/CFP ratios were calculated. For single time point gradient measurements, the line-scan function of MetaMorph was used to measure YFP/CFP ratios along 4 μm wide strips connecting the nucleus to the leading edge in the direction of cell motility. Because of variability in cell size, the resulting sets of measurements were of different lengths. Comparison of these values was made possible by resizing data set length to 20 categories, by aggregating and averaging initial measurements. Next, the first value of each data set (corresponding to the FRET measurements closest to the nucleus) was taken as reference to estimate the relative evolution of FRET along the direction of motility. The plotted points are the means of measurements for each category of the cell population.

Immunoprecipitations

For the Sec8 immunoprecipitation shown in Figure 1C, protein lysates from one 10 cm dish of DNA-transfected 293T cells were prepared in 1 ml lysis buffer A (50 mM Tris-HCl [pH 7.5], 150 mM NaCl, 1% Triton, 1 mM EDTA, freshly supplemented with a protease inhibitor mixture [Roche, #1836170]) and then incubated for 2 hr with 25 μl of beads covalently coupled to a mixture of monoclonal anti-Sec8 antibodies (Yeaman et al., 2001). For the HA immunoprecipitations shown in Figures 1D and 1E, protein lysates from one 6 cm dish of DNA-transfected 293T cells were prepared in 600 μl of lysis buffer B (20 mM Tris-HCl [pH 7.4], 100 mM NaCl, 5 mM MgCl$_2$, 1% Triton, 10% glycerol, freshly supplemented with 1 mM dithiothreitol and the protease inhibitor mixture) and then incubated for 1 hr with a monoclonal anti-HA antibody (3F10, 1 μg), and then for a further 1 hr after, 1 mg of G-coupled magnetic beads (Invitrogen, #100-04D) was added. The immobilized immune complexes were washed three times with 1 ml of lysis buffer and finally boiled in gel-loading buffer. The whole-lysate inputs represent 1.6% (Figure 1C) or 6% (Figures 1D and 1E) of the immunoprecipitated material.

Morphodynamics Analysis

The videos of motile cells expressing RFP-CAAX to track the cell periphery were generated from a series of images taken at 10 min time intervals and were visually analyzed as follows. For each cell and each time interval, the cell periphery was inspected to identify portions that expanded in an apparently coordinated way from time T to time T+1, and each of these portions was scored as an active protrusion. For each cell, the average number of protrusions per time point and the mean values for all of the observed cells were calculated. In order to score protrusion positioning, we traced an angle of 120° facing the direction of motility (front), a mirror angle of 120° (rear),

facing the wound (within a 120° angle); rear, when protrusions were opposite the wound (within a 120° angle); and side, when protrusions were inside the two lateral 60°C angles.

(C and E) Edge velocity maps. Computer-assisted analysis was used to establish edge velocity maps for a representative control (siLuc-treated) cell (C) (see Movie S4 for the corresponding video sequence) and a representative SH3BP1-depleted cell (siSH3BP1-2-treated) (E) (see Movie S5 for the corresponding video sequence).

(D and F) Autocorrelation maps. Autocorrelation maps for the control cell (D) whose edge velocity map is shown in (C) and for the SH3BP1-depleted cell (F) whose edge velocity map is shown in (E). Broken white arrows indicate the temporal autocorrelation functions at ΔCell periphery = 0 degree; these values were used for the analysis shown in (H).

(G) Analysis of edge velocities. Edge fractions were classified into three categories (retracting < −2.5 μm/10 min; −2.5 μm/10 min < static < 2.5 μm/10 min; protruding > 2.5 μm/10 min) and quantified in control (siLuc-treated; n = 5) and siSH3BP1-treated (n = 5) cells. ** indicates p < 0.01 and *p < 0.05 (Student's t test). Bars represent standard deviation (SD).

(H) Temporal analysis of autocorrelation. Temporal cuts (ΔCell periphery = 0 degree) of autocorrelation maps are shown for control (siLuc-treated; blue, n = 3) and siSH3BP1-treated (red, n = 4) cells. Symbols indicate results of the Student's t test analysis. Differences between experimental and control cells are significant both at 10 min (**p < 0.01) and 20 min (*p < 0.05).

(I) Wild-type SH3BP1, but not GAP-deficient SH3BP1 mutant, rescues the morphodynamics of SH3BP1-depleted cells. NRK cells were transfected with siLuc or siSH3BP1-2, with a GFP-CAAX-expressing plasmid, and the indicated cherry constructs. Red-fluorescent cells were video imaged, and autocorrelation coefficients at 10 min were measured. n = 8 for each condition. See Movie S6 for representative videos. See Figure S5A for temporal autocorrelation analysis of all analyzed cells. ** indicate p < 0.01 and *p < 0.05 (Student's t test). Bars represent SEM.
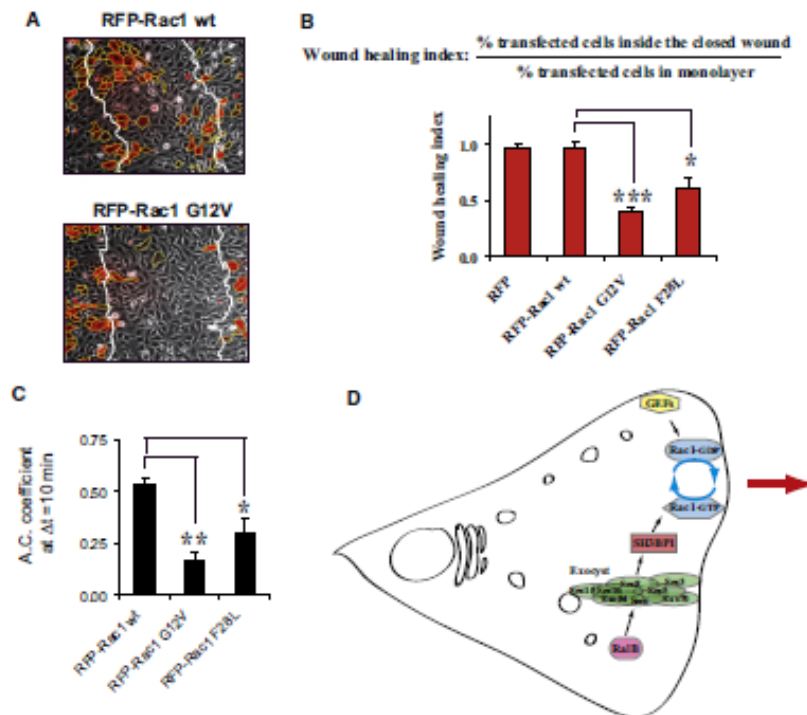
Figure 7. The Inactivation of Rac1 Is a Requirement for Cell Motility

(A) Expression of Rac1 GV12, but not of wild-type Rac1, inhibits cell migration in wound-healing assay. NRK cells were transfected with vectors expressing RFP-fused Rac1 wild-type or carrying the G12V mutation. Representative fields showing the closed wound after migration are shown. Note that transfection efficiency was intentionally low.

(B) Quantitative comparison of Rac1 alleles. The effects of the expression of three Rac1 alleles (wild-type, GTPase-deficient G12V, fast-cycling F28L) on motility were quantified using the wound-healing index (see Figure S5C and the Supplemental Experimental Procedures). Expression levels of RFP constructs were similar. Bars represent SEM.

(C) Temporal autocorrelation analysis. Effects of the expression of the three Rac1 alleles on morphodynamics were quantified as Figure 6I. See Movie S7 for representative videos. See Figure S5B for detailed temporal graphics of all analyzed cells. Bars represent SEM.

(D) A model for the interplay between Ral and Rac in the regulation of cell migration. In motile cells the RalB GTPase controls the association of the subunits of its effector the exocyst complex and promotes localization of the exocyst at leading edge. The exocyst physically interacts with and brings to the leading edge the GAP protein SH3BP1, which stimulates the hydrolysis of bound GTP to GDP on Rac1 at the front. Several GEFs activate Rac1 at the front by replacing bound GDP with GTP. Therefore, Rac1 undergoes locally multiple activation-inactivation cycles, and this Rac1 cycling is necessary for the spatiotemporal regulation of the protrusions during directional motility. RalB, via the exocyst, participates to define where Rac1 cycling occurs and promotes protruding activity.

and two lateral angles of 60° (sides). At each time interval, each observed protrusion was scored as belonging to one of these three categories. To measure edge velocities, we developed simple computer-assisted methods that will soon be described in detail elsewhere (K.K., K.A., and M.M., unpublished data). See the Supplemental Experimental Procedures for more details.

SUPPLEMENTAL INFORMATION

Supplemental Information includes five figures, seven movies, Supplemental Experimental Procedures, and Supplemental References and can be found with this article online at doi:10.1016/j.molcel.2011.03.032.

149

REFERENCES

Barale, S., McCusker, D., and Arkowitz, R.A. (2006). Cdc42p GDP/GTP cycling is necessary for efficient cell fusion during yeast mating. Mol. Biol. Cell 17, 2824–2838.

Bos, J.L., Rehmann, H., and Wittinghofer, A. (2007). GEFs and GAPs: critical elements in the control of small G proteins. Cell 129, 865–877.

Cantor, S.B., Urano, T., and Feig, L.A. (1995). Identification and characterization of Ral-binding protein 1, a potential downstream target of Ral GTPases. Mol. Cell. Biol. 15, 4578–4584.

Cicchetti, P., Mayer, B.J., Thiel, G., and Baltimore, D. (1992). Identification of a protein that binds to the SH3 region of Abl and is similar to Bcr and GAP-rho. Science 257, 803–806.

Cicchetti, P., Ridley, A.J., Zheng, Y., Cerione, R.A., and Baltimore, D. (1995). 3BP-1, an SH3 domain binding protein, has GAP activity for Rac and inhibits growth factor-induced membrane ruffling in fibroblasts. EMBO J. 14, 3127–3135.

Dobereiner, H.G., Dubin-Thaler, B.J., Hofman, J.M., Xenias, H.S., Sims, T.N., Giannone, G., Dustin, M.L., Wiggins, C.H., and Sheetz, M.P. (2006). Lateral membrane waves constitute a universal dynamic pattern of motile cells. Phys. Rev. Lett. 97, 038102.

Etienne-Manneville, S. (2004). Cdc42—the centre of polarity. J. Cell Sci. 117, 1291–1300.

He, B., and Guo, W. (2009). The exocyst complex in polarized exocytosis. Curr. Opin. Cell Biol. 21, 537–542.

Itoh, R.E., Kurokawa, K., Ohba, Y., Yoshizaki, H., Mochizuki, N., and Matsuda, M. (2002). Activation of rac and cdc42 video imaged by fluorescent resonance energy transfer-based single-molecule probes in the membrane of living cells. Mol. Cell. Biol. 22, 6582–6591.

Itoh, R.E., Kiyokawa, E., Aoki, K., Nishioka, T., Akiyama, T., and Matsuda, M. (2008). Phosphorylation and activation of the Rac1 and Cdc42 GEF Asef in A431 cells stimulated by EGF. J. Cell Sci. 121, 2635–2642.

Jullien-Flores, V., Dorseuil, O., Romero, F., Letourneur, F., Saragosti, S., Berger, R., Tavitian, A., Gacon, G., and Camonis, J.H. (1995). Bridging Ral GTPase to Rho pathways. RLIP76, a Ral effector with CDC42/Rac GTPase-activating protein activity. J. Biol. Chem. 270, 22473–22477.

Karlsson, R., Pedersen, E.D., Wang, Z., and Brakebusch, C. (2009). Rho GTPase function in tumorigenesis. Biochim. Biophys. Acta 1796, 91–98.

Kraynov, V.S., Chamberlain, C., Bokoch, G.M., Schwartz, M.A., Slabaugh, S., and Hahn, K.M. (2000). Localized Rac activation dynamics visualized in living cells. Science 290, 333–337.

Kurokawa, K., Itoh, R.E., Yoshizaki, H., Nakamura, Y.O., and Matsuda, M. (2004). Coactivation of Rac1 and Cdc42 at lamellipodia and membrane ruffles induced by epidermal growth factor. Mol. Biol. Cell 15, 1003–1010.

Ligeti, E., Dagher, M.C., Hernandez, S.E., Koleske, A.J., and Settleman, J. (2004). Phospholipids can switch the GTPase substrate preference of a GTPase-activating protein. J. Biol. Chem. 279, 5055–5058.

Lim, K.H., O'Hayer, K., Adam, S.J., Kendall, S.D., Campbell, P.M., Der, C.J., and Counter, C.M. (2006). Divergent roles for RalA and RalB in malignant growth of human pancreatic carcinoma cells. Curr. Biol. 16, 2385–2394.

Lin, R., Bagrodia, S., Cerione, R., and Manor, D. (1997). A novel Cdc42Hs mutant induces cellular transformation. Curr. Biol. 7, 794–797.

Lu, W., and Mayer, B.J. (1999). Mechanism of activation of Pak1 kinase by membrane localization. Oncogene 18, 797–806.

Maeda, Y.T., Inose, J., Matsuo, M.Y., Iwaya, S., and Sano, M. (2008). Ordered patterns of cell shape and orientational correlation during spontaneous cell migration. PLoS ONE 3, e3734. 10.1371/journal.pone.0003734.

Miller, A.L., and Bement, W.M. (2009). Regulation of cytokinesis by Rho GTPase flux. Nat. Cell Biol. 11, 71–77.

Nakamura, T., Kurokawa, K., Kiyokawa, E., and Matsuda, M. (2006). Analysis of the spatiotemporal activation of rho GTPases using Raichu probes. Methods Enzymol. 406, 315–332.

Osmani, N., Vitale, N., Borg, J.P., and Etienne-Manneville, S. (2006). Scrib controls Cdc42 localization and activity to promote cell polarization during astrocyte migration. Curr. Biol. 16, 2395–2405.

Oxford, G., Owens, C.R., Titus, B.J., Foreman, T.L., Herlevsen, M.C., Smith, S.C., and Theodorescu, D. (2005). RalA and RalB: antagonistic relatives in cancer cell migration. Cancer Res. 65, 7111–7120.

Palamidessi, A., Frittoli, E., Garre, M., Faretta, M., Mione, M., Testa, I., Diaspro, A., Lanzetti, L., Scita, G., and Di Fiore, P.P. (2008). Endocytic trafficking of Rac is required for the spatial restriction of signaling in cell migration. Cell 134, 135–147.

Pankov, R., Endo, Y., Even-Ram, S., Araki, M., Clark, K., Cukierman, E., Matsumoto, K., and Yamada, K.M. (2005). A Rac switch regulates random versus directionally persistent cell migration. J. Cell Biol. 170, 793–802.

Raftopoulou, M., and Hall, A. (2004). Cell migration: Rho GTPases lead the way. Dev. Biol. 265, 23–32.

Ridley, A.J., Schwartz, M.A., Burridge, K., Firtel, R.A., Ginsberg, M.H., Borisy, G., Parsons, J.T., and Horwitz, A.R. (2003). Cell migration: integrating signals from front to back. Science 302, 1704–1709.

Rosse, C., Hatzoglou, A., Parrini, M.C., White, M.A., Chavrier, P., and Camonis, J. (2006). RalB mobilizes the exocyst to drive cell migration. Mol. Cell. Biol. 26, 727–734.

Rosse, C., Formstecher, E., Boeckeler, K., Zhao, Y., Kremerskothen, J., White, M.D., Camonis, J.H., and Parker, P.J. (2009). An aPKC-exocyst complex controls paxillin phosphorylation and migration through localised JNK1 activation. PLoS Biol. 7, e1000235. 10.1371/journal.pbio.1000235.

Sahai, E., and Marshall, C.J. (2002). RHO-GTPases and cancer. Nat. Rev. Cancer 2, 133–142.

Sakurai-Yageta, M., Recchi, C., Le Dez, G., Sibarita, J.B., Daviet, L., Camonis, J., D'Souza-Schorey, C., and Chavrier, P. (2008). The interaction of IQGAP1 with the exocyst complex is required for tumor cell invasion downstream of Cdc42 and RhoA. J. Cell Biol. 181, 985–998.

Sanz-Moreno, V., Gadea, G., Ahn, J., Paterson, H., Marra, P., Pinner, S., Sahai, E., and Marshall, C.J. (2008). Rac activation and inactivation control plasticity of tumor cell movement. Cell 135, 510–523.

Schmidt, A., and Hall, A. (2002). Guanine nucleotide exchange factors for Rho GTPases: turning on the switch. Genes Dev. 16, 1587–1609.

ten Klooster, J.P., Jaffer, Z.M., Chernoff, J., and Hordijk, P.L. (2006). Targeting and activation of Rac1 are mediated by the exchange factor beta-Pix. J. Cell Biol. 172, 759–769.

Wu, Y.I., Frey, D., Lungu, O.I., Jaehrig, A., Schlichting, I., Kuhlman, B., and Hahn, K.M. (2009). A genetically encoded photoactivatable Rac controls the motility of living cells. Nature 461, 104–108.

Yeaman, C., Grindstaff, K.K., Wright, J.R., and Nelson, W.J. (2001). Sec6/8 complexes on trans-Golgi network and plasma membrane regulate late stages of exocytosis in mammalian cells. J. Cell Biol. 155, 593–604.

150

Supplemental Information

SH3BP1, an Exocyst-Associated RhoGAP, Inactivates Rac1 at the Front to Drive Cell Motility

Maria Carla Parrini, Amel Sadou-Dubourgnoux, Kazuhiro Aoki, Katsuyuki Kunida, Marco Biondini, Anastassia Hatzoglou, Patrick Poullet, Etienne Formstecher, Charles Yeaman, Michiyuki Matsuda, Carine Rossé, and Jacques Camonis

INVENTORY OF SUPPLEMENTAL INFORMATION

- **Figures S1 to S5**

- **Movies S1 to S7**

- **Supplemental Experimental Procedures**

- **Supplemental References**

Figure S1 relates to Figure 2

Figure S2 and Movie S1 relate to Figure 3

Figure S3 relates to Figure 4

Figure S4 and Movie S2 relate to Figure 5

Figure S5 relates to Figure 6 and 7

Movies S3, Movies S4, Movie S5 and Movie S6 relate to Figure 6

Movie S7 relates to Figure 7

SUPPLEMENTAL FIGURES
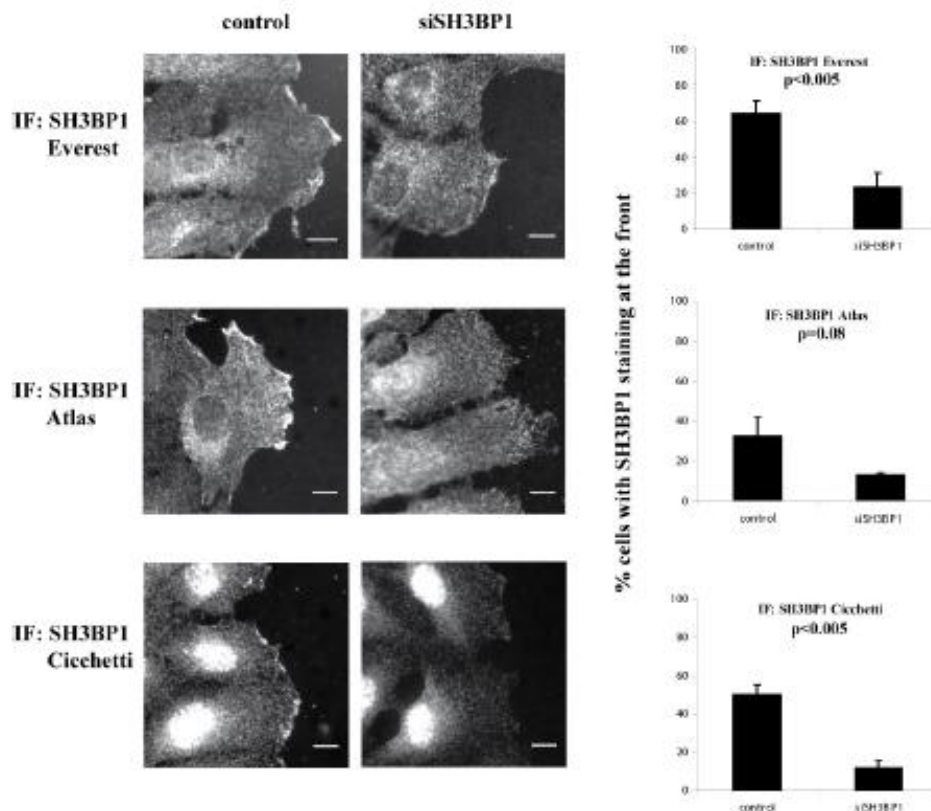
Figure S1. Immuno-fluorescence staining for SH3BP1.
Motile control or SH3BP1depleted NRK cells were co-stained with one of three different antibodies against SH3BP1 (two were purchased from Everest Biotech and Atlas Antibodies, and one was a gift from Dr. P. Cicchetti). Representative wide-field microscope images are shown. The cells with a clear fluorescent signal at the leading edge were counted (at least 100 cells per condition per experiment), in 3 to 4 independent experiments per antibody, and the mean percentages of stained cells were used for quantification. Note the presence of a non-specific nuclear signal in the case of the Cicchetti antibody. Bars on images indicate 10 microns. Bars on graphics represent SEM.
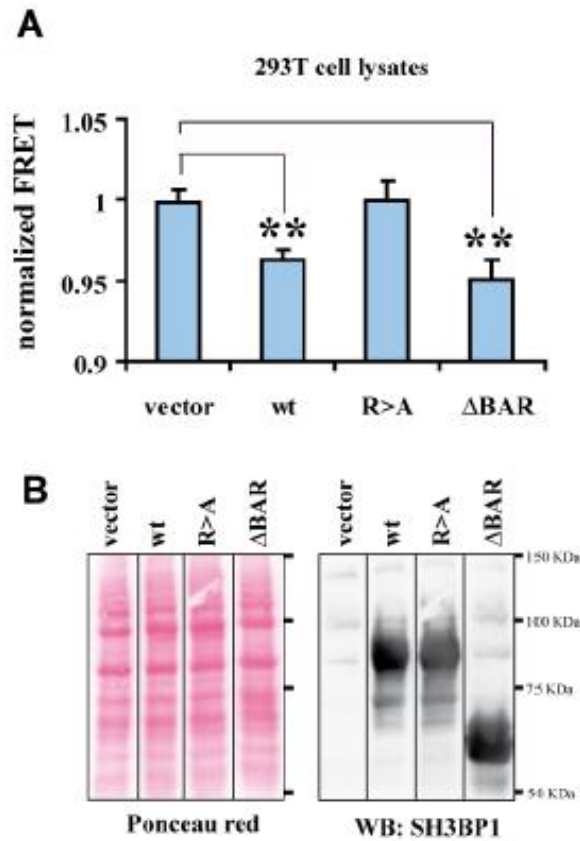
Figure S2.

A. GAP activity on Rac1 of wild-type SH3BP1 and mutated forms.

293T cells were transfected with Raichu-Rac1 (K-Ras C-ter), together with a vector expressing wild-type SH3BP1 (wt), a mutated version (R>A or ΔBAR) or with empty vector (vector). Two-days after transfection, cell lysates were prepared in 20mM TrisHCl pH=7.5, 100mM NaCl, 5mM MgCl2, 0.5% Triton, freshly supplemented with protease inhibitors. Emission spectra of lysates were quickly acquired using a Fluorimeter at 433 nm excitation wavelength. The emission ratios for YFP/CFP (525 nm/ 475 nm), as a measurement of Raichu FRET, were calculated based on the normalized spectra and then expressed as fraction of the empty-vector condition. Number of experiments n=7. Bars represent SEM. ** indicates p<0.01 (Student t-test).

B. Whole cell lysates were analyzed by Ponceau Red staining and anti-SH3BP1 Western blot in order to verify protein expression.
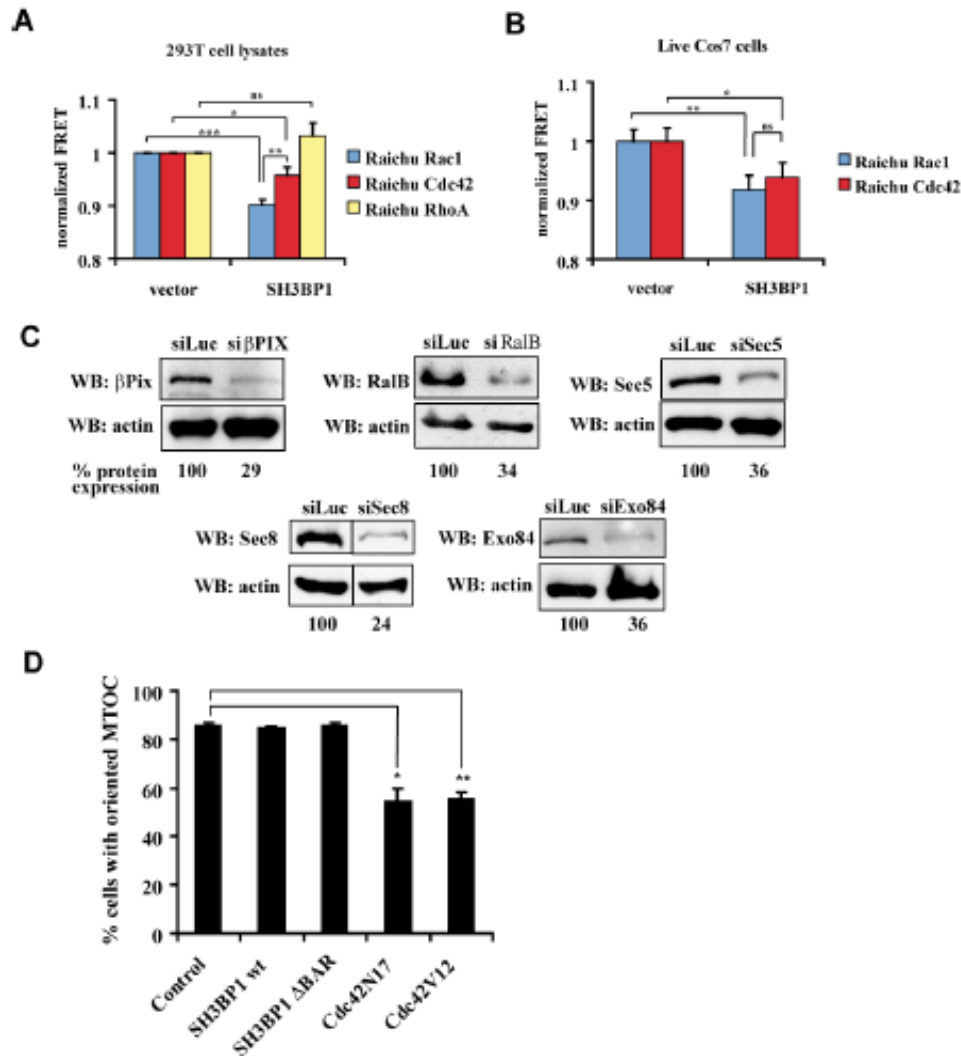
Figure S3.
A. Substrate specificity of full-length SH3BP1: FRET measurements in whole-cell lysates. 293T cells were transfected with Raichu-Rac1, Raichu-Cdc42 or Raichu-RhoA (all with K-Ras membrane-targeting sequence at the C-terminus), together with SH3BP1-expression vector (SH3BP1) or with empty vector (vector). FRET measurements were performed as in Figure S2A. Number of experiments n=10 for Raichu-Rac1, n=6 for Raichu-Cdc42 and n=3 for Raichu-RhoA.
B. FRET measurements in living cells. Cos-7 cells were transfected with Raichu-Rac1 (Rac1Cter) or Raichu-Cdc42 (Cdc42Cter), together with SH3BP1-expression vector (SH3BP1) or with empty vector (vector). YFP and CFP microscope images were acquired for each cell and mean intensities were measured for the whole cell surface. Single-cell FRET=YFP/CFP ratios (indicators of Rac1 and Cdc42 activities) were calculated and

normalized against the mean FRET of empty-vector transfected cells. Number of cells n=39 (Raichu-Rac1, vector), n=24 (Raichu-Rac1, SH3BP1), n=30 (Raichu-Cdc42, vector), n=26 (Raichu-Cdc42, SH3BP1).

C. Validation of protein depletion in MTOC reorientation experiments. NRK cells were treated with siLuc, siβPIX, siRalB, siSec5, siSec8 or siExo84, and subjected to either MTOC staining (Figure 4) or lysis. Lysates were analyzed with the indicated antibodies. Quantification was performed using ImageJ, and protein expression levels, after normalization of protein loads using actin, are expressed as percentage of the control under each panel.

D. Expression of wild-type SH3BP1 or ΔBAR mutant does not perturb MTOC orientation. NRK cells were transfected with plasmids expressing wild-type SH3BP1 (wt), SH3BP1 ΔBAR, dominant-negative Cdc42N17 or dominant-active Cdc42V12. Wound-closing cells were fixed and subjected to MTOC staining together with SH3BP1 or Cdc42 staining, in order to detect and score only cells expressing exogenous proteins. Analysis was performed as in Figure 4 from two experiments. Results show that neither forms of SH3BP1 impact MTOC orientation, while perturbation of Cdc42 activity did prevent correct cell polarization, as expected.

A

Raichu-Rac1
1011x

Raichu-Rac1 Y40C
1016x

Raichu-Pak-Rho
1110x

control

siSH3BP1

FRET
(YFP/CFP)

2.2

1.3

FRET
(YFP/CFP)

1.3

0.9

FRET
(YFP/CFP)

1.2

0.8

B

Raichu-Rac1 (Rac1Cter)

control

CFP   FRET

siSH3BP1

CFP   FRET

1.9

1.4

FRET
(YFP/CFP)

Rac1
activity

C

ns

D

control
siSH3BP1

Distance nucleus-leading edge (20 categories)
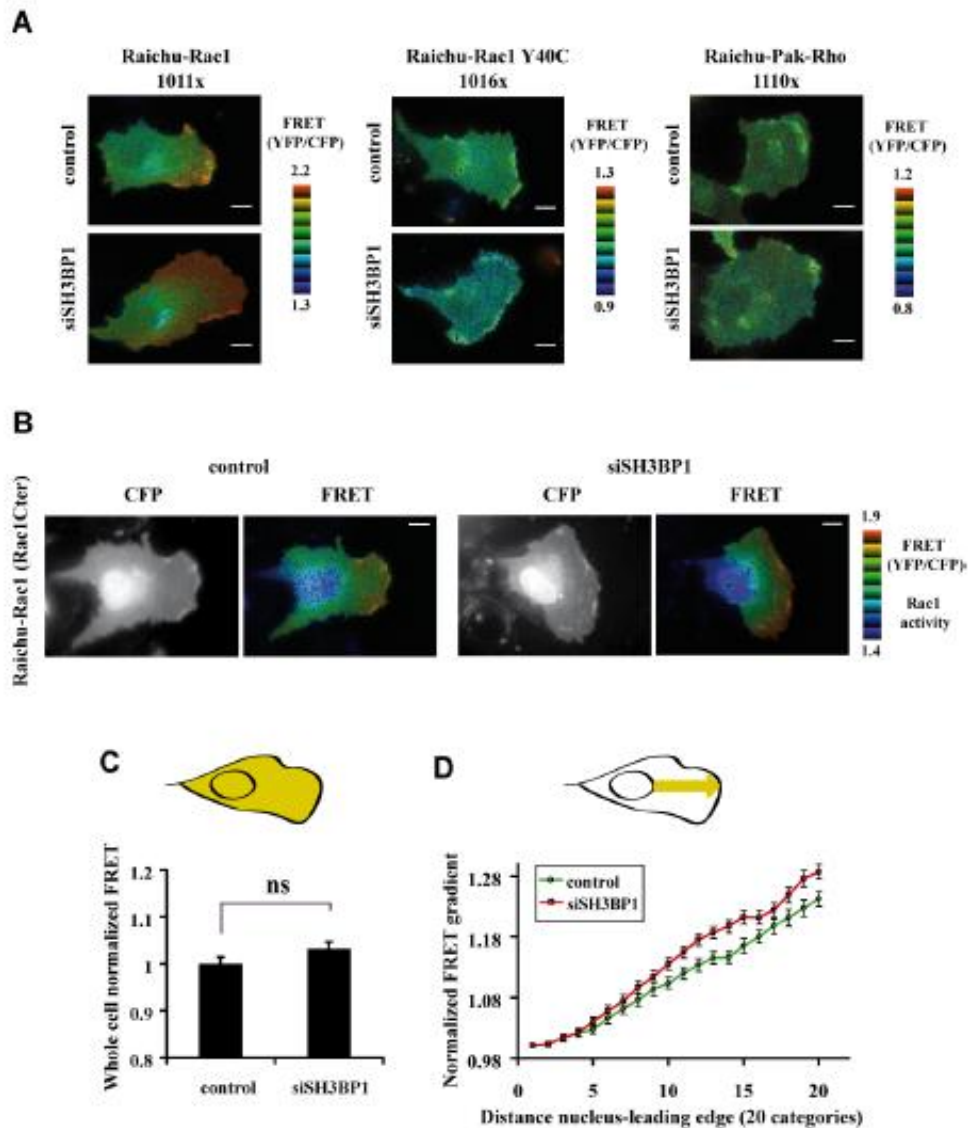
Figure S4.
A. Negative controls for FRET imaging.
NRK cells were transfected with siLuc (control) or siSH3BP1-2, twenty four hours later transfected with plasmids expressing Raichu-Rac1 (1011x), Raichu-Rac1 Y40C (1016x) (http://www.path1.med.kyoto-u.ac.jp/mm/e-phogemon/vector.htm) or Raichu-Pak-Rho (1110x) (Yoshizaki et al., 2003), wounded, and visualized by live FRET microscopy. Raichu-Rac Y40C carries a mutation in the Rac effector domain impairing the intra-molecular interaction with the GBD (GTPase Binding Domain) of Pak1. Raichu-Pak-Rho contains Rho sequence instead of Rac sequence. Note that, contrary to Raichu-Rac1, the two control probes

do not present a FRET gradient pattern and do not show any difference following SH3BP1 depletion. These results show the specificity of results reported on Figure 5.

B. Spatial regulation of Rac1 activity in motile cells requires SH3BP1. Visualization of Rac1 activity by FRET. Experiments were done performed as described in legend of Figure 5, but using the Raichu-Rac1 (Rac1Cter) probe instead of the Raichu-Rac1 (KRasCter) probe.

C. Whole-cell Rac1 activity. n=36 for control siLuc and n=30 for siSH3BP1, with cells from three independent experiments. Bars represent SEM. p value = 0.06 (Student t-test).

D. Gradients of Rac1 activity. . n=36 for control siLuc and n=30 for siSH3BP1, with cells from three independent experiments. Bars represent SEM. Student t-test: p<0.05 for categories 16 and 18; p<0.01 for categories 10, 11, 12, 13, 15, 19 and 20; p<0.001 for category 14.
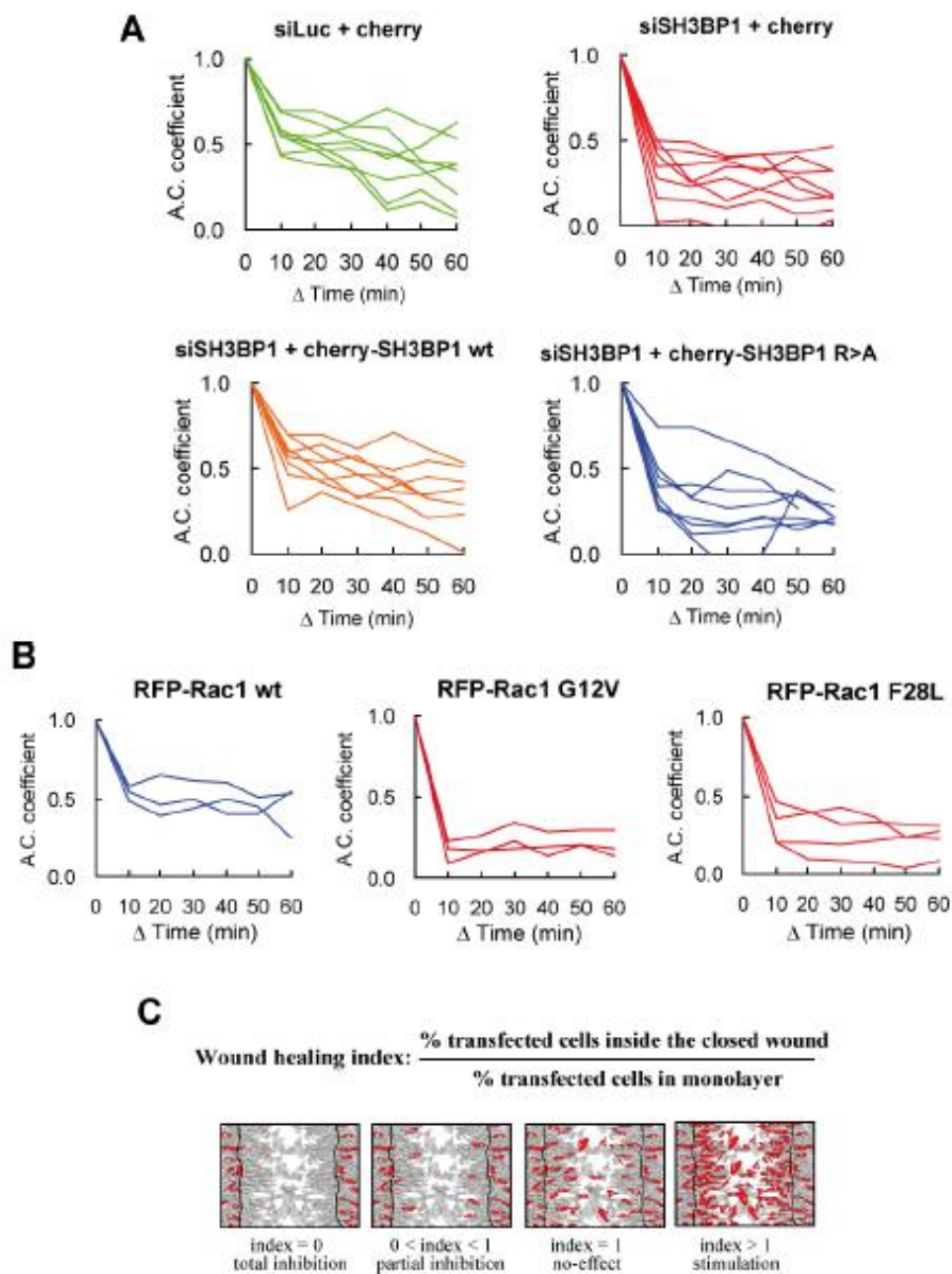
Figure S5.
A. Temporal autocorrelation analysis. Cells analyzed for Figure 6I.
B. Temporal autocorrelation analysis. Cells analyzed for Figure 7C.
C. Depiction of "wound index healing" method.

LEGENDS OF SUPPLEMENTAL MOVIES

Movie S1. Wound-healing: comparison between control and SH3BP1-depleted cells. Observation time: 9 hrs. Control sample is in the left panel and SH3BP1-depleted sample in the right panel.

Movie S2. Raichu-Rac (KRasCter): comparison between control and SH3BP1-depleted cells. Observation time: 120 min. Control sample is the left panel and SH3BP1-depleted sample in the right panel.

Movie S3. Protrusion dynamics (RFP-CAAX): comparison between control and SH3BP1-depleted cells. Observation time: 180 min. Control sample is in the left panel and SH3BP1-depleted sample in the right panel.

Movie S4. Control motile cell used for analysis of Figure 6C and 6D.

Movie S5. SH3BP1-depleted motile cell used for analysis of Figure 6E and 6F.

Movie S6. Rescue of morphodynamics defects (GFP-CAAX).
Observation time: 90 min. Cells were transfected with the indicated siRNAs and DNAs.
(Upper left panel)   siLuc + cherry
(Upper right panel)   siSH3BP1 + cherry
(Lower left panel)   siSH3BP1 + cherry-SH3BP1 wt
(Lower right panel)   siSH3BP1 + cherry-SH3BP1 R>A

Movie S7. Protrusion dynamics (GFP-CAAX): comparison between wild-type Rac1 and constitutively active mutant Rac1 G12V.
Observation time: 95 min. A cell expressing wild-type Rac1 is in the left panel and a cell expressing Rac1 G12V is in the right panel.

SUPPLEMENTAL EXPERIMENTAL PROCEDURES

Antibodies

For SH3BP1 proteins, we used 3 different antibodies: a goat polyclonal which can be purchased from Everest Biotech (#EB06271) or AbCam (#ab10103), a rabbit polyclonal purchased from Atlas Antibodies (#HPA000757) and a rabbit polyclonal gift of Dr. Piera Cicchetti (batch #6) (Cicchetti et al., 1995). For Exo84, Sec15 and Sec5 proteins, we used antibodies produced in the C. Yeaman laboratory. Commercial mouse monoclonal antibodies used were: anti-Sec8, anti-βPIX and anti-p190RhoGAP from BD Transduction Laboratories (#610659, #611648 and #610150), and anti-actin from Sigma (#A5441). The rat monoclonal antibody anti-HA (clone 3F10) used was from Roche (#11867423001). The commercial rabbit polyclonal antibodies used were: anti-pericentrin from Covance (#PRB-432C), anti-RalB and anti-RLIP76/RalBP1 from Cell Signalling Technology (#3523 and #3630).

Western blotting

For the Western blots of immunoprecipitation experiments the primary antibodies were: Atlas Antibodies anti-SH3BP1, dilution 1/250; anti-Sec8, dilution 1/1000; anti-HA, dilution 1/1000. For the Western blots on whole cell lysates, we verified protein expression using the following conditions: Cicchetti anti-SH3BP1, dilution 1/500; anti-actin, dilution 1/100000; anti-βPIX, dilution, 1/500; anti-RalB, dilution 1/250; Yeaman laboratory monoclonal anti-Sec5, dilution 1/1000; Yeaman laboratory monoclonal anti-Exo84, dilution 1/1000; anti-Sec8, dilution 1/1000; anti-p190RhoGAP, dilution 1/250; anti-RLIP76, dilution 1/1000. The TBST buffer (150 mM NaCl, 10 mM Tris pH=8, 0.05% Tween-20) was used for Western blotting, with the addition of 5% BSA (bovine serum albumin) for saturation and 1% BSA for antibody reactions. The secondary antibodies were horseradish peroxidase-conjugated (Jackson ImmunoResearch) and the detection was achieved with the ECL chemiluminescence method (PerkinElmer, #NEL104001EA).

siRNA sequences

For depletion of proteins by RNAi, sequences of siRNAs used in this work were
CGUACGCGGAAUACUUCGAdTdT (siLuciferase)
GCCUUAGAGAUGAGCUGUGdTdT (siSH3BP1-1)
GAGAAAGGUGGAACAGUGCdTdT (siSH3BP1-2)

GGGUUCGAUACGACUGCCAdTdT (siβPIX)

UGACGAGUUUGUAGAAGACdTdT (siRalB)

GGUCGGAAAGACAAGGCAGAUdTdT (siSec5)

GGUCCUGAUGACAACUUAAdTdT (siSec8)

UGGGCAUGUUCGUGGAUGCdTdT (siExo84)

CAGAAAUGGAAAGUUUGCAAAGACAdTdT (sip190RhoGAP)

GUAGAGAGGACCAUGAUGUdTdT (siRLIP76)

Immunofluorescence staining

In wound-healing experiments, motile NRK cells on collagen-coated cover slips were fixed with 4% paraformaldehyde 4-5 hr post-wounding, and permeabilized with 0.1% Triton X-100 in PBS buffer. Saturation and incubation with antibodies were carried out in PBS containing 10% foetal bovine serum. Primary antibodies were: anti-SH3BP1 as indicated in figure legends (Everest Biotech antibody, 1/50 dilution; Atlas antibody, 1/50 dilution; Cicchetti antibody, 1/20 dilution); anti-Exo84 (Yeaman laboratory; 1/1000 dilution); anti-Sec15 (Yeaman laboratory; 1/500 dilution); and Sec8 monoclonal antibody (BD Transduction Laboratories, 1/100 dilution). Secondary antibodies and Prolong mounting medium were from Invitrogen and were used according to manufacturer's instructions.

Yeast two-hybrid methods

The coding sequences for human Exo84 (GenBank gi: 58331103) and human Sec8 (Genbank gi: 82546829) were cloned into plasmid pB27 as a C-terminal fusion to LexA. The constructs were used as baits to screen at saturation a highly complex, random-primed human placenta cDNA library constructed into plasmid pP6. pB27 and pP6 were derived from the original pBTM116 (Vojtek and Hollenberg, 1995) and pGADGH (Bartel and Fields, 1995) plasmids, respectively. More than 50 million clones (5-fold the complexity of the library) were screened with each bait, using a mating approach involving the Y187 (MATα) and L40ΔGal4 (MATa) yeast strains as previously described (Formstecher et al., 2005). Positive colonies were selected on a medium lacking tryptophan, leucine and histidine; this was supplemented with 2 mM or 5 mM 3-aminotriazole for Exo84 and Sec8 screens, respectively. The prey fragments of the positive clones were amplified by PCR and sequenced at their 5' and 3' junctions. The resulting sequences were used to identify the corresponding interacting proteins in the GenBank database (NCBI) using a fully automated procedure. 18 and 6 clones coding for SH3BP1 fragments were found in the Exo84 and Sec8 screens, respectively.

161

Microscopy setting

For video-microscopy experiments, starting from 3 hrs post-wounding, the cells were imaged on a Leica DMIRE2 inverted microscope equipped with a motorized stage for multi-positioning, a CoolSNAP HQ2 camera (Roper Scientific), filter wheels (Ludl Electronic Products), a "Box"-heated chamber and "Brick" CO_2 controller (Life Imaging Services), under control of the MetaMorph software (Universal Imaging).

For dual-emission ratiometric FRET imaging, we used a D440/20x excitation filter, a 455DCLP dichroic mirror, and the two D485/40m (CFP) and D535/30m (YFP) emission filters (Chroma, Filter Set #71007a). Cells were illuminated with a 103 W Mercury lamp (Osram) through a 5% transmission neutral density (ND) filter. The exposure time was a few hundred msec with a camera binning of 4 x 4. Image processing was performed using the MetaMorph software.

Transwell assay

The Boyden-chamber migration assay was performed using Transwells with 8-μm pore-size membranes (Corning, #3422) as previously published (Rosse et al., 2006). 75,000 cells were loaded into the upper compartment and allowed to migrate through the pores for 6 to 12 hr in the standard culture medium. Cells that had not migrated were removed from the upper compartment using a cotton swab. Cells that had migrated to the lower surface of the membrane were fixed and stained with 0.2% crystal violet in 20% methanol for 30 min. Cells were then lysed with 20% acetic acid, and absorbance was measured at 584 nm. The absorbance measurements were directly proportional to the density of migrated cells. The measurements were calculated from the means of duplicate or triplicate wells, for each of the four independent experiments performed.

"Wound healing index" method

As an alternative to manual tracking to analyze cells expressing exogenous fluorescent proteins, we developed a novel method based on quantification of the capacity of the transfected cells to repopulate a wound as compared to non-transfected cells (**Figure S5C**). A "wound healing index" is defined as the ratio between "the percentage of transfected cells inside the closed wound" and "the percentage of transfected cells in the monolayer". The numerator is measured by counting the fluorescent and non-fluorescent cells in the wounded area. The denominator is measured by counting the fluorescent and non-fluorescent cells

before wounding the monolayer. If transfected cells behave as non-transfected cells, the index will be 1, which indicates that the expressed protein does not impact migration of the cell population. An index = 0 indicates that the fluorescent fusion totally inhibits migration; an index between 0 and 1 indicates a partial inhibition, while an index > 1 indicates that the expression of the expressed protein stimulates motility. This method requires an intentionally modest DNA transfection efficiency (5-20 %) and provides a quick evaluation of many cells and conditions. It is particularly convenient in order to compare the effect of the expression of various alleles of a gene of interest.

Edge velocity measurements

Coordinate values of the cell periphery were traced from images of migrating cells by the MetaMorph software. The data were then exported into Matlab (version R2008b; The Mathworks Inc.) to implement the following processes. First, in a target image at time = T, normal vectors were generated for each point along the cell perimeter. Second, acute changes of vector angles caused by local membrane deformation were smoothed by correction with the average of ten neighboring vector angles. Third, the point at which each corrected vector intersected with the cell periphery at time = T + 1 was traced. Last, edge velocity was calculated as the distance between the point at time = T and the intersection point at time = T + 1 divided by elapsed time (10 min). Autocorrelation functions of edge velocities were calculated according to a previous report (Maeda et al., 2008).

SUPPLEMENTAL REFERENCES

Bartel, P. L., and Fields, S. (1995). Analyzing protein-protein interactions using two-hybrid system. Methods Enzymol *254*, 241-263.

Formstecher, E., Aresta, S., Collura, V., Hamburger, A., Meil, A., Trehin, A., Reverdy, C., Betin, V., Maire, S., Brun, C., *et al.* (2005). Protein interaction mapping: a Drosophila case study. Genome Res *15*, 376-384.

Vojtek, A. B., and Hollenberg, S. M. (1995). Ras-Raf interaction: two-hybrid analysis. Methods Enzymol *255*, 331-342.

Yoshizaki, H., Ohba, Y., Kurokawa, K., Itoh, R. E., Nakamura, T., Mochizuki, N., Nagashima, K., and Matsuda, M. (2003). Activity of Rho-family GTPases during cell division as visualized with FRET-based probes. J Cell Biol *162*, 223-232.

BIBLIOGRAPHY

Abercrombie M, Heaysman JE, Pegrum SM. 1971. The locomotion of fibroblasts in culture. IV. Electron microscopy of the leading lamella. Exp Cell Res. Aug;67(2):359-67.

Abercrombie, M., Heaysman, J.E., and Pegrum, S.M. 1970. The locomotion of fibroblasts in culture. II. Cell Res. 60, 437–444.

Amann, K.J., and Pollard, T.D. 2001. The Arp2/3 complex nucleates actin filament branches from the sides of pre-existing filaments. Nature Cell Biology . 3(3):306-310.

Awasthi S, Singhal SS, Awasthi YC, Martin B, Woo JH, Cunningham CC, Frankel AE. 2008. RLIP76 and Cancer. Clin Cancer Res. 14(14):4372-7.

Barr FA, Gruneberg U. 2007. Cytokinesis: placing and making the final cut. Cell. Nov 30;131(5):847-60.

Baek, K., Knodler, A., Lee, S. H., Zhang, X., Orlando, K., Zhang, J., Foskett, T. J., Guo, W. and Dominguez, R. 2010. Structure-function study of the N-terminal domain of exocyst subunit Sec3. J. Biol. Chem. 285, 10424–1043.

Balakireva M, Rossé C, Langevin J, Chien Y-chen, Gho M, Gonzy-Treboul G, Voegeling-Lemaire S, Aresta S, Lepesant J-A, Bellaiche Y, White M & Camonis J. 2006. The Ral/exocyst effector complex counters c-Jun N-terminal kinase-dependent apoptosis in Drosophila melanogaster. Mol. Cell. Biol 26: 8953-8963.

Bhattacharya, M., Anborgh, P.H., Babwah, A.V., Dale, L.B., Dobransky, T., Benovic, J.L., Feldman, R.D., Verdi, J.M., Rylett, R.J., and Ferguson, S.S. 2002. Beta-arrestins regulate a Ral-GDS Ral effector pathway that mediates cytoskeletal reorganization. Nat. Cell Biol. 4, 547–555.

Beronja S, Laprise P, Papoulas O, Pellikka M, Sisson J, Tepass U. 2005. Essential function of Drosophila Sec6 in apical

exocytosis of epithelial photoreceptor cells. J Cell Biol. 169(4):635-46.

Biesova Z, Piccoli C, Wong WT. 1997. Isolation and characterization of e3B1, an eps8 binding protein that regulates cell growth. Oncogene;14:233–41.

Blankenship JT, Fuller MT, Zallen JA. 2007. The Drosophila homolog of the Exo84 exocyst subunit promotes apical epithelial identity. J Cell Sci. 120(Pt 17):3099-110.

Bodemann BO, Orvedahl A, Cheng T, Ram RR, Ou Y-H, Formstecher E, Maiti M, Hazelett CC, Wauson EM, Balakireva M, Camonis JH, Yeaman C, Levine B & White MA. 2011. RalB and the Exocyst Mediate the Cellular Starvation Response by Direct Activation of Autophagosome Assembly. Cell 144: 253-267.

Bodemann BO and White MA. 2008. Ral GTPases and cancer: linchpin support of the tumorigenic platform. Nat. Rev. Cancer 8: 133-140.

Boujemaa-Paterski, R., E. Gouin, G. Hansen, S. Samarin, C. Le Clainche, D. Didry, P. Dehoux, P. Cossart, C. Kocks, M.F. Carlier, and D. Pantaloni. 2001. Listeria protein ActA mimics WASp family proteins: it activates filament barbed end branching by Arp2/3 complex. Biochemistry. 40:11390–11404.

Boyd C, Hughes T, Pypaert M, Novick P. 2004. Vesicles carry most exocyst subunits to exocytic sites marked by the remaining two subunits, Sec3p and Exo70p. J Cell Biol. Dec 6;167(5):889-901.

Bretscher, M. S., and C. Aguado-Velasco. 1998. Membrane traffic during cell locomotion. Curr. Opin. Cell Biol. 10:537-541.

Brown FC, Pfeffer SR. 2010. An update on transport vesicle tethering. Molecular Membrane Biology, November; 27(8): 457–461.

Brymora A, Valova VA, Larsen MR, Roufogalis BD, Robinson PJ. 2001. The brain exocyst complex interacts with RalA in a GTP-dependent manner: identification of a novel mammalian Sec3 gene and a second Sec15 gene. J Biol Chem. 276(32):29792-7.

Buccione R, Orth JD, McNiven MA. 2004. Foot and mouth: podosomes, invadopodia and circular dorsal ruffles. Nat Rev Mol Cell Biol. Aug;5(8):647-57.

Buchsbaum RJ. 2007. Rho activation at a glance. J Cell Sci. 120(Pt 7):1149-52.

Camonis JH and White MA. 2005. Ral GTPases: corrupting the exocyst in cancer cells. Trends Cell Biol 15: 327-332.

Campellone, K. G., Webb, N. J., Znameroski, E. A. and Welch, M. D. 2008. WHAMM is an Arp2/3 complex activator that binds microtubules and functions in ER to Golgi transport. Cell 134, 148-161.

Carlier M-F. 1991. Actin: protein structure and filament dynamics. The Journal of biological chemistry 266(1):1-4.

Cascone I, Selimoglu R, Ozdemir C, Del Nery E, Yeaman C, White M & Camonis J. 2008. Distinct roles of RalA and RalB in the progression of cytokinesis are supported by distinct RalGEFs. EMBO J 27: 2375-2387.

Chardin P and Tavitian A. 1989. Coding sequences of human ralA and ralB cDNAs. Nucleic Acids Res 17: 4380.

Chardin P and Tavitian A. 1986. The ral gene: a new ras related gene isolated by the use of a synthetic probe. EMBO J 5: 2203-2208.

Cantor, S B; Urano T, Feig L A; 1995; Identification and characterization of Ral-binding protein 1, a potential downstream target of Ral GTPases. Mol. Cell. Biol. 15 (8): 4578–84.

Chen X-W, Leto D, Xiong T, Yu G, Cheng A, Decker S & Saltiel AR. 2011. A Ral GAP complex links PI 3-kinase/Akt signaling to RalA activation in insulin action. Mol. Biol. Cell 22: 141-152.

Chen Z, Borek D, Padrick SB, Gomez TS, Metlagel Z, Ismail AM, Umetani J, Billadeau DD, Otwinowski Z, Rosen MK. 2010. Structure and control of the actin regulatory WAVE complex. Nature 468(7323):533-8.

Chien Y, Kim S, Bumeister R, Loo YM, Kwon SW, Johnson CL, Balakireva MG, Romeo Y, Kopelovich L, Gale Jr M, Yeaman C, Camonis JH, Zhao Y, White MA. 2006. RalB GTPase-mediated activation of the IkappaB family kinase TBK1 couples innate immune signaling to tumor cell survival. Cell 127: 157–170.

Chien Y, and White MA. 2003. RAL GTPases are linchpin modulators of human tumour-cell proliferation and survival. EMBO Rep 4: 800–806.

Cicchetti P. and Baltimore D. 1995. Identification of 3BP-1 in cDNA expression library by SH3 domain screening. Methods Enzymol. 1995;256:140-8.

Cicchetti P, Ridley AJ, Zheng Y, Cerione RA, Baltimore D. 1995. 3BP-1, an SH3 domain binding protein, has GAP activity for Rac and inhibits growth factor-induced membrane ruffling in fibroblasts. EMBO J. 14(13):3127-35.

Cicchetti P, Mayer BJ, Thiel G and Baltimore D. 1992. Identification of a protein that binds to the SH3 region of Abl and is similar to Bcr and GAP. Science, 257, 803–806.

Clough RR, Sidhu RS, Bhullar RP. 2002. Calmodulin binds RalA and RalB and is required for the thrombin-induced activation of Ral in human platelets. J Biol Chem. Aug 9;277(32):28972-80.

Croteau, N. J., Furgason, M. L., Devos, D. and Munson, M. 2009. Conservation of helical bundle structure between the exocyst subunits. PLoS ONE 4, e4443.

van Dam EM & Robinson PJ. 2006. Ral: mediator of membrane trafficking. Int. J. Biochem. Cell Biol 38: 1841-1847.

Davidson AJ, Insall RH. 2011. Actin-based motility: WAVE regulatory complex structure reopens old SCARs. Curr Biol. 25;21(2):R66-8.

DeMali, K. A., Barlow, C. A. and Burridge, K. 2002. Recruitment of the Arp2/3 complex to vinculin: coupling membrane protrusion to matrix adhesion. J. Cell Biol. 159, 881-891.

Dent, E. W., Kwiatkowski, A. V., Mebane, L. M., Philippar, U., Barzik, M., Rubinson, D. A., Gupton, S., van Veen, J. E., Furman, C., Zhang, J. et al. 2007. Filopodia are required for cortical neurite initiation. Nat. Cell Biol. 9, 1347–1359.

Derry, J.M., Ochs, H.D., and Francke, U. 1994. Isolation of a novel gene mutated in Wiskott-Aldrich syndrome. Cell 78, 635–644.

Derivery E, Gautreau A. 2010. Generation of branched actin networks: assembly and regulation of the N-WASP and WAVE molecular machines. Bioessays 32(2):119-31.

Dobbelaere, J., and Y. Barral. 2004. Spatial coordination of cytokinetic events by compartmentalization of the cell cortex. Science 305: 393–396.

Donaldson JG, Porat-Shliom N, Cohen LA. 2009. Clathrin-independent endocytosis: a unique platform for cell signaling and PM remodeling. Cell Signal. 21(1):1-6.

Dong, G., Hutagalung, A. H., Fu, C., Novick, P. and Reinisch, K. M. 2005. The structures of exocyst subunit Exo70p and the Exo84p C-terminal domains reveal a common motif. Nat. Struct. Mol. Biol. 12, 1094–1100.

Dotti, C. G., Sullivan, C. A. and Banker, G. A. 1988. The establishment of polarity by hippocampal neurons in culture. J. Neurosci. 8, 1454–1468.

Downward J. 2003. Targeting RAS signalling pathways in cancer therapy. Nat Rev Cancer. 3(1):11-22.

Eden S, Rohatgi R, Podtelejnikov AV, Mann M and Kirschner MW. 2002. Mechanism of regulation of WAVE1-induced actin nucleation by Rac1 and Nck. Nature, 418, 790–793.

Egile C., Loisel T.P., Laurent V., Li R., Pantaloni D., Sansonetti P.J., Carlier M-F. 1999. Activation of the Cdc42 effector N-WASP by the Shigella flexneria IcsA protein promotes actin nucleation by Arp2/3complex and bacterial actin-based motility. J. Cell Biol. 146:1319–1332.

Emkey R, Freedman S and Feig LA. 1991. Characterization of a GTPase-activating protein for the Ras-related Ral protein. Journal of Biological Chemistry 266: 9703 -9706.

Etienne-Manneville S. 2004. Cdc42 the centre of polarity. J Cell Sci. Mar 15;117(Pt 8):1291-300.

Etienne-Manneville S. 2004. Actin and microtubules in cell motility: which one is in control? Traffic. Jul;5(7):470-7.

Fenwick RB, Prasannan S, Campbell LJ, Nietlispach D, Evetts KA, Camonis J, Mott HR & Owen D. 2009. Solution structure and dynamics of the small GTPase RalB in its active conformation: significance for effector protein binding. Biochemistry 48: 2192-2206.

Fernandez RM, Ruiz-Miró M, Dolcet X, Aldea M, Garí E. 2011. Cyclin D1 interacts and collaborates with Ral GTPases enhancing cell detachment and motility. Oncogene. 21;30(16):1936-46.

Finger FP and Novick P. 1998. Spatial regulation of exocytosis: lessons from yeast. J. Cell Biol 142: 609-612.

Frankel P, Aronheim A, Kavanagh E, Balda MS, Matter K, Bunney TD & Marshall CJ. 2005. RalA interacts with ZONAB in a cell density-dependent manner and regulates its transcriptional activity. EMBO J 24: 54-62.

Fukai S, Matern HT, Jagath JR, Scheller RH, Brunger AT. 2003. Structural basis of the interaction between RalA and Sec5, a subunit of the sec6/8 complex. EMBO J 22: 3267–3278.

Gautreau, A., Ho, H. Y., Steen, H., Gygi, S. P. and Kirschner, M. W. 2004. Purification and architecture of the ubiquitous WAVE complex. Proc. Natl. Acad. Sci. USA 101, 4379-4383.

Godin CM, Ferreira LT, Dale LB, Gros R, Cregan SP & Ferguson SSG. 2010. The small GTPase Ral couples the angiotensin II type 1 receptor to the activation of phospholipase C-delta 1. Mol. Pharmacol 77: 388-395.

Goley ED, Welch MD. 2006. The ARP2/3 complex: an actin nucleator comes of age. Nat Rev Mol Cell Biol 7 (10): 713–726.

Goldfinger LE, Ptak C, Jeffery ED, Shabanowitz J, Hunt DF, Ginsberg MH. 2006. RLIP76 (RalBP1) is an R-Ras effector that mediates adhesion-dependent Rac activation and cell migration. J Cell Biol. Sep 11;174(6):877-88.

Gonzalez-García A, Pritchard CA, Paterson HF, Mavria G, Stamp G & Marshall CJ. 2005. RalGDS is required for tumor formation in a model of skin carcinogenesis. Cancer Cell 7: 219-226.

Grindstaff KK, Yeaman C, Anandasabapathy N, Hsu SC, Rodriguez-Boulan E, Scheller RH, Nelson WJ. 1998. Sec6/8 complex is recruited to cell-cell contacts and specifies transport vesicle delivery to the basal-lateral membrane in epithelial cells. Cell. 93(5):731-40.

Gromley A, Yeaman C, Rosa J, Redick S, Chen C-T, Mirabelle S, Guha M, Sillibourne J & Doxsey SJ. 2005. Centriolin

anchoring of exocyst and SNARE complexes at the midbody is required for secretory-vesicle-mediated abscission. Cell 123: 75-87.

Guo W, Tamanoi F, Novick P. 2001. Spatial regulation of the exocyst complex by Rho1 GTPase. Nat Cell Biol;3:353–60.

Guo, W., Sacher, M., Barrowman, J., Ferro-Novick, S., and Novick, P. 2000. Trends Cell Biol. 10, 251–255.

Guo W, Roth D, Walch-Solimena C & Novick P. 1999. The exocyst is an effector for Sec4p, targeting secretory vesicles to sites of exocytosis. EMBO J 18: 1071-1080.

Guo, W., Grant, A., and Novick, P. 1999b. J. Biol. Chem. 274, 23558–23564.

Hahn WC, Counter CM, Lundberg AS, Beijersbergen RL, Brooks MW & Weinberg RA. 1999. Creation of human tumour cells with defined genetic elements. Nature 400: 464-468.

Hamad NM, Elconin JH, Karnoub AE, Bai W, Rich JN, Abraham RT, Der CJ & Counter CM. 2002. Distinct requirements for Ras oncogenesis in human versus mouse cells. Genes Dev 16: 2045-2057.

Hamburger, Z. A., Hamburger, A. E., West, Jr, A. P. and Weis, W. I. 2006. Crystal structure of the S. cerevisiae exocyst component Exo70p. J. Mol. Biol. 356, 9–21.

Hancock JF, Paterson H, Marshall CJ. 1990. A polybasic domain or palmitoylation is required in addition to the CAAX motif to localize p21ras to the plasma membrane. Cell. Oct 5;63(1):133-9.

Hancock JF, Magee AI, Childs JE, Marshall CJ. 1989. All ras proteins are polyisoprenylated but only some are palmitoylated. Cell. Jun 30;57(7):1167-77.

Hazuka CD, Foletti DL, Hsu SC, Kee Y, Hopf FW, Scheller RH. 1999. The sec6/8 complex is located at neurite outgrowth

and axonal synapse-assembly domains. J Neurosci. 19(4):1324-34.

He B, Guo W. 2009. The exocyst complex in polarized exocytosis. Curr Opin Cell Biol. Aug;21(4):537-42.

He, B., Xi, F., Zhang, X., Zhang, J. and Guo, W. 2007. Exo70 interacts with phospholipids and mediates the targeting of the exocyst to the plasma membrane. EMBO J 26, 4053–4065.

Heasman, S.J. and Ridley, A.J. 2008. Mammalian Rho GTPases: new insights into their functions from in vivo studies. Nat. Rev. Mol. Cell Biol. 9, 690–701.

Hertzog M. and Chavrier P. 2011. Cell polarity during motile processes: keeping on track with the exocyst complex. Biochem. J. (2011) 433, 403–409.

Higgs, H. N. and Pollard, T. 1999. Regulation of actin polymerization by Arp2/3 complex and WASp/Scar proteins. J. Biol. Chem. 274, 32531- 32534.

Hofer F, Berdeaux R & Martin GS. 1998. Ras-independent activation of Ral by a Ca(2+)-dependent pathway. Curr. Biol 8: 839-842.

Hsu SC, Ting AE, Hazuka CD, Davanger S, Kenny JW, Kee Y, Scheller RH. 1996. The mammalian brain rsec6/8 complex. Neuron. 17(6):1209-19.

Huang L, Hofer F, Martin GS, Kim SH. 1998. Structural basis for the interaction of Ras with RalGDS. Nat Struct Biol. Jun;5(6):422-6.

Ibarra N, Pollitt A, Insall RH. 2006. Regulation of actin assembly by SCAR/WAVE proteins. Biochem Soc Trans. 33(Pt 6):1243-6.

Innocenti, M., Zucconi, A., Disanza, A., Frittoli, E., Areces, L. B., Steffen, A., Stradal, T. E., Di Fiore, P. P., Carlier, M. F. and Scita, G. 2004. Abi1 is essential for the formation and

activation of a WAVE2 signalling complex. Nat. Cell Biol. 6, 319-327.

Insall RH. 2011. Dogma bites back--the evidence for branched actin. Trends Cell Biol. Jan;21(1):2; author reply 4-5.

Issaq SH, Lim KH, Counter CM. 2010. Sec5 and Exo84 foster oncogenic ras-mediated tumorigenesis. Mol Cancer Res. 8(2):223-31.

Itoh, R.E., Kiyokawa, E., Aoki, K., Nishioka, T., Akiyama, T., and Matsuda, M. 2008. Phosphorylation and activation of the Rac1 and Cdc42 GEF Asef in A431 cells stimulated by EGF. J. Cell Sci. 121, 2635–2642.

Jenkins G. M. and Frohman M. A. 2005. Phospholipase D: a lipid centric review. Cell. Mol. Life. Sci 62:2305–2316.

Jiang H, Luo JQ, Urano T, Frankel P, Lu Z, Foster DA, Feig LA. 1995. Involvement of Ral GTPase in v-Src-induced phospholipase D activation. Nature. Nov 23;378(6555):409-12.

Jin, R., Junutula, J. R., Matern, H. T., Ervin, K. E., Scheller, R. H. and Brunger, A. T. 2005. Exo84 and Sec5 are competitive regulatory Sec6/8 effectors to the RalA GTPase. EMBO J. 24, 2064–2074.

Jullien-Flores V, Mahé Y, Mirey G, Leprince C, Meunier-Bisceuil B, Sorkin A & Camonis JH. 2000. RLIP76, an effector of the GTPase Ral, interacts with the AP2 complex: involvement of the Ral pathway in receptor endocytosis. J. Cell. Sci 113 (Pt 16): 2837-2844.

Jullien-Flores V, Dorseuil O, Romero F, Letourneur F, Saragosti S, Berger R, Tavitian A, Gacon G & Camonis JH. 1995. Bridging Ral GTPase to Rho pathways. RLIP76, a Ral effector with CDC42/Rac GTPase-activating protein activity. J. Biol. Chem 270: 22473-22477.

Kato, M., Miki, H., Kurita, S., Endo, T., Nakagawa, H., Miyamoto, S. & Takenawa, T (2002) WICH, a novel verprolin homology domain-containing protein that functions cooperatively with N-WASP in actin-microspike formation. Biochem. Biophys. Res. Commun. 291, 41–47.

Kelly AE, Kranitz H, Dötsch V, Mullins RD. 2006. Actin binding to the central domain of WASP/Scar proteins plays a critical role in the activation of the Arp2/3 complex. J Biol Chem. 281(15):10589-97.

Kelleher, J. F., Atkinson, S. J. and Pollard, T. D. 1995. Sequences, structural models and subcellular localization of the actin-related proteins Arp2 and Arp3 from Acanthamoeba. J. Cell Biol. 131, 385-397.

Kim, A.S., Kakalis, L.T., Abdul-Manan, M., Liu, G.A., and Rosen, M.K. 2000. Autoinhibition and activation mechanisms of the Wiskott-Aldrich syndrome protein. Nature 404, 151–158.

Kinsella BT, Erdman RA, Maltese WA. 1991. Carboxyl-terminal isoprenylation of ras-related GTP-binding proteins encoded by rac1, rac2, and ralA. J Biol Chem. May 25;266(15):9786-94.

Kobayashi K, Kuroda S, Fukata M, Nakamura T, Nagase T, Nomura N, Matsuura Y, Yoshida-Kubomura N, Iwamatsu A, Kaibuchi K. 1998. p140Sra-1 (specifically Rac1-associated protein) is a novel specific target for Rac1 small GTPase. J Biol Chem. Jan 2;273(1):291-5.

Kovacs, E. M., Goodwin, M., Ali, R. G., Paterson, A. D. and Yap, A. S. 2002 Cadherin-directed actin assembly: E-cadherin physically associates with the Arp2/3 complex to direct actin assembly in nascent adhesive contacts. Curr. Biol. 12, 379-382.

Kunda, P., G. Craig, V. Dominguez, and B. Baum. 2003. Abi, Sra1, and Kette control the stability and localization of

SCAR/WAVE to regulate the formation of actin-based protrusions. Curr. Biol. 13:1867–1875.

Lalli G. 2009. RalA and the exocyst complex influence neuronal polarity through PAR-3 and aPKC. J Cell Sci. 122(Pt 10):1499-506.

Lalli G and Hall A. 2005. Ral GTPases regulate neurite branching through GAP-43 and the exocyst complex. J Cell Biol. 171(5):857-69.

Langevin J, Morgan MJ, Sibarita JB, Aresta S, Murthy M, Schwarz T, Camonis J, Bellaïche Y. 2005. Drosophila exocyst components Sec5, Sec6, and Sec15 regulate DE-Cadherin trafficking from recycling endosomes to the plasma membrane. Dev Cell. 9(3):365-76.

Lebensohn, R., Montagnat, M., Mansuy, P., Duval, P., Meysonnier, J., and Philip, A. 2009. Modeling viscoplastic behavior and heterogeneous intracrystalline deformation of columnar ice polycrystals. Acta Materiala, 57:1405–1415.

Lee T, Feig L & Montell DJ. 1996. Two distinct roles for Ras in a developmentally regulated cell migration. Development 122: 409-418.

Letinic K, Sebastian R, Toomre D, Rakic P. 2009. Exocyst is involved in polarized cell migration and cerebral cortical development. Proc Natl Acad Sci U S A. Jul 7;106(27):11342-7.

Lim K-H, Brady DC, Kashatus DF, Ancrile BB, Der CJ, Cox AD & Counter CM. 2010. Aurora-A phosphorylates, activates, and relocalizes the small GTPase RalA. Mol. Cell. Biol 30: 508-523.

Lim K-H, O'Hayer K, Adam SJ, Kendall SD, Campbell PM, Der CJ & Counter CM. 2006. Divergent roles for RalA and RalB in malignant growth of human pancreatic carcinoma cells. Curr. Biol 16: 2385-2394.

Lim, K.L., Chew C.M.K., Tan, M.M. J., Wang C., Chung, K.K.K., Zhang, Y., Tanaka Y., Smith, W.L., Engelender, S., Ross, Dawson C.A., V.L. and Dawson, T. M. 2005. Parkin mediates non-classical, proteasomal-independent, ubiquitination of Synphilin-1: Implications for Lewy Body formation. Journal of Neuroscience, 25, 2002-2009.

Linardopoulou EV, Parghi SS, Friedman C, Osborn GE, Parkhurst SM, Trask BJ. 2007. Human subtelomeric WASH genes encode a new subclass of the WASP family. PLoS Genet. 3(12):e237.

Lipschutz JH, Guo W, O'Brien LE, Nguyen YH, Novick P, Mostov KE. 2000. Exocyst is involved in cystogenesis and tubulogenesis and acts by modulating synthesis and delivery of basolateral plasma membrane and secretory proteins. Mol Biol Cell. 11(12):4259-75.

Liu, J., Zuo, X., Yue, P. and Guo, W. 2007. Phosphatidylinositol 4,5-bisphosphate mediates the targeting of the exocyst to the plasma membrane for exocytosis in mammalian cells. Mol. Biol. Cell 18, 4483–4492.

Luo JQ, Liu X, Frankel P, Rotunda T, Ramos M, Flom J, Jiang H, Feig LA, Morris AJ, Kahn RA & Foster DA. 1998. Functional association between Arf and RalA in active phospholipase D complex. Proc. Natl. Acad. Sci. U.S.A 95: 3632-3637.

Machacek M, Hodgson L, Welch C, Elliott H, Pertz O, Nalbant P, Abell A, Johnson GL, Hahn KM, Danuser G. 2009. Coordination of Rho GTPase activities during cell protrusion. Nature. 461(7260):99-103.

Machesky, L. M., Mullins, R. D., Higgs, H. N., Kaiser, D. A., Blanchoin, L., May, R. C., Hall, M. E. and Pollard, T. D. 1999. Scar, a WASprelated protein, activates nucleation of actin filaments by the Arp2/3 complex. Proc. Nat. Acad. Sci. USA 96, 3739-3744.

Machesky LM and Insall RH. 1998. Scar1 and the related Wiskott–Aldrich syndrome protein, WASP, regulate the actin cytoskeleton through the Arp2/3 complex. Curr Biol, 8, 1347–1356.

Machesky, L. M., Atkinson, S. J., Ampe, C., Vandekerckhove, J. and Pollard, T. D. 1994. Purification of a cortical complex containing two unconventional actins from Acanthamoeba by affinity chromatography on profilin-agarose. J. Cell Biol. 127, 107-115.

Maehama, T., Tanaka, M., Nishina, H., Murakami, M., Kanaho, Y. & Hanada, K. 2008. RalA functions as an indispensable signal mediator for the nutrient-sensing system. J. Biol. Chem. 283, 35053–35059.

Mattila PK, Lappalainen P. 2008. Filopodia: molecular architecture and cellular functions. Nat. Rev. Mol. Cell Biol. 9: 446-454.

Miki, H., Yamaguchi, H., Suetsugu, S. and Takenawa, T. 2000. IRSp53 is an essential intermediate between Rac and WAVE in the regulation of membrane ruffling. Nature 408, 732-735.

Miki, H., Suetsugu, S. and Takenawa, T. 1998a. WAVE, a novel WASP family protein involved in actin reorganization induced by Rac. EMBO J. 17, 6932-6941.

Miki, H., Sasaki, T., Takai, Y., and Takenawa, T. 1998b. Induction of filopodium formation by a WASP-related actin-depolymerizing protein N-WASP. Nature 391, 93–96.

Miki, H., Miura, K., and Takenawa, T. 1996. N-WASP, a novel actindepolymerizing protein, regulates the cortical cytoskeletal rearrangement in a PIP2-dependent manner downstream of tyrosine kinases. EMBO J. 15, 5326–5335.

Mirey, G., M. Balakireva, S. L'Hoste, C. Rosse, S. Voegeling, and J. H. Camonis. 2003. A RalGEF-Ral pathway is conserved in Drosophila melanogaster and sheds new light on the

connectivity of the Ral, Ras, and Rap pathways. Mol. Cell. Biol. 23:1112–1124.

Moore, B. A., Robinson, H. H. and Xu, Z. 2007. The crystal structure of mouse Exo70 reveals unique features of the mammalian exocyst. J. Mol. Biol. 371, 410–421.

Moskalenko S, Tong C, Rosse C, Mirey G, Formstecher E, Daviet L, Camonis J, White MA. 2003. Ral GTPases regulate exocyst assembly through dual subunit interactions. J Biol Chem. Dec 19;278(51):51743-8.

Moskalenko S, Henry DO, Rosse C, Mirey G, Camonis JH & White MA. 2002. The exocyst is a Ral effector complex. Nat. Cell Biol 4: 66-72.

Mullins , R.D. , J.A. Heuser , and T.D. Pollard. 1998. The interaction of Arp2/3 complex with actin: nucleation, high affi nity pointed end capping, and formation of branching networks of fi laments. Proc. Natl. Acad. Sci. USA . 95 : 6181 – 6186.

Munson M, Novick P. 2006. The exocyst defrocked, a framework of rods revealed. Nat Struct Mol Biol;13:577–81.

Murthy M, Ranjan R, Denef N, Higashi ME, Schupbach T, Schwarz TL. 2005. Sec6 mutations and the Drosophila exocyst complex. J Cell Sci. 2005 Mar 15;118(Pt 6):1139-50.

Murthy M, Garza D, Scheller RH, Schwarz TL. 2003. Mutations in the exocyst component Sec5 disrupt neuronal membrane traffic, but neurotransmitter release persists. Neuron. 37(3):433-47.

Nakashima, S., Morinaka, K., Koyama, S., Ikeda, M., Kishida, M., Okawa, K., Iwamatsu, A., Kishida, S. and Kikuchi, A. 1999. Small G protein Ral and its downstream molecules regulate endocytosis of EGF and insulin receptors. EMBO J. 18, 3629-3642.

Nicely NI, Kosak J, de Serrano V, Mattos C. 2004. Crystal structures of Ral-GppNHp and Ral-GDP reveal two binding sites that are also present in Ras and Rap. Structure. Nov;12(11):2025-36.

Novick P, Field C & Schekman R. 1980. Identification of 23 complementation groups required for post-translational events in the yeast secretory pathway. Cell 21: 205-215.

Nozumi, M., Nakagawa, H., Miki, H., Takenawa, T. and Miyamoto, S. 2003. Differential localization of WAVE isoforms in filopodia and lamellipodia of the neuronal growth cone. J. Cell Sci. 116, 239-246.

Oikawa, T., H. Yamaguchi, T. Itoh, M. Kato, T. Ijuin, D. Yamazaki, S. Suetsugu, and T. Takenawa. 2004. PtdIns(3,4,5)P3 binding is necessary for WAVE2-induced formation of lamellipodia. Nat. Cell Biol. 6:420–426.

Osmani N, Vitale N, Borg JP, Etienne-Manneville S. 2006. Scrib controls Cdc42 localization and activity to promote cell polarization during astrocyte migration. Curr Biol. Dec 19;16(24):2395-405.

Oxford G, Owens CR, Titus BJ, Foreman TL, Herlevsen MC, Smith SC & Theodorescu D. 2005. RalA and RalB: antagonistic relatives in cancer cell migration. Cancer Res 65: 7111-7120.

Palamidessi A, Frittoli E, Garré M, Faretta M, Mione M, Testa I, Diaspro A, Lanzetti L, Scita G, Di Fiore PP. 2008. Endocytic trafficking of Rac is required for the spatial restriction of signaling in cell migration. Cell. 134(1):135-47.

Panchal, S.C., D.A. Kaiser, E. Torres, T.D. Pollard, and M.K. Rosen. 2003. A conserved amphipathic helix in WASP/Scar proteins is essential for activation of Arp2/3 complex. Nat. Struct. Biol. 10:591–598.

Pankov, R., Y. Endo, S. Even-Ram, M. Araki, K. Clark, E. Cukierman, K. Matsumoto, and K.M. Yamada. 2005. A Rac switch regulates random versus directionally persistent cell migration. J. Cell Biol. 170:793–802.

Pantaloni, D., C. L. Clainche, and M. F. Carlier. 2001. Mechanism of actinbased motility. Science. 292:1502–1506.

Pantaloni, D., Boujemaa, R., Didry, D., Gounon, P. and Carlier, M.-F. 2000. The Arp2/3 complex branches filament barbed ends: functional antagonism with capping proteins. Nat. Cell Biol. 2, 385-391.

Parrini MC, Sadou-Dubourgnoux A, Aoki K, Kunida K, Biondini M, Hatzoglou A, Poullet P, Formstecher E, Yeaman C, Matsuda M, Rossé C, Camonis J. 2011. SH3BP1, an exocyst-associated RhoGAP, inactivates Rac1 at the front to drive cell motility. Mol. Cell 42, 650–661.

Pokutta S, Drees F, Yamada S, Nelson WJ, Weis WI. 2008. Biochemical and structural analysis of alpha-catenin in cell-cell contacts. Biochem Soc Trans. Apr;36(Pt 2):141-7.

Pollard,T.D. and Borisy,G.G. 2003. Cellular Motility Driven by Assembly and Disassembly of Actin Filaments. Cell. 112;453-465.

Pollitt AY, Insall RH. 2008. Abi mutants in Dictyostelium reveal specific roles for the SCAR/WAVE complex in cytokinesis. Curr Biol. 18(3):203-10.

Polzin A, Shipitsin M, Goi T, Feig LA, Turner TJ. 2002. Ral-GTPase influences the regulation of the readily releasable pool of synaptic vesicles. Mol Cell Biol. 22(6):1714-22.

Raftopoulou, M. and Hall, A. (2004). Cell migration: Rho GTPases lead the way. Dev. Biol. 265, 23-32.

Ramesh, N., Anton, I. M., Hartwig, J. H. and Geha, R. S. 1997. WIP, a protein associated with the Wiskott-Aldrich syndrome

protein, induces actin polymerization and redistribution in lymphoid cells. Proc. Natl. Acad. Sci. USA 94, 14671-14676.

Rangarajan A, Hong SJ, Gifford A & Weinberg RA. 2004. Species- and cell type-specific requirements for cellular transformation. Cancer Cell 6: 171-183.

Rebhun JF, Chen H & Quilliam LA. 2000. Identification and characterization of a new family of guanine nucleotide exchange factors for the ras-related GTPase Ral. J. Biol. Chem 275: 13406-13410.

Ridley, A.J., Schwartz, M.A., Burridge, K., Firtel, R.A., Ginsberg, M.H., Borisy, G., Parsons, J.T., and Horwitz, A.R. 2003. Cell migration: integrating signals from front to back. Science 302, 1704–1709.

Robinson RC, Turbedsky K, Kaiser DA, Marchand JB, Higgs HN, Choe S, Pollard TD. 2001. Crystal structure of Arp2/3 complex. Science. 294(5547):1679-84.

Robinson NG, Guo L, Imai J, Toh EA, Matsui Y, Tamanoi F. Rho3 of Saccharomyces cerevisiae, which regulates the actin cytoskeleton and exocytosis, is a GTPase which interacts with Myo2 and Exo70. Mol Cell Biol 1999;19:3580–7.

Rohatgi R., Ho H.-y.H., Kirschner M.W. 2000. Mechanism of N-WASP activation by Cdc42 and phosphatidylinositol 4,5-bisphosphate. J. Cell Biol.;150:1299–1309.

Rohatgi, R., L. Ma, H. Miki, M. Lopez, T. Kirchhausen, T. Takenawa, and M.W. Kirschner. 1999. The interaction between N-WASP and the Arp2/3 complex links Cdc42-dependent signals to actin assembly. Cell. 97:221–231.

Rossé C, Hatzoglou A, Parrini M-C, White MA, Chavrier P & Camonis J. 2006. RalB mobilizes the exocyst to drive cell migration. Mol. Cell. Biol 26: 727-734.

Rossé C, L'Hoste S, Offner N, Picard A & Camonis J. 2003. RLIP, an effector of the Ral GTPases, is a platform for Cdk1 to

phosphorylate epsin during the switch off of endocytosis in mitosis. J. Biol. Chem 278: 30597-30604.

Rosse, C., Formstecher, E., Boeckeler, K., Zhao, Y., Kremerskothen, J., White, M. D., Camonis, J. H. and Parker, P. J. 2009. An aPKC–exocyst complex controls paxillin phosphorylation and migration through localised JNK1 activation. PLoS Biol. 7, e1000235.

Rottner K, Hänisch J, Campellone KG. 2010. WASH, WHAMM and JMY: regulation of Arp2/3 complex and beyond. Trends Cell Biol. Nov;20(11):650-61.

Rouiller I, Xu XP, Amann KJ, Egile C, Nickell S, Nicastro D, Li R, Pollard TD, Volkmann N, Hanein D. 2008. The structural basis of actin filament branching by the Arp2/3 complex. J Cell Biol. 180(5):887-95.

de Ruiter ND, Wolthuis RM, van Dam H, Burgering BM & Bos JL. 2000. Ras-dependent regulation of c-Jun phosphorylation is mediated by the Ral guanine nucleotide exchange factor-Ral pathway. Mol. Cell. Biol 20: 8480-8488.

Sablina AA, Chen W, Arroyo JD, Corral L, Hector M, Bulmer SE, DeCaprio JA & Hahn WC. 2007. The tumor suppressor PP2A Abeta regulates the RalA GTPase. Cell 129: 969-982.

Sanz-Moreno, V., Gadea, G., Ahn, J., Paterson, H., Marra, P., Pinner, S., Sahai, E., and Marshall, C.J. 2008. Rac activation and inactivation control plasticity of tumor cell movement. Cell 135, 510–523.

Schmidt M, Voss M, Thiel M, Bauer B, Grannass A, Tapp E, Cool RH, de Gunzburg J, von Eichel-Streiber C, Jakobs KH. 1998. Specific inhibition of phorbol ester-stimulated phospholipase D by Clostridium sordellii lethal toxin and Clostridium difficile toxin B-1470 in HEK-293 cells. Restoration by Ral GTPases. J Biol Chem. Mar 27;273(13):7413-22.

Scita G, Tenca P, Areces LB, et al. 2001. An effector region in Eps8 is responsible for the activation of the Rac-specific GEF activity of Sos-1 and for the proper localization of the Rac-based actin-polymerizing machine. J Cell Biol;154:1031–44.

Shipitsin M, Feig LA. 2004. RalA but not RalB enhances polarized delivery of membrane proteins to the basolaterla surface of epithelial cells. Mol Cell Biol 24: 5746–5756.

Shirakawa R, Fukai S, Kawato M, Higashi T, Kondo H, Ikeda T, Nakayama E, Okawa K, Nureki O, Kimura T, Kita T & Horiuchi H. 2009. Tuberous sclerosis tumor suppressor complex-like complexes act as GTPase-activating proteins for Ral GTPases. J. Biol. Chem 284: 21580-21588.

Sidhu RS, Elsaraj SM, Grujic O, Bhullar RP. 2005. Calmodulin binding to the small GTPase Ral requires isoprenylated Ral. Biochem Biophys Res Commun. Oct 14;336(1):105-9.

Sidhu RS, Clough RR & Bhullar RP. 2005. Regulation of phospholipase C-delta1 through direct interactions with the small GTPase Ral and calmodulin. J. Biol. Chem 280: 21933-21941.

Sivaram, M. V., Furgason, M. L., Brewer, D. N. and Munson, M. 2006. The structure of the exocyst subunit Sec6p defines a conserved architecture with diverse roles. Nat. Struct. Mol. Biol. 13, 555–556.

Sivaram MV, Saporita JA, Furgason ML, Boettcher AJ, Munson M. 2005. Dimerization of the exocyst protein Sec6p and its interaction with the t-SNARE Sec9p. Biochemistry 44:6302–6311.

Sjoblom T, Jones S, Wood LD, Parsons DW, Lin J, Barber TD, Mandelker D, Leary RJ, Ptak J, Silliman N, Szabo S, Buckhaults P, Farrell C, Meeh P, Markowitz SD, Willis J, Dawson D, Willson JKV, Gazdar AF, Hartigan J, et al (2006)

The Consensus Coding Sequences of Human Breast and Colorectal Cancers. Science 314: 268 -274.

Small JV. 2010. Dicing with dogma: de-branching the lamellipodium. Trends Cell Biol. Nov;20(11):628-33.

Smith SC, Oxford G, Baras AS, Owens C, Havaleshko D, Brautigan DL, Safo MK, Theodorescu D. 2007. Expression of ral GTPases, their effectors, and activators in human bladder cancer. Clin Cancer Res. 13(13):3803-13.

Sossey-Alaoui, K., Li, X., Ranalli, T.A., Cowell, J.K. J. Biol. Chem. 2005. WAVE3-mediated cell migration and lamellipodia formation are regulated downstream of phosphatidylinositol 3-kinase.

Steffen, A., Rottner, K., Ehinger, J., Innocenti, M., Scita, G., Wehland, J., and Stradal, T.E.B. 2004. Sra-1 and Nap1 link Rac to actin assembly driving lamellipodia formation. EMBO J. 23, 749–759.

Stovold, C. F., Millard, T. F. and Machesky, L. M. 2005. Inclusion of Scar/WAVE3 in a similar complex to Scar/WAVE1 and 2. BMC Cell Biol. 6, 11.

Suetsugu, S., D. Yamazaki, S. Kurisu, and T. Takenawa. 2003. Differential roles of WAVE1 and WAVE2 in dorsal and peripheral ruffle formation for fibroblast cell migration. Dev. Cell. 5:595–609.

Suetsugu, S., Miki, H. & Takenawa, T. 2001. Identification of another actin-related protein (Arp) 2/3 complex binding site in neural Wiskott-Aldrich syndrome protein (N-WASP) that complements actin prolymerization induced by the Arp2/3 complex activating (VCA) domain of N-WASP. J.Biol.Chem. 276, 33175-33180.

Suetsugu, S., Miki, H. and Takenawa, T. 1999. Identification of two human WAVE/SCAR homologues as general actin

regulatory molecules which associate with the Arp2/3 complex. Biochem. Biophys. Res. Commun. 260, 296-302

Suetsugu, S., Miki, H. and Takenawa, T. 1998. The essential role of profilin in the assembly of actin for microspike formation. EMBO J. 17, 6516-6526.

Sugihara K, Asano S, Tanaka K, Iwamatsu A, Okawa K, Ohta Y. 2002. The exocyst complex binds the small GTPase RalA to mediate filopodia formation. Nat Cell Biol. 4(1):73-8.

Suzuki J, Yamazaki Y, Li G, Kaziro Y, Koide H & Guang L. 2000. Involvement of Ras and Ral in chemotactic migration of skeletal myoblasts. Mol. Cell. Biol 20: 4658-4665.

Svitkina, T. M. and Borisy, G. G. 1999. Arp2/3 complex and actin depolymerizing factor/cofilin in dendritic organization and treadmilling of actin filament arrays in lamellipodia. J. Cell Biol. 145, 1009-1026.

Takenawa T, Miki H. 2001. WASP and WAVE family proteins: key molecules for rapid rearrangement of cortical actin filaments and cell movement. J Cell Sci. May;114(Pt 10):1801-9.

Tchevkina E, Agapova L, Dyakova N, Martinjuk A, Komelkov A, Tatosyan A. 2005. The small G-protein RalA stimulates metastasis of transformed cells. Oncogene. Jan 13;24(3):329-35.

TerBush DR, Maurice T, Roth D, Novick P. 1996. The Exocyst is a multiprotein complex required for exocytosis in Saccharomyces cerevisiae. EMBO J. Dec 2;15(23):6483-94.

TerBush DR, Novick P. 1995. Sec6, Sec8, and Sec15 are components of a multisubunit complex which localizes to small bud tips in Saccharomyces cerevisiae. J Cell Biol. Jul;130(2):299-312.

Tian X, Rusanescu G, Hou W, Schaffhausen B, Feig LA. 2002. PDK1 mediates growth factor-induced Ral-GEF activation by

a kinase-independent mechanism. EMBO J. Mar 15;21(6):1327-38.

Urano T, Ihara H, Takada Y, Nagai N, Takada A. 1996. The inhibition of human factor Xa by plasminogen activator inhibitor type 1 in the presence of calcium ion, and its enhancement by heparin and vitronectin. Biochim Biophys Acta. Dec 5;1298(2):199-208.

Urban E, Jacob S, Nemethova M, Resch GP, Small JV. 2010. Electron tomography reveals unbranched networks of actin filaments in lamellipodia. Nat Cell Biol. May;12(5):429-35.

Van Aelst L, White MA, Wigler MH. 1994. Ras partners. Cold Spring Harb Symp Quant Biol.59:181-6.

Varambally S, Yu J, Laxman B, Rhodes DR, Mehra R, Tomlins SA, Shah RB, Chandran U, Monzon FA, Becich MJ, et al. 2005. Integrative genomic and proteomic analysis of prostate cancer reveals signatures of metastatic progression. Cancer Cell 8, 393–406.

VerPlank L, Li R. 2005. Cell cycle-regulated trafficking of Chs2 controls actomyosin ring stability during cytokinesis. Mol Biol Cell. May;16(5):2529-43.

Vetter IR, Wittinghofer A. 2001. The guanine nucleotide-binding switch in three dimensions. Science. Nov 9;294(5545):1299-304.

Vetterkind S, Miki H, Takenawa T, Klawitz I, Scheidtmann KH, Preuss U. 2002. The rat homologue of Wiskott-Aldrich syndrome protein (WASP)-interacting protein (WIP) associates with actin filaments, recruits N-WASP from the nucleus, and mediates mobilization of actin from stress fibers in favor of filopodia formation. J Biol Chem. Jan 4;277(1):87-95.

Vicente-Manzanares, M., Choi, C. K. & Horwitz, A. R. 2009. Integrins in cell migration the actin connection. J. Cell Sci. 122, 199–206.

Volkman BF, Prehoda KE, Scott JA, Peterson FC, Lim WA. 2002. Structure of the N-WASP EVH1 domain-WIP complex: insight into the molecular basis of Wiskott-Aldrich Syndrome. Cell. Nov 15;111(4):565-76.

Voss M, Weernink PA, Haupenthal S, Möller U, Cool RH, Bauer B, Camonis JH, Jakobs KH, Schmidt M. 1999. Phospholipase D stimulation by receptor tyrosine kinases mediated by protein kinase C and a Ras/Ral signaling cascade. J Biol Chem. Dec 3;274(49):34691-8.

Wallar BJ, Alberts AS. 2003. The formins: active scaffolds that remodel the cytoskeleton. Trends Cell Biol. Aug;13(8):435-46.

Wang H, Owens C, Chandra N, Conaway MR, Brautigan DL, Theodorescu D. 2010. Phosphorylation of RalB is important for bladder cancer cell growth and metastasis. Cancer Res. Nov 1;70(21):8760-9.

Wang H, Tang X, Liu J, Trautmann S, Balasundaram D, McCollum D, Balasubramanian MK. 2002. The multiprotein exocyst complex is essential for cell separation in Schizosaccharomyces pombe. Mol Biol Cell. Feb;13(2):515-29.

Ward Y, Wang W, Woodhouse E, Linnoila I, Liotta L, Kelly K. 2001. Signal pathways which promote invasion and metastasis: critical and distinct contributions of extracellular signal-regulated kinase and Ral-specific guanine exchange factor pathways. Mol Cell Biol. Sep;21(17):5958-69.

Welch MD, DePace AH, Verma S, Iwamatsu A, Mitchison TJ. 1997. The human Arp2/3 complex is composed of evolutionarily conserved subunits and is localized to cellular regions of

dynamic actin filament assembly. J Cell Biol. Jul 28;138(2):375-84.

Welch MD, Mullins RD. 2002. Cellular control of actin nucleation. Annu Rev Cell Dev Biol.;18:247-88.

White MA, Vale T, Camonis JH, Schaefer E, Wigler MH. 1996. A role for the Ral guanine nucleotide dissociation stimulator in mediating Ras-induced transformation. J Biol Chem. Jul 12;271(28):16439-42.

Whyte JR, Munro S. 2002. Vesicle tethering complexes in membrane traffic. J Cell Sci. Jul 1;115(Pt 13):2627-37.

Wu H, Brennwald P. 2010. The function of two Rho family GTPases is determined by distinct patterns of cell surface localization. Mol Cell Biol. Nov;30(21):5207-17.

Wu Z, Owens C, Chandra N, Popovic K, Conaway M, Theodorescu D. 2010. RalBP1 is necessary for metastasis of human cancer cell lines. Neoplasia. Dec;12(12):1003-12.

Wu, S., Mehta, S. Q., Pichaud, F., Bellen, H. J. and Quiocho, F. A. 2005. Sec15 interacts with Rab11 via a novel domain and affects Rab11 localization in vivo. Nat. Struct. Mol. Biol. 12, 879–885.

Yamashita, M., Kurokawa, K., Sato, Y., Yamagata, A., Mimura, H., Yoshikawa, A., Sato, K., Nakano, A. and Fukai, S. 2010. Structural basis for the Rho- and phosphoinositidedependent localization of the exocyst subunit Sec3. Nat. Struct. Mol. Biol. 17, 180–186.

Yamazaki D, Fujiwara T, Suetsugu S, Takenawa T. 2005. A novel function of WAVE in lamellipodia: WAVE1 is required for stabilization of lamellipodial protrusions during cell spreading. Genes Cells. May;10(5):381-92.

Yamazaki Y, Takani K, Atoda H, Morita T. 2003. Snake venom vascular endothelial growth factors (VEGFs) exhibit potent

activity through their specific recognition of KDR (VEGF receptor 2). J Biol Chem. Dec 26;278(52):51985-8.

Yan C, Martinez-Quiles N, Eden S, Shibata T, Takeshima F, Shinkura R, Fujiwara Y, Bronson R, Snapper SB, Kirschner MW, Geha R, Rosen FS, Alt FW. 2003. WAVE2 deficiency reveals distinct roles in embryogenesis and Rac-mediated actin-based motility. EMBO J. Jul 15;22(14):3602-12.

Yang C, Svitkina T. 2011.Visualizing branched actin filaments in lamellipodia by electron tomography. Nat Cell Biol. Sep 2;13(9):1012-3; author reply 1013-4.

Yang P, Fox L, Colbran RJ, Sale WS. 2000. Protein phosphatases PP1 and PP2A are located in distinct positions in the Chlamydomonas flagellar axoneme. J Cell Sci. Jan;113 (Pt 1):91-102.

Yarar D, D'Alessio JA, Jeng RL, Welch MD. 2002. Motility determinants in WASP family proteins. Mol Biol Cell. Nov;13(11):4045-59.

Yarar D, To W, Abo A, Welch MD. 1999. The Wiskott-Aldrich syndrome protein directs actin-based motility by stimulating actin nucleation with the Arp2/3 complex. Curr Biol. May 20;9(10):555-8.

Yeaman C, Grindstaff KK, Nelson WJ. 2004. Mechanism of recruiting Sec6/8 (exocyst) complex to the apical junctional complex during polarization of epithelial cells. J Cell Sci. Feb 1;117(Pt 4):559-70.

Yin J, Pollock C, Tracy K, Chock M, Martin P, Oberst M, Kelly K. 2007. Activation of the RalGEF/Ral pathway promotes prostate cancer metastasis to bone. Mol Cell Biol. Nov;27(21):7538-50.

Zhang X, Bi E, Novick P, Du L, Kozminski KG, Lipschutz JH, et al. 2001. Cdc42 interacts with the exocyst and regulates polarized secretion. J Biol Chem;276:46745–50.

Zettl M, Way M. 2002. The WH1 and EVH1 domains of WASP and Ena/VASP family members bind distinct sequence motifs. Curr Biol. Sep 17;12(18):1617-22.

Zuchero JB, Coutts AS, Quinlan ME, Thangue NB, Mullins RD. 2009. p53-cofactor JMY is a multifunctional actin nucleation factor. Nat Cell Biol. Apr;11(4):451-9.

Zuo X, Zhang J, Zhang Y, Hsu SC, Zhou D, Guo W. 2006. Exo70 interacts with the Arp2/3 complex and regulates cell migration. Nat Cell Biol. Dec;8(12):1383-8.